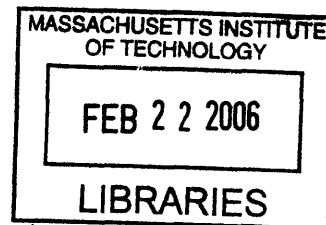


Microvessel Structure Formation in a 3D Perfused Co-culture of Rat Hepatocytes and Liver Endothelial Cells

By

Albert J. Hwa



Bachelor of Science (Magna Cum Laude), Chemical Engineering
Cornell University, 2000

Submitted to the Biological Engineering Division in partial fulfillment of the requirements for the degree of

Doctor of Philosophy
at the
Massachusetts Institute of Technology

February, 2006

©2006 Massachusetts Institute of Technology
All Rights Reserved

ARCHIVES!

Signature of author: _____
Biological Engineering Division

Certified by: _____
Linda Griffith
Professor of Biological Engineering and Mechanical Engineering
Thesis Advisor

Accepted by: _____
Douglas Lauffenburger
Professor and Director of Biological Engineering Division

This doctoral thesis has been examined by a committee of the Biological Engineering Division as follows:

Chairperson, Graduate Thesis Committee: _____
Roger D. Kamm
Professor of Biological Engineering and Mechanical Engineering
MIT

Thesis Advisor, Committee Member: _____
Linda G. Griffith
Professor of Biological Engineering and Mechanical Engineering
MIT

Thesis Committee Member: _____
Donna B. Stolz
Professor of Cell Biology and Physiology
University of Pittsburgh

Thesis Committee Member: _____
Peter T. So
Professor of Biological Engineering and Mechanical Engineering
MIT

Microvessel Structure Formation in a 3D Perfused Co-culture of Rat Hepatocytes and Liver Endothelial Cells

By

Albert J. Hwa

Submitted to the Biological Engineering Division
on January 13, 2006 in Partial Fulfillment of the Requirements
for the Degree of Doctor of Philosophy in Bioengineering

Abstract

Many liver physiological and pathophysiological behaviors are not adequately captured by current *in vitro* hepatocyte culture methods. A 3D perfused microreactor previously demonstrated superior hepatic functional maintenance than conventional 2D cultures, and was hypothesized to provide an environment favorable to endothelial cell maintenance and morphogenesis. This dissertation focuses on characterizing the 3D perfused co-culture of primary hepatocyte fraction with primary rat liver endothelial isolate. Scanning electron microscopy revealed significantly higher numbers of pore-like structures on the co-culture tissue surface resembling liver sinusoids compared to cultures containing only the hepatocytes fraction (mono-culture). EGFP-labeled endothelial cells proliferated moderately and organized into microvessel-like structures as observed by *in situ* multi-photon microscopy. By mixing female endothelial cells with male hepatocytes, the female cell population increased from initially ~7% on day 1 to ~12% on day 13, as determined by quantitative PCR on genomic DNA. The maintenance and morphogenesis of endothelial cells were not observed in parallel 2D collagen gel sandwich cultures. Immunohistochemistry further confirmed the presence of sinusoidal endothelia within the 3D co-culture tissue, as well as other non-parenchymal cells in both 3D mono-culture and co-culture. Global transcriptional profiling confirmed the loss of endothelia in 2D culture as the comparison between mono-culture and co-culture showed substantial differential expression levels only in the 3D format. The majority of the genes expressed substantially higher in 3D co-culture than mono-culture was found to be endothelia-specific. A group of key liver metabolism genes, however, do not show significant expression differences between the 3D cultures. This study concludes that the 3D perfused microreactor maintains non-parenchymal cells better than the 2D format, and the retention of non-parenchymal cells in the primary hepatocyte fraction likely contributes to the maintenance of key hepatic function gene expression. Additional endothelial cells organize into microvessel-like structures in this environment, but exert little influence on the gene expression of most key liver transcription factors and metabolism enzymes. Therefore 3D cultures may eliminate the need of co-cultures for applications focusing on metabolic behaviors of hepatocytes, and 3D endothelial-hepatocyte co-cultures may prove useful in studies where proper endothelium structure is required, such as cancer metastasis.

Thesis Advisor: Linda G. Griffith

Title: Professor of Biological Engineering and Mechanical Engineering

Acknowledgements

I would like to thank my advisor Linda Griffith for giving me the opportunity to work on this topic and allowing me freedom to explore many different directions this project could take. I also want to express my deepest gratitude to Donna Stolz, whose vast knowledge on liver biology and imaging taught me more than I could have imagined. I also want to thank my other committee members Peter So and Roger Kamm for giving me great suggestions and help me step back to look at the overall big picture.

This work could not have been possible without the contribution from so many wonderful people I worked with. I especially want to thank Katy Wack, Joe Moritz, and Anand Sivaraman for helping me break through many research problems. Everyone else in the BPEC lab including Dan Bauer, Emily Larson, Megan Whittemore, Dena Janigan, Laura Vineyard, Mark Powers, Artemis Kalezi, Nate Tedford, Ben Cosgrove, and Karel Domansky provided me with either technical assistance or tremendously helpful discussions.

The folks at University of Pittsburgh made my summer of 2003 such a productive period – a big thank-you to Mark Ross, Fengli Guo, Ana Bursick, Glenn Papworth, Katie O’Callaghan, Bill Bowen and the entire Alan Wells lab. Nicki Watson at Whitehead Institute was the MIT imaging guru for all my experiments, trouble-shooting for my many unusual samples. Every conversation with Nicki was always a pleasure.

One of the most challenging parts of this work was working with the two-photon microscope. Its operation was made much more manageable with the help of Maxine Jonas, Judy Su, Michael Previte, and Siavash Yazdanfar. I want to thank Peter So for being particularly patient with me and giving me constant technical pointers and encouragement.

I could not have imagined ever finishing the microarray experiments without the help of Rebecca Fry, Brad Hogan, Manlin Luo, and Sanchita Bhattacharya. And the central part of my thesis was made possible with Professor Okabe’s permission to use his green rats. I want to thank Glenda Inciong, Bob Marini, Suzan Erdman, and Katie Madden, for helping me with keeping these little fellows.

Working in the lab was not always fun and laughs. I want to thank the friends I made at in the LGG and DAL labs: Anand, Artemis, Joe M., Joe S., Nate, Csani, Megan, Emily, Laura, Dan, Vivian, Kevin, John, Maria, Eileen, Kathryn, Ada, Ajit, and Lily. You guys were the highlights of my life in the lab.

Last but not the least; I want to thank Michael Carney, my parents, and my friends for their unwavering love and support. My sincere gratitude to all of you for encouraging me – I could not have done this without you.

Albert Hwa

Abstract	3
Acknowledgements	4
Chapter 1	9
Introduction and Background	9
1.1 Liver function and structure	9
1.2 Cell types in liver	11
1.2.1 Hepatocyte	12
1.2.2 Sinusoidal Endothelial Cell	12
1.2.3 Kupffer Cell.....	14
1.2.4 Stellate Cell.....	14
1.2.5 Other cells types	15
1.3 State of the art in vitro liver cell co-culture methods.....	15
1.4 3D perfusion microreactor	18
1.5 Shear stress – an important stimulus.....	19
1.6 Liver regeneration.....	20
1.7 Imaging techniques relevant for 3D structures.....	21
1.7.1 Epifluorescence (single-photon fluorescence)	21
1.7.2 Two-photon microscopy	22
1.7.3 Scanning Electron Microscopy (SEM)	22
1.7.4 General histology.....	22
1.8 Hypotheses and specific thesis aims.....	23
Chapter 2	24
Development of the Co-culture Protocol	24
2.1 Introduction and design rationale	24
2.2 Materials and methods.....	25
2.2.1 Isolation of liver endothelial cells.....	25
2.2.2 Approach 1: Seeding hepatocyte spheroids into endothelium-lined channels: Protocol Development of Endothelium-lined Channel Walls	26
2.2.3 Approach 2: Seeding hepatocyte spheroids into scaffold with top surface coated with liver endothelial cells.....	27
2.2.4 Approach 3: Pre-aggregate liver endothelial cells with hepatocytes into spheroids prior to reactor seeding.....	28
2.3 Results.....	29
2.3.1 Primary liver endothelial isolation	29
2.3.2 Approach 1: Coating channel walls with endothelium.....	30

2.3.3 Approach 2: Seeding hepatocyte spheroids into scaffold with top surface covered with liver endothelial cells	31
2.3.4 Approach 3: Pre-aggregate Liver Endothelial Cells with hepatocytes into spheroids prior to reactor seeding.....	34
2.4 Discussion and conclusion	37
Chapter 3.....	40
Testing of Methodologies to Visualize Cell Types and Their Morphology within the 3D	
Microreactor	40
3.1 Introduction	40
3.2 Materials and methods.....	41
3.2.1 Compatibility of AcLDL with the microreactor	41
3.2.2 EGFP-positive Endothelial Cells	41
3.2.2 Visualization of Fluid Space within the 3D Tissue Using Two-photon Microscopy	42
3.2.3 Immunohistochemistry on the Microreactor 3D Tissue.....	43
3.3. Results.....	44
3.3.1 DiI-AcLDL is trapped in reactor filter	44
3.3.2 EGFP labeled liver endothelial cells.....	45
3.3.2 Fluid channel visualization using 2-photon microscopy	47
3.3.3 Immunohistochemistry on liver tissue embedded in Technovit8100.....	48
3.4 Discussion and conclusion	50
Chapter 4.....	53
Morphological Study on 3D Microperfused Co-cultures of Rat Hepatocytes and Liver	
Endothelial Cells	53
4.1 Introduction	53
4.2 Materials and methods.....	54
4.2.1 Culture media	54
4.2.2 Cell isolation.....	54
4.2.3 Microreactor seeding and maintenance	55
4.2.4 2D collagen gel sandwich.....	55
4.2.5 SEM and image analysis.....	56
4.2.6 <i>In situ</i> two-photon microscopy and image analysis	56
4.2.7 RNA and DNA isolation	57
4.2.8 Quantification of EGFP cell percentages in co-cultures.....	57
4.2.9 Immunohistochemistry.....	58
4.3 Results.....	58
4.3.1 Co-culture with endothelium alters tissue surface morphology.....	58
4.3.2 The endothelial cell fraction proliferates and forms 3D networks in 3D perfusion culture, but is lost in 2D culture.....	60
4.3.3 Quantification of EGFP-positive population	66
4.3.4 Immunohistochemical identification of endothelial cells in microreactor culture.....	68

4.4 Discussion.....	69
Chapter 5.....	73
Effects of rat liver endothelia on Gene Expression in 3D Perfusion Hepatocyte Co-culture 73	
5.1 Introduction	73
5.2 Materials and Methods	74
5.2.1 Cell Isolation and Culture	74
5.2.2 Microreactor seeding and maintenance	75
5.2.3 2D Collagen Gel Sandwich (CGS)	75
5.2.4 RNA Isolation	76
5.2.5 Immunohistochemistry.....	76
5.2.6 Global Transcriptional Profiling and Analysis of Expression Data.....	76
5.3 Results.....	77
5.3.1 Immunohistochemical Identification of Non-Parenchymal Cells in Microreactor Culture	77
5.3.2 Endothelial Cells Contribute to Gene Expression in 3D Cultures but not in 2D Cultures	81
5.3.3 Most Genes with Higher Expression Levels in 3D Co-culture than Mono-culture are Endothelia-associated Genes.....	83
5.3.4 Liver-Enriched Metabolism Gene Expression is Preferentially Maintained in 3D Regardless of Endothelial Cell Addition	87
5.4 Discussion.....	91
Chapter 6.....	94
Gene Expression Profile Comparison to Liver Regeneration and Stellate Cell-specific Gene Sets.....	94
6.1 Introduction	94
6.2 Materials and Methods	95
6.3 Results.....	96
6.4 Discussion and Conclusion.....	101
Chapter 7.....	105
Conclusions and Future Recommendations.....	105
7.1 Summary and Conclusions	105
7.2 Future Recommendations.....	106
References.....	108
Appendix 1 - Isolation and Viability Test of Primary Liver Endothelial Cells	123

Appendix 2 - HGM formulation.....	125
Appendix 3 - Protocol for Assembling Milli-F Reactors.....	127
Appendix 4 - Co-culture spheroid formation and bioreactor seeding protocol.....	131
Appendix 5 - Bioreactor cross-flow reversal, medium change protocol.....	133
Appendix 6 - Sample Preparation for Scanning Electron Microscopy	134
Appendix 7 - Protocol for RNA isolation from samples in Trizol	136
Appendix 8 - Protocol for DNA Isolation from Samples in Trizol	138
Appendix 9 - Protocol for Tissue Cryosectioning and Immunostaining.....	139
Appendix 10 - Embedding tissue samples in Technovit8100 and immunohistochemistry...141	
Appendix 11 - Notes on maintaining EGFP rat colonies.....	144
Appendix 12 – Collagen Gel Sandwich Preparation.....	145

Chapter 1

Introduction and Background

1.1 Liver function and structure

Liver carries out a multitude of functions besides metabolizing drugs and toxins. It synthesizes urea, removes metabolic wastes, and produces proteins, lipids, cholesterol, and carbohydrates. It also serves as an important storage for iron, copper, glycogen, fat-soluble vitamins (A, D, E, and K), and blood. These functions are made possible by the complex interactions between the blood flow and the cells of the liver, facilitated by the intricate architecture of the parenchyma and its cell arrangement [1].

Liver is a highly vascularized organ with a complex structure. Two models of liver organization exist: the lobule and the acinus [1]. In Kiernan's lobule model [2], the cells are arranged in hexagonal repeated patterns, with three corners occupied by the portal triads (composed of bile duct, hepatic artery, and portal vein) and the central vein in the center (Figure 1.1A). Oxygenated blood from the heart is introduced through hepatic artery, and enriched blood from digestive tracts flow through portal vein. All the blood flows through the tissue and drains into central veins. Bile duct drains bile from individual small bile ducts in opposite direction of blood flow.

In Rappaport's acinar model (Figure 1.2B), he noted that as blood travels through the liver capillaries, called sinusoids, the oxygen content and dissolved solutes are continuously being modified by the neighboring cells. Therefore the cells at different distances away from central vein should be considered heterogeneous. The acinus is divided into three zones characterized by the depleted oxygen and metabolite levels in the red blood cells as they flow along the length of a sinusoid [3].

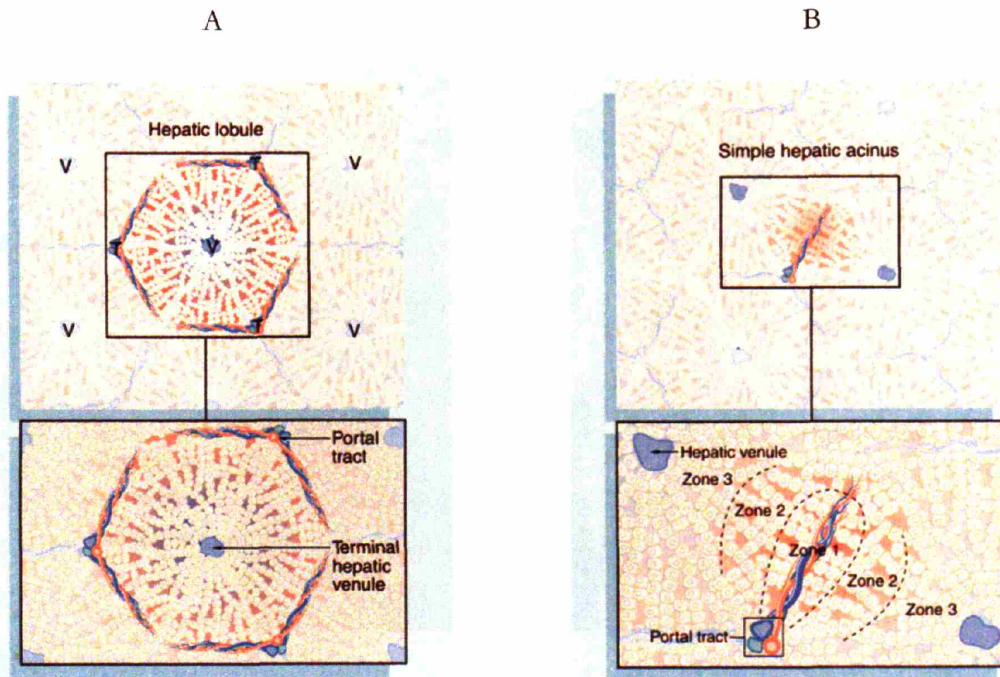
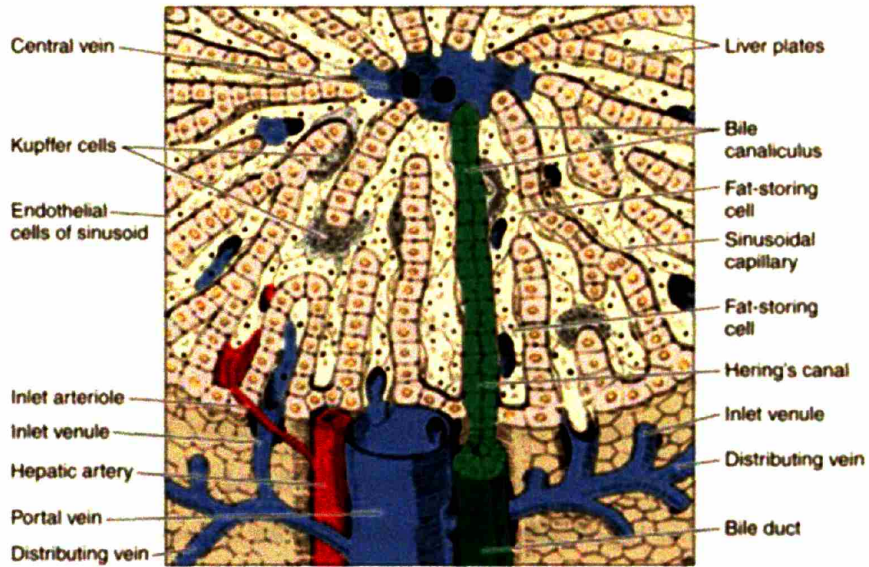


Figure 1.1: Two views on basic liver structural unit: (A) Kiernan's Lobule model and (B) Rappaport's acinar model.

Images taken from Wheater's Functional Histology: A Text and Colour Atlas

At the cellular level, the organization is equally intricate. This complexity may be required to achieve proper liver function. The main cell type in liver, hepatocytes, are arranged into plates of single cell thickness, known as the parenchyma. Cell plates extend from the portal triads to the central veins, and they are separated by sinusoids (Figure 1.2A). Within the parenchyma, hepatocytes have three cell domains: the apical domain forms bile canalicular networks involved in secretion of bile components and metabolites of xenobiotics; the basal domain faces the ECM-rich region (Space of Disse) and is involved in cell signaling; the lateral domain forms tight junctions with neighboring hepatocytes. Sinusoids are lined with sinusoidal endothelial cells (SEC), which contain fenestrations that allow passage of small solutes into the Space of Disse [4]. Kupffer cells, the resident macrophages in liver, interact with SEC's within the sinusoid. Fibroblast-like cells in the liver, called stellate cells, are distributed within the Space of Disse, forming cell-cell contacts with SEC's and hepatocytes.

A



B

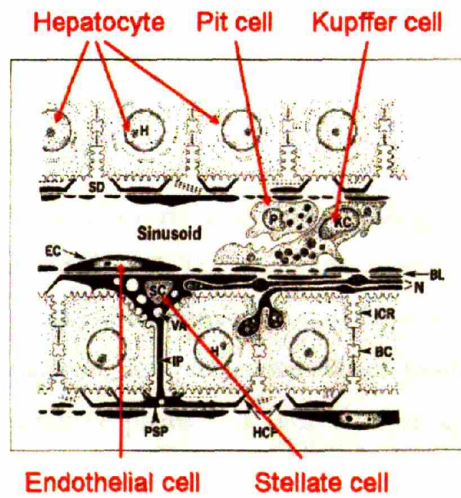


Figure 1.2: Cell arrangement in Liver. (A) A closer look at a lobule. (B) A cross-section of a sinusoid.

Image A taken from Junqueira and Carneiro, *Basic Histology, a text and atlas* [5]. Image B adapted from Wake et al. [6].

1.2 Cell types in liver

1.2.1 Hepatocyte

Hepatocytes are the main cell type in the liver, constituting 60-65% of total cells by number and ~80% by volume [1]. They are a highly differentiated epithelial cell type. Most major liver functions are carried out by hepatocytes, including: detoxification of blood; secretion of plasma proteins, growth factors, and bile; metabolism of proteins, fat, and steroids; and storage of vitamin, iron, and glycogen [7, 8].

The differentiated functions of hepatocytes are notoriously hard to maintain for an extended period of time *in vitro*, mainly due to the multitude of environmental cues *in vivo* that are not recapitulated *in vitro*. These include direct heterotypic and homotypic cell-cell interactions, soluble factors, cell-ECM interactions, and mechanical stress signals. Hence a variety of different culturing methods have been developed to address these issues. Collagen-gel sandwich (to address cell-matrix interactions and cell cytoskeletal structures), medium formulation (to address soluble signals), and co-culturing with non-parenchymal cells (to address heterotypic cell-cell interactions) have all been shown to enhance and maintain some hepatic features for a period of time [8-10].

1.2.2 Sinusoidal Endothelial Cell

Liver sinusoidal endothelial cells form a continuous lining on the sinusoidal wall as a barrier between the parenchyma and blood [11-13]. They compose about 19-21% of all liver cells [1]. Their morphology is marked by broad cytoplasmic extensions with numerous tiny pores called fenestrations. These fenestrations, with an average diameter of 160nm, are clustered in groups of 10 to 50, commonly referred to as sieve plates [12]. The number and size of fenestrations vary in different zonations and can change in response to a variety of hormones, drugs, toxins, diseases, and underlying ECM [12]. Liver sinusoidal endothelium also differs from endothelium in other parts of the body in the lack of basal lamina underneath the cells [1].

The major function of sinusoidal endothelium is thought to be a selective barrier determining passage of macromolecules in and out of the Space of Disse and their contact with hepatocytes and stellate cells. This selection is partly determined by the dynamic size of fenestrae on endothelial surface [4].

Sinusoidal endothelial cells are also considered as a scavenger cell type [14]. They possess a number of receptors involved in receptor-mediated endocytosis. These include the scavenger receptor (which binds denatured proteins), hyaluronan receptor, mannose receptor, and Fc receptor (which recognizes the Fc domain of immunoglobulin G) [14]. A common endothelial marker, acetylated low density lipoprotein (AcLDL), is specifically taken up by the scavenger receptor [15]. Through endocytosis using the hyaluronan receptor, liver sinusoidal endothelial cells are considered to be the major site of clearance of hyaluronic acid [16, 17]. Sinusoidal endothelial cells are also able to transport macromolecules from blood to Space of Disse through receptor-mediated transcytosis [15]. Therefore sinusoidal endothelium is a selective barrier between blood and the parenchyma through discriminations against sizes and binding properties of macromolecules.

Long-term *in vitro* culture of sinusoidal endothelial cells has been difficult to maintain. These cells do not have very high plating efficiency [18]. In the absence of vascular endothelial growth factor (VEGF) they quickly undergo apoptosis (<12 hours), which may be delayed by adding glycine to the medium [19, 20]. Molecules such as dexamethasone, heparin, and insulin can be added to culture medium to improve cell survival [21]. VEGF has been reported to induce their DNA synthesis and proliferation [19, 22]. Serum-free hepatocyte-conditioned medium can improve the survival of these cells in culture for 5-6 days, but it also stimulated overgrowth of stellate cells after one week [18]. Indeed a paracrine relationship between hepatocytes and sinusoidal endothelial cells has been found such that hepatocyte-made VEGF induces sinusoidal endothelial cells to secrete hepatocyte growth factor (HGF) as a survival factor for the parenchyma [23]. These reports suggest that endothelial cells and hepatocytes share an intimate relationship in organ maintenance and protection during injury [24], and co-culturing with hepatocytes may mimic *in vivo* environmental cues to help maintain sinusoidal endothelial cell survival and functions.

Many typical endothelial cell markers are not applicable to sinusoidal endothelial cells. Up until recently, there has been a disagreement on whether platelet-endothelial cell adhesion molecule (PECAM, or CD31) is expressed on sinusoidal endothelial cells. PECAM is present at cell-cell junctions on most endothelium, but its presence on liver endothelium is controversial [25-28]. Deleve et al. reported that surface expression of PECAM on sinusoidal endothelial cells is a de-differentiation marker, and normally it is expressed intracellularly [29]. Appearance of PECAM on cell surface seemed to coincide with the disappearance of fenestrations. On large-vessel endothelium,

however, PECAM is always strongly expressed. An antibody specific for rat sinusoidal endothelial cell, SE-1, was discovered in 1993 [30]. SE-1 only targets the sinusoids, sparing the large-vessel endothelium. To date the functional aspect of the antigen targeted by SE-1 is still not clear, but highly pure primary sinusoidal endothelial cells can be isolated using this antibody [31]. It is possible that the antigen may be involved with the differentiated state of sinusoidal endothelial cells. As stated earlier, another endothelial marker, AcLDL, can be taken up by sinusoidal endothelium through its scavenger receptor-mediated endocytosis. This mechanism, however, is not exclusive to sinusoidal endothelial cells – Kupffer cells and large-vessel endothelium can also take up AcLDL. Overall, the differentiated state of sinusoidal endothelium should be marked by presence of fenestrations, positive staining of SE-1, and absence of surface expression of PECAM.

1.2.3 Kupffer Cell

Kupffer cells are the resident macrophages in the liver and account for more than 50% of all macrophages in the body and about 8-12% of all liver cells [32, 33]. They are situated within the sinusoids, forming cellular extensions over the endothelial lining. Their extensions sometimes reach through the endothelial fenestrations and into the parenchyma [1]. Their population is heterogeneously distributed though they preferentially localize to the periportal region, a strategic location for monitoring the blood flow into the liver. Kupffer cells at different regions also differ in their size and expression of enzymes, receptors, and subcellular structures [34]. As a major immune defense cell type to preserve homeostasis, their main function is to remove foreign materials from portal blood. Through endocytosis, phagocytosis, and production of cytokines, Kupffer cells remove a variety of substances from blood, such as bacterial components, endotoxins, and immune complexes [1]. Kupffer cells can be identified by macrophage markers ED1 and ED2 [34].

1.2.4 Stellate Cell

Stellate cells are also called fat-storing cells, Ito cells, or lipocytes. They are located in the Space of Disse, and have important functions including: retinoid storage and homeostasis; remodeling of extracellular matrix; production of growth factors and cytokines; and contraction and dilation of the sinusoidal lumen in response to endothelin, angiotensin, thromboxane, or prostaglandins [35]. They comprise about 5-8% of all liver cells [36]. The stellate cell population can

be broadly separated into two phenotypes. In healthy liver, their quiescent phenotype is marked by large lipid droplets and expression of moderate amounts of cytoskeleton elements. Classic markers of stellate cells include desmin, glial fibrillary acidic protein (GFAP), and vimentin. In chronically diseased liver, they take on an activated phenotype. They proliferate rapidly with features of myofibroblasts, extensive expression of microtubules, intermediate filaments, and bundles of actin filaments. These changes are usually accompanied by synthesis of basal lamina-like material and collagen fibers and loss of lipid droplets [1]. Smooth muscle actin (α -SMA) is a standard marker for activated stellate cells.

1.2.5 Other cells types

Other cells include pit cells and bile duct epithelial cells (cholangiocytes). Cholangiocytes constitute by number ~3-5% of all liver cells, forming the lining of bile ducts, which are responsible for draining bile from the parenchyma and delivering it to the intestine [1]. They participate in secretory and absorptive activities during the formation of bile [1]. They can also proliferate and reconstitute injured parenchyma under specific conditions [37]. Cholangiocytes are also found to interact with the immune system and microorganisms [38, 39]. Pit cells are natural killer cells residing in the sinusoids. They display defensive mechanisms against viral infections and tumor metastasis [40].

1.3 State of the art *in vitro* liver cell co-culture methods

When hepatocytes are isolated from the liver and cultured under conventional 2D culture conditions, many liver-specific functions (protein synthesis, xenobiotic metabolism, cytochrome P450 activity) are lost rapidly [8]. The progress in understanding the factors that contribute to hepatocyte phenotype has led to development of various culturing techniques with the goal of maintaining liver-specific functions *in vitro*. The following factors are considered important for maintaining liver-specific structure and function *in vitro*: extracellular matrix environment, medium formulation/soluble factors, cell-cell interactions, and maintenance of cell shape and tissue organization [8, 10].

Among many approaches to reestablish hepatocyte functions *in vitro*, co-culturing hepatocytes with other cell types has been found to help maintain cell morphology and metabolic activities. First shown by Guguen-Guillouzo et al., co-culturing hepatocytes with liver-derived epithelial cells on a petri dish resulted in maintenance of high albumin secretion rates and long-term survival of hepatocytes [41]. This is not very surprising in light of the liver biology: hepatocytes in their native environment are in constant communication with their surroundings, including direct contact with neighboring hepatocytes and close association with other sinusoidal cells, as well as soluble factors and ECM secreted by sinusoidal cells. Many *in vitro* methods through the use of porous membranes, conditioned medium, coverslips in wells, and seeding density have tried to separate the effects exerted by ECM, soluble factors, and cell-cell contact. None was able to systematically vary the degree of heterotypic cell interaction, but only proved that a complete lack of such interaction does not support differentiated hepatocyte functions. (For a review, see [9, 42]) To truly control the degree of cell-cell contact, surfaces that are patterned through the use of photolithography [43], elastomeric stamping [44], or temperature-sensitive polymer surfaces [45] that foster attachment of different cell types in specific regions are useful. These experiments demonstrated that higher degrees of heterotypic cell interaction better preserves differentiated hepatocyte functions. These static 2D culture formats, however, lack dynamic fluid flow and also are limited in terms of their potential for cells to form 3D *in vivo* structures [9, 43, 46-67].

Other co-culturing methods developed sought to include flow conditions and/or construct three-dimensional structures. Several 2D constructs were implemented with various flow systems, showing better maintenance of hepatic functions [68-72]. Three-dimensional spheroidal structures produced either by culturing hepatocytes on poorly-adhesive surfaces or in spinner flasks were found to maintain hepatocyte viability and functions [73, 74]. Packed-bed and hollow-fiber bioreactors were developed as bioartificial liver systems for clinical use, in which anchored single hepatocytes or hepatocyte spheroids were used to support patient metabolism [75]. Gerlach et al. furthered the hollow-fiber reactor concept and developed a woven capillary reactor where hepatocytes are strategically located, and metabolite and gas exchanges occur through different capillaries [76, 77]. A similar compartmentalized reactor system was created with layers of hepatocytes in collagen gel sandwiches separated and anchored by membranes, which provide medium and gas exchanges [68]. Other culturing methods include roller bottle cultures without carrier beads and with beads followed by implantation in Matrigel [78, 79] and using polymer

scaffolds with or without flow conditions [47, 80-83]. These methods produced more *in vivo*-like structures, but the complexity also made it difficult to control seeding parameters in the case of co-culture. Gerlach et al. mentioned co-culturing of SEC's and hepatocytes in the woven capillary reactors, but no details of co-culture seeding method were described [84]. Bader et al. attempted to reproduce the spatial arrangement in sinusoids by placing NPC's on top of the sandwiched hepatocyte layer [46]. This system was not implemented with medium flow, however, and it remained as a flat culture without any true 3D structure formations. Pollock et al. reported that sinusoidal endothelial cells are located on the outer lining of their co-culture spheroids, but no definitive sinusoidal endothelial markers or resemblance to *in vivo* liver structures were demonstrated [47]. Michalopoulos et al. described structures of plates and ducts and an Factor VIII+ endothelium lining in cultures formed on beads followed by implantation in Matrigel [78]. Another report of their cultures without the addition of beads or Matrigel was stained positive for ICAM-1, another pan-endothelium marker [79]. These reports demonstrated that the roller bottle culture format encourages formation of endothelium at the tissue-fluid interface, but whether these *in vitro* structures represent physiologically relevant sinusoidal endothelium is unknown because the definitive markers were not shown (SE-1 or fenestrations).

Overall, there were few systematic and quantitative attempts taken to study the morphological outcome of co-culture in these culturing techniques. Often the need to anchor cells prevents further 3D tissue morphogenesis, as in the case of Bader's design. Different cell populations used and differences in ECM and growth factors in the medium further complicate comparison between each culturing method and make it difficult to interpret results.

Furthermore, it is important to remember the interdependencies among liver cell types. While a large part of liver research has focused on hepatic metabolism functions, many liver physiological and pathological behaviors are the results of cooperation among all liver cells: changes in underlying ECM alter sinusoidal endothelial phenotype; loss of fenestrations and capillarization of sinusoidal endothelium can lead to abnormal exchange of macromolecules between blood and the parenchyma; certain cytokines secreted by Kupffer cells can activate stellate cells or cause injuries on endothelial cells and hepatocytes; activated stellate cells secrete many ECM molecules not found in normal liver and participate in the capillarization of sinusoids. It is therefore necessary to construct an *in vitro* liver cell co-culture that not only affords differentiated hepatocyte functions, but also

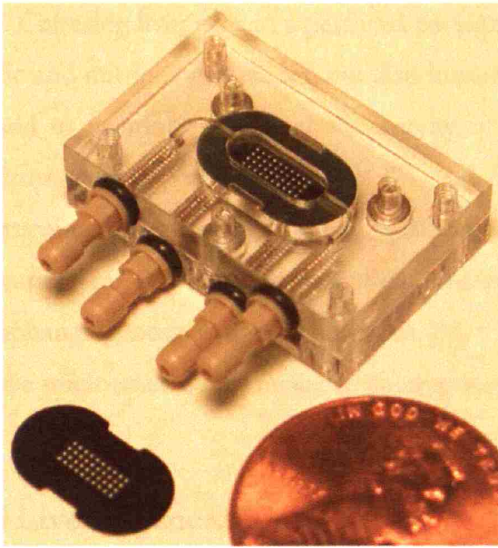
maintains physiological non-parenchymal cell presentation. Such a model will be immensely helpful in studying various liver physiological and pathophysiological behaviors.

1.4 3D perfusion microreactor

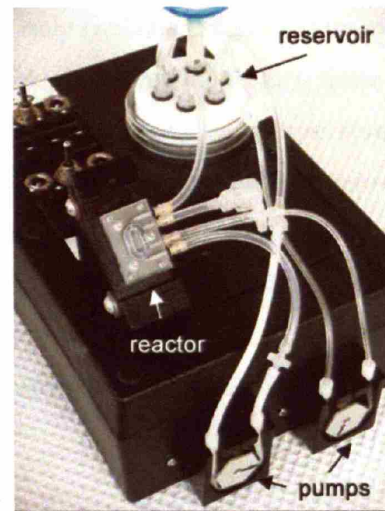
None of the current culture methods has shown robust capability for hepatitis viral replication, tumor metastasis, and other important physiological and pathophysiological liver behaviors. Hierarchical tissue structures and consequent intrinsic mechanisms of ECM and growth factor signaling may be essential to reproduce these complex liver functions *in vitro*. For example, solutes in blood normally need to pass through the endothelium before they contact parenchymal cells, and only particles smaller than fenestrations on SEC's are allowed to freely enter the space of Disse [12]. However, various stimuli such as shear stress, soluble substances, and ECM have been shown to influence fenestration size, which is thought to regulate the extraction rate of dietary cholesterol in liver [4]; cancer cells metastasizing to form liver tumors have to extravasate through the endothelium before taking residence in the parenchyma [85]. Both of these phenomena would require a proper sinusoidal cell arrangement to take place.

To address the various factors that influence hepatocyte culture, namely cell-cell interaction, cell-ECM interaction, and medium flow, a 3D perfused microreactor was developed (Figure 1.3A) [86]. The microreactor contains a silicon scaffold with an array of channels with cell-adhesive walls. Cells or cell aggregates are seeded into these channels while re-circulating medium flows across the top of the scaffold and through the channels. The physical setup of the reactor with peristaltic pumps is shown in Figure 1.3B, and the cross-sectional view of the reactor is shown in Figure 1.3C. The microreactor facilitates evolution of tissue-like morphological structures [86]. Functional studies have shown that albumin secretion and ureagenesis rates can be maintained for at least two weeks when these microreactors were seeded with pre-aggregated hepatocytes [10, 87, 88]. The microreactor culture format was also able to maintain the gene expressions of important liver transcription factors and metabolic enzymes better than 2D collagen gel sandwich cultures [10].

A



B



C

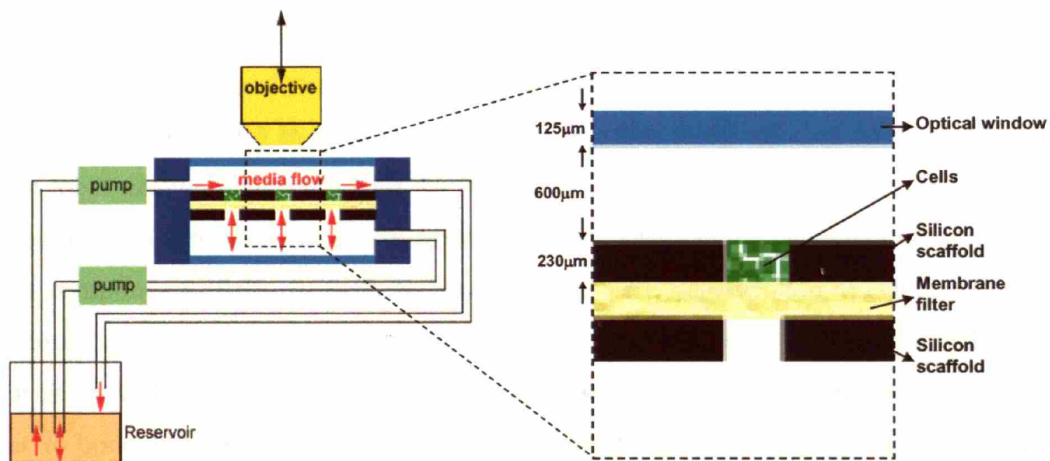


Figure 1.3: (A) A close-up picture of an assembled microreactor; (B) A reactor with complete fluidics and peristaltic pumps; (C) A schematic drawing of the cross-sectional view of the reactor.

1.5 Shear stress – an important stimulus

Effects of shear stress and mechanical strain may play big roles in liver biology, but quantitative studies on these effects have been scarce. Endothelial cells in sinusoids are subjected to varied mechanical stresses induced by blood flow. Many reports described how mechanical forces influence phenotypes of smooth muscle cells and vascular endothelial cells of human aortic or umbilical vein origin. It has been proposed that intracellular signaling events are generated when

mechanical forces are sensed by membrane proteins, ion channels, cytoskeleton, integrins, etc. [89-91]. Culturing liver cells in a perfused environment will not only facilitate effective mass exchange of toxic and nutrient substances, but also introduce this physiological stimulus. In fact, shear stress was found to promote the metabolic activity of hepatocytes in a monolayer co-culture system with a mixture of non-parenchymal cells [71, 92]. It was also found that endothelial cells (possibly from contamination during hepatocyte isolation) may have migrated to the tissue-fluid interface during culturing in the microreactor [93]. Interstitial flow also was found to be a stimulus for lymphangiogenesis and vasculogenesis [94, 95]. These findings suggest that a flow environment such as the microreactor may facilitate the migration and self-organization of endothelial cells.

1.6 Liver regeneration

Liver has the amazing capability to regulate its size and growth. Extensive functional deficits created by loss of tissue elicit proliferative processes that eventually restore liver function and architecture [96, 97]. The commonly accepted experimental model for studying liver regeneration is partial hepatectomy (PHx) in which lobes comprising two thirds of a rat liver are removed. The residual lobes enlarge to make up for the lost mass within five to seven days [1]. This process is achieved only when there is precise coordination among hepatocytes, various non-parenchymal cells, and the components of the extracellular matrix (ECM) [96]. Regeneration of cell populations within the remnant liver initiates with hepatocytes between 24 to 48 hours, followed by biliary epithelial cells at 36 to 48 hours, Kupffer and stellate cells at 48 hours, and finally the sinusoidal endothelial cells at 96 hours [97]. At 72 hours after PHx, hepatocytes have proliferated from original cell plates into avascularized clusters of 10 to 12 hepatocytes. Stellate cells then extend their processes into these clusters and secrete ECM. Surrounding sinusoidal endothelial cells follow and infiltrate into these avascularized islands and proliferate, eventually restore the normal cell plate architecture (Figure 1.4). Precise coordination of growth factor secretion, regulation of cell surface receptors, and ECM modification orchestrate the proliferation, migration, and functional patterns of these cells [22, 98-100]. The liver regeneration process shows that, given correct signals, liver cells have the capability to proliferate and recreate the original tissue architecture. The liver regeneration phenomenon inspired several designs of co-culture protocols in this thesis.

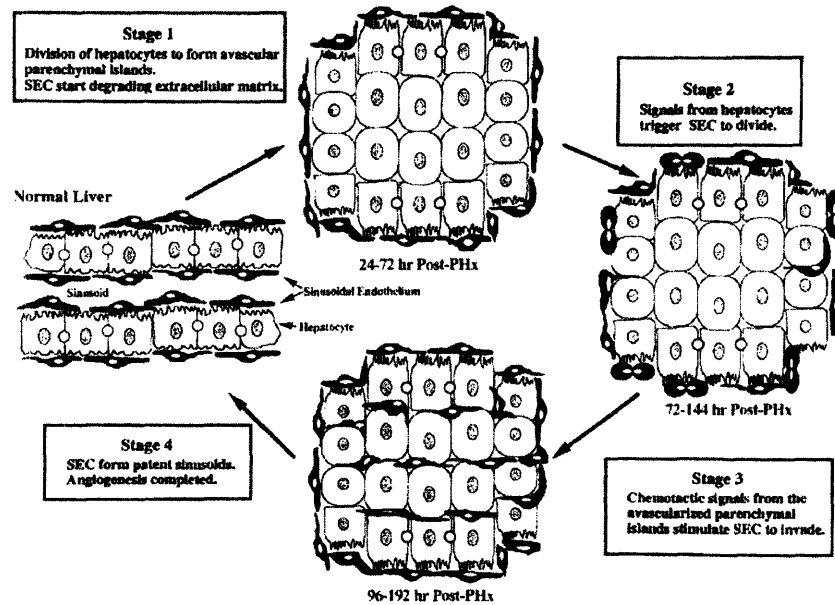


Figure 1.4: Sequential events during liver regeneration. *Image reprinted from Ross et al. [22]*

1.7 Imaging techniques relevant for 3D structures

This thesis aims to visualize and quantify specific cells within 3D tissue. Below is a brief review on various imaging techniques used in this project:

1.7.1 Epifluorescence (single-photon fluorescence)

This is the most common fluorescence microscopy. The light source in the UV range comes from a mercury arc lamp at a power output of around 100W. The excitation light goes through an optical filter to hit the sample at a certain wavelength, and the emission light goes through another filter to be captured at another wavelength. This method can be broadly applied to most two-dimensional samples. Samples labeled with different fluorescent markers can be easily viewed by changing the filter sets. Three-dimensional objects cannot be clearly viewed with this method. The excitation light is uniform regardless of the focal plane, causing high noise-to-signal ratio because emission signals can come from all planes above and below the focal plane. Also long exposure of

the sample to the excitation light may cause photobleaching – a term used to describe fading or loss of fluorescence due to photon-induced chemical damage and covalent modification.

1.7.2 Two-photon microscopy

Two-photon microscopy was invented by Denk et al. in 1990 to facilitate imaging 3D objects [101, 102]. A fluorophore is excited simultaneously by two photons to a higher energy state, and returns to its normal state while emitting a photon in the observable wavelength. The low-energy photons are in the infrared range, providing better depth penetration into 3D objects due to its reduced scattering and absorption. The excitation laser beam only excites a very small volume around the focal point (about one femtoliter) and its intensity exponentially decreases with distance away from it. This feature reduces photobleaching and photodamaging to the specimen, and provides high signal-to-noise ratio. A possible side effect of two-photon microscopy is sample overheating from the infrared light.

1.7.3 Scanning Electron Microscopy (SEM)

Fine structures on sample surfaces can be viewed under SEM. A beam of electrons scans across the sample surface in a vacuum, and the secondary electrons that bounce off the sample are detected and converted to photons. These signals are correlated with the scanning positions to generate a topographical image of the sample. Only the top surface of the sample can be viewed with SEM. Therefore the interior of a sample must be exposed prior to observation. Samples need to be processed to preserve their surface features and to enhance contrast under SEM. Therefore it is generally not applicable to live samples.

1.7.4 General histology

Tissue samples can be fixed, dehydrated, processed, and embedded within paraffin, plastic, or resin, to indefinitely preserve their structures. Three-dimensional samples can be cut into 2-dimensional sections that allow staining and observation. Cell components are generally colorless. Various stains such as H&E and Toluidine Blue stain different components to provide contrast and allow identification of tissue organization and pathological states to trained eyes. Immunostaining is

often not applicable to many embedding materials because they are hydrophobic and antibodies do not have access to antigens. Choosing hydrophilic embedding materials and careful sample processing that preserves antigen reactivity are essential to successful immunohistochemistry [103].

1.8 Hypotheses and specific thesis aims

This thesis is born out of the following hypotheses: 1. the microreactor provides a better environment than conventional 2D culture formats for maintaining the survival of non-parenchymal cells, particularly endothelial cells. 2. This culture format with perfusion flow may be conducive to formation of blood vessels. 3. Addition of non-parenchymal cells to the hepatocyte culture in the microreactor may enhance hepatic functions.

The specific aims of this thesis are:

1. To develop a quantitative protocol of establishing a co-culture of hepatocytes and liver endothelial cells while addressing the starting cell populations and viabilities.
2. To define and implement appropriate imaging tools for visualization of the additional endothelial cells in the microreactor and to quantify the morphological outcome.
3. To quantify the additional endothelial cell population.
4. To determine the difference in functional behavior between mono-culture and co-culture in the microreactor as well as in the conventional 2D culture format.

Chapter 2

Development of the Co-culture Protocol

2.1 Introduction and design rationale

The goal of this co-culture protocol is to produce a starting cell population in reactors containing mixtures of hepatocytes and endothelial cells. Furthermore, the viability and cell population from primary endothelial cell isolations should be quantitatively defined.

Liver endothelial cells do not have direct cell-cell contact with hepatocytes *in vivo*. They are associated with each other through ECM interactions in the Space of Disse. During liver regeneration, they first surround avascularized hepatocyte islands and then invade them to reform the sinusoid structures [22, 96, 97]. Previous reports on co-cultures of hepatocytes and human umbilical vein endothelial cells also reported that endothelial cells can migrate and self-organize into structures in response to environmental cues [104]. In culture systems with flow conditions, endothelial cells or non-parenchymal cells were also observed to self-organize into layers at the tissue-fluid interface [47, 71, 78, 79]. These observations suggested that given an appropriate environment, endothelial cells may secrete their own ECM and self-organize with hepatocytes into structures resembling *in vivo* sinusoids. Three approaches were selected based on this philosophy and are illustrated in Figure 2.1. The first approach cultures both cell types in a spinner flask, a conventional method to produce hepatocyte spheroids [73]. The second approach aims to coat channel walls with endothelium so that the relative locations of hepatocytes and endothelial cells resemble those seen in liver regeneration. The third approach is a variation on approach 2 by changing the initial location of endothelial cells. This chapter examines the effectiveness of these approaches in encouraging heterotypic interactions between hepatocytes and endothelial cells.

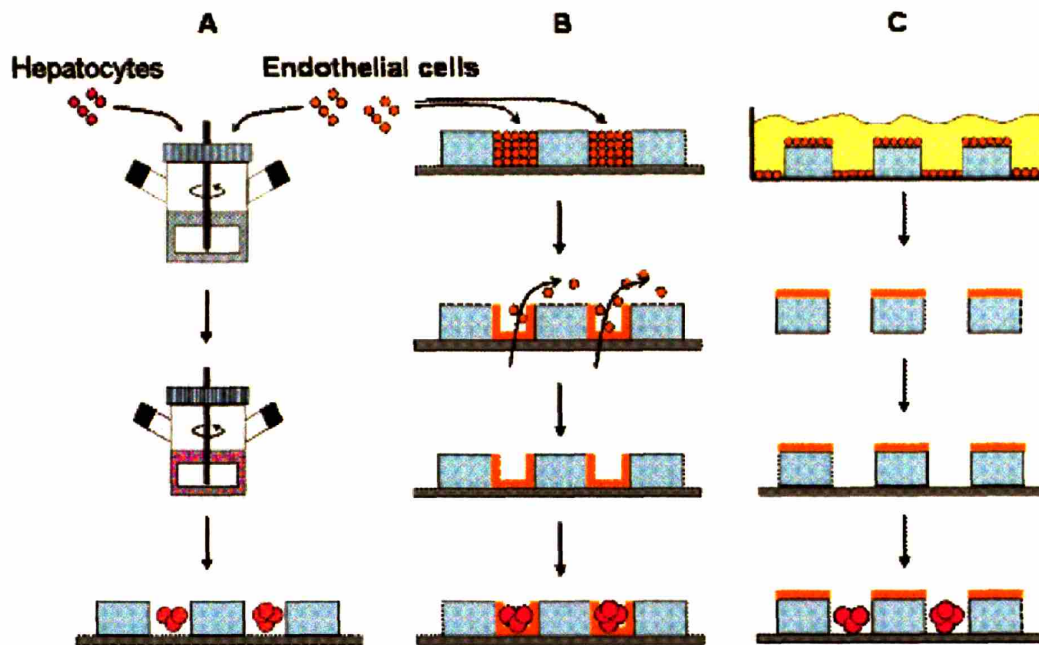


Figure 2.1: Three approaches to foster endothelial-hepatocyte interaction: (A) endothelial cells and hepatocyte are grown into spheroids in a spinner flask before being seeded into reactors. (B) Endothelial cells are grown into monolayers onto channel walls in the scaffold prior to seeding of spheroids made with enriched hepatocyte fraction. (C) Endothelial cells are grown into monolayers on the top surface of scaffolds before reactor assembly. Hepatocyte spheroids are then introduced.

2.2 Materials and methods

2.2.1 Isolation of liver endothelial cells

Cells were isolated from male Fischer rats within the 150g-250g range using a modification of Seglen's two-step collagenase perfusion procedure [10]. Enriched hepatocytes were obtained after repeated 50g centrifugation and washing cycles. Endothelial cells were isolated using a modified version of the two-step Percoll density gradient [105]. The supernatant from the 50g spins was subjected to a 5-minute 100g spin to remove small hepatocytes. Cells in the remaining supernatant were collected into pellets with 7 minutes of 350g spin. After re-suspending the cells in PBS (Gibco), the cell solution was loaded on top of a two-step Percoll density gradient in a 50ml conical tube. The top layer of Percoll (Sigma-Adrich), 25% in PBS, was placed in the tube first. The bottom layer, 50%

Percoll in PBS, was carefully and slowly loaded underneath the 25% layer. The tubes containing three layers of solutions were subjected to 20 minutes of 900g spin with the lowest acceleration and brake settings. Due to their specific density, endothelial cells were captured at the interface. A volume of 10 mL around the interface was collected, diluted 1:1 with PBS, and subjected to 10 minutes of 900g spin. The resultant pellet contained non-parenchymal cells highly enriched in liver endothelial cells. Previous studies by Brent Schreiber determined this isolation procedure produced 87% endothelial, 10% Kupffer, and 3% Stellate cells, averaged over 6 biological replicates [106]. The viability and concentration of primary endothelial cells isolations were determined by Hoechst (Molecular Probes) and Sytox Orange (Molecular Probes) staining, because the small cell size was not compatible with conventional Trypan blue exclusion test. Hoechst stained all nuclei, while Sytox Orange stained nuclei of only cells with compromised membrane. Cells were viewed on a hemacytometer with epifluorescence through the DAPI filter. Blue nuclei were deemed live and orange ones dead. The viability was consistently above 90%. (For detailed isolation protocol, see Appendix 1)

Sterilized coverslips (No.1 10mm, VWR) were coated with 30 mg/mL collagen (Cohesion) in PBS (Gibco) for 2hr at 37°C and allowed to dry at room temperature for 1hr after collagen solution was removed. Endothelial cells were seeded at 1 million cells/mL and 300 µl/well on collagen-coated glass coverslips in 24-well plates (Falcon) in EGM-2 (Cambrex). Cells were allowed to attach to the coverslips for 4 hours before they were washed in PBS and fixed in 2% paraformaldehyde (EMS) for 20 min. Each coverslip was stained with primary antibodies SE-1 (IBL America) or anti-CD31 (Chemicon), followed by secondary antibody goat-anti-mouse Cy3 (Jackson ImmunoResearch) and Hoechst nuclei stain (Molecular Probes). Two biological replicates and at least 6 images per replicate per group were used to quantify the percentage of SE-1+ and CD31+ cells. Images were imported into Metamorph (Universal Imaging) for quantitation.

2.2.2 Approach 1: Seeding hepatocyte spheroids into endothelium-lined channels: Protocol Development of Endothelium-lined Channel Walls

Because of the time-consuming and expensive nature of isolating primary liver endothelial cells, initial testing of protocols was carried out with primary rat lung microvessel endothelial cells (RLMVECs, VEC Technologies, Inc., Rensselaer, NY). Microreactors were assembled according to

standard protocol (Appendix 3) and primed with MCDB-131 Complete medium (VEC Technologies) for an hour at 37°C before cell seeding using a syringe filled with 1mL medium with 1×10^6 RLMVEC/mL. Typically only ~0.5 mL of cell solution was seeded due to blockage of flow from too many cells. The reactors were operated at 37°C and 5% CO₂ with or without 0.5 ml/min axial flow and 40 µl/min cross flow for 24 hours. Reactors were disassembled and the scaffolds were incubated in the Cell Viability Kit (Molecular Probes, Carlsbad, CA) according to manufacturer's instructions. Under epifluorescence live cells expressed green cytoplasm (Calcein AM, $\lambda_{ex}/\lambda_{em}=495/515\text{nm}$) and dead cells appeared with red nuclei (EthD-1, $\lambda_{ex}/\lambda_{em}=495/635\text{nm}$). Following epifluorescence observation, the scaffolds were fixed in 2.5% Glutaraldehyde (EMS) in PBS for 20 min at room temperature and processed for SEM observation. (See Appendix 6 for standard SEM protocol) Samples were viewed under a JEOL JSM-5600 LV scanning electron microscope.

The same protocol was used with primary isolations of liver endothelial cells, except EGM-2 (Cambrex) was used in place of MCDB-131 Complete medium. To encourage cell adhesion, the cross flow rate was reduced to 30 µl/min or shut off for the first 1, 2, or 4 hours. Due to the smaller size of liver endothelial cells, an alternative reactor filter membrane with 3 µm pore size (SSSWP04700N, Millipore) was also used to compare cell retention rate against the standard filter (5 µm-pore size Durapore membrane, Millipore). Fibronectin (Sigma-aldrich) at 50 µg/mL was used as an alternative ECM coating on the scaffold.

2.2.3 Approach 2: Seeding hepatocyte spheroids into scaffold with top surface coated with liver endothelial cells

This approach required a scaffold covered with a monolayer of endothelial cells on the top. The scaffold was coated for 30 minutes with 30 µg/mL of collagen (Cohesion) in PBS and placed in a 35mm Petri dish (Falcon). A seeding density of 1×10^6 primary liver endothelial cells in EGM-2 (Cambrex) was used. To assess the endothelium coverage and its phenotype after 24 hours of culturing at 37°C and 5% CO₂, scaffolds were first incubated in the Live/dead assay (Molecular Probes) according to manufacturer's protocol and observed on a epifluorescence microscope. Following the observation, the scaffolds were processed for SEM (see Appendix 6 for standard SEM protocol) and viewed under a JEOL JSM-5600LV scanning electron microscope.

Incorporation of liver endothelial cells into hepatic tissue was qualitatively assessed by epifluorescence microscopy. Liver endothelial cells on scaffolds were labeled with DiI-AcLDL at 1 $\mu\text{g}/\text{mL}$ in medium (Molecular Probes) before reactor assembly (Appendix 3). Hepatocyte spheroids were prepared from cells isolated from the previous day and seeded into reactors immediately after reactor assembly according to the standard protocol (Appendix 4-5). Images were taken using the Rhodamine filter on day 1, 2, and 3 post-seeding.

2.2.4 Approach 3: Pre-aggregate liver endothelial cells with hepatocytes into spheroids prior to reactor seeding

The co-culture medium was made with EGM-2 (Cambrex) mixed at a 1:1 (v/v) ratio with HGM (see Appendix 2 for HGM formulation), called HEGM. It was used in co-culture spinner flasks and reactors. The spinner flask culture volume was kept the same as mono-cultures at 100 mL. To accommodate metabolic demands from additional endothelial cells, hepatocyte concentration was lowered to 20×10^6 cells/flask. Since no direct cell-cell adhesion was expected between these two cell types, the incorporation rate was expected to be low. The typical yield of primary liver endothelial isolation from one rat liver is about 75×10^6 cells. Because few endothelial cells were required for other experiments, in the interest of optimizing the incorporation rate, 75×10^6 endothelial cells per spinner flask were used to produce co-culture spheroids.

To confirm and characterize endothelial presence within the co-culture spheroids, they were processed for cryosectioning and immunostaining. Spheroids ranged between 100-300 μm in diameter were spun down at 40g for 2 minutes and resuspended in 2% paraformaldehyde (EMS Sciences) at room temperature for 30 minutes. Following 3 washes in PBS, spheroids were stored in PBS at 4°C. On the day of cryosectioning, spheroids were collected into pellets after 2 minutes of 40g spin and resuspended in ~ 100 -200 μL of 37°C agarose (Sigma-aldrich) solution (1% w/v in milli-Q water) in an eppendorf tube. After agarose solidified, the cell-gel was placed on a piece of 42 filter paper (Whatman). The cell-gel was submerged for 30 seconds in 2-methylbutane (Fluka) at its freezing point, and another 10 seconds in liquid nitrogen. The frozen sample was stored at -80°C. Samples were sectioned into 8 μm thickness and stained with primary mouse-anti-rat antibodies SE-1 (IBL America), ED1 (Serotec), and desmin (BD Biosciences) followed by Cy3-conjugated goat-anti-

mouse antibodies (Jackson Immunoresearch) and Hoechst nuclear stain (Molecular Probes). (See appendix 9 for detailed protocol) Images were viewed under 200x magnification and then imported into Metamorph (Universal Imaging) for quantification. Nuclei associated with positive staining and total nuclei were counted. Ten images per sample and two biological replicates of 1-day old mono-culture and co-culture spheroids were used for quantification. (This work was performed in collaboration with Katie O'Callaghan and Donna Stolz at University of Pittsburgh)

2.3 Results

2.3.1 Primary liver endothelial isolation

Previous study had showed that primary endothelial isolate contains about 10% Kupffer cells, 3% stellate cells, and by balance 87% endothelial cells [106]. The endothelial population may contain both large-vessel endothelium and sinusoidal endothelium. To confirm the presence of sinusoidal endothelium, briefly cultured liver endothelial isolate was immunostained with SE-1 and anti-CD31 antibodies for sinusoidal endothelium and large-vessel endothelium, respectively. Staining showed that the majority of these cells are sinusoidal in origin (Figure 2.2). Of the total cells, $89.3 \pm 2.5\%$ were SE-1+ and $8.7 \pm 2.0\%$ were CD31+.

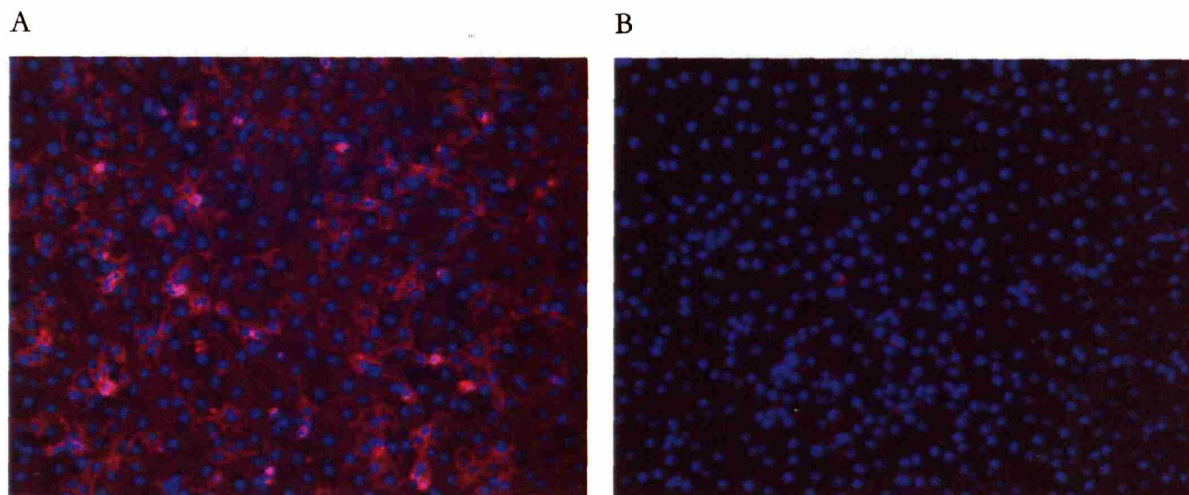


Figure 2.2: Primary liver endothelial isolate was cultured briefly and immunostained with SE-1 (A) or anti-CD31 (B) and Hoechst nuclei stain. Red: SE-1 or anti-CD31; blue: Hoechst

2.3.2 Approach 1: Coating channel walls with endothelium

After several trials of various flow rates, it was found that RLMVECs adhered better to walls when cross flow was shut off for the first four hours of culture, and axial flow was maintained for all 24 hours. Cells appeared live and covered the channel walls completely. (Figure 2.3)

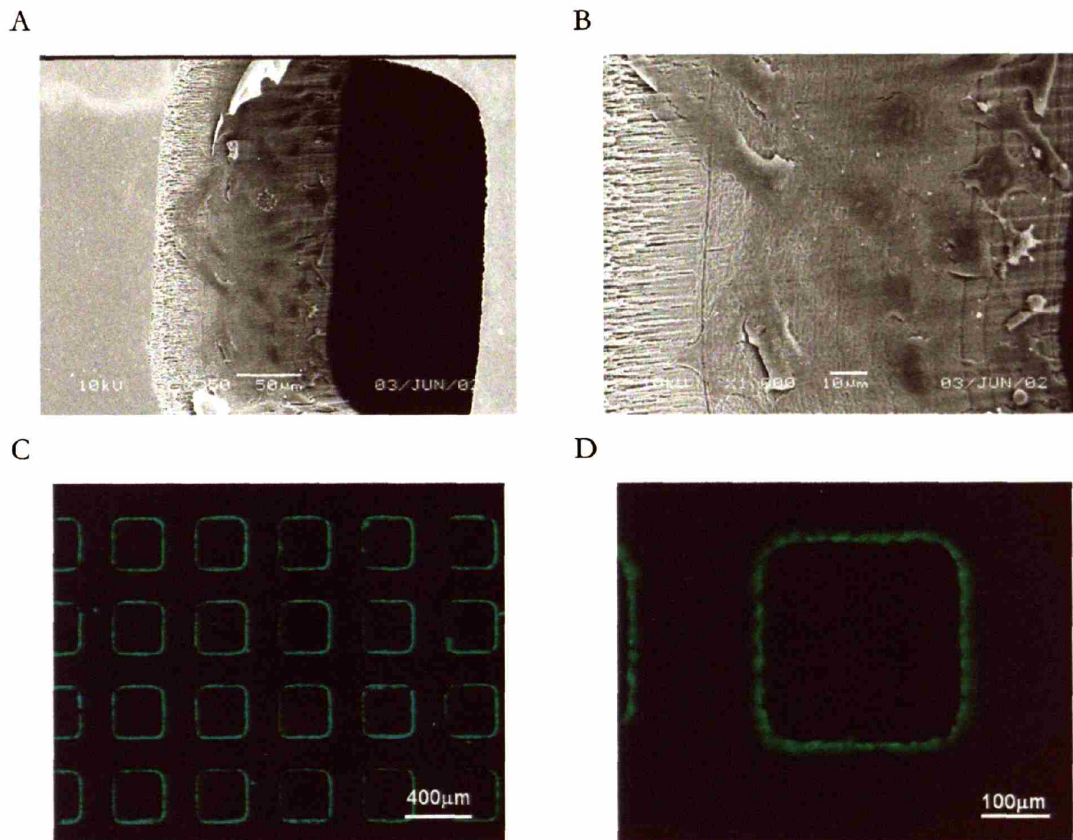


Figure 2.3: SEM images showed channel walls were covered with a monolayer of RLMVECs (A,B). Live/dead assay showed all RLMVECs were alive on channel walls.

The same protocol was then applied to primary liver endothelial cells using EGM-2 medium (EGM-2 bulletkit, Cambrex, Walkersville, MD). Due to their smaller size, liver endothelial cells passed through reactor filter membrane of 5 μm-pore size readily and rarely had time to stay within channels to adhere to the walls. Various parameters were tested: fibronectin and collagen I coating on channels walls; a filter membrane with 3 μm-pore size; longer interruption of cross flow; higher

and lower seeding concentration. But none produced satisfactory monolayer of liver endothelial cells. This approach was determined to be impractical for liver endothelial cells (Figure 2.4).

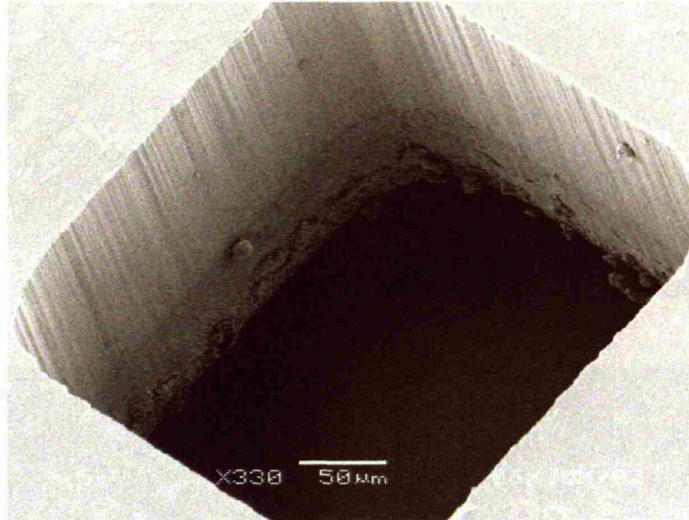


Figure 2.4: an SEM image of a reactor channel 24 hours after seeding with liver endothelial cell fraction. Few cells adhered to the vertical channel walls.

2.3.3 Approach 2: Seeding hepatocyte spheroids into scaffold with top surface covered with liver endothelial cells

Silicon scaffolds were coated with type I collagen and liver endothelial cells were seeded on top of the scaffolds. After 24 hours of culturing, the scaffolds were treated with the live/dead stain, showing live cells in green and dead cells in red. Most cells on the scaffold appear live (Figure 2.5C, D). Using SEM, the morphology of liver endothelial cells was confirmed to be consistent with regular tissue culture, and the top surface of scaffold was covered with endothelial cells. (Figure 2.5A, B)

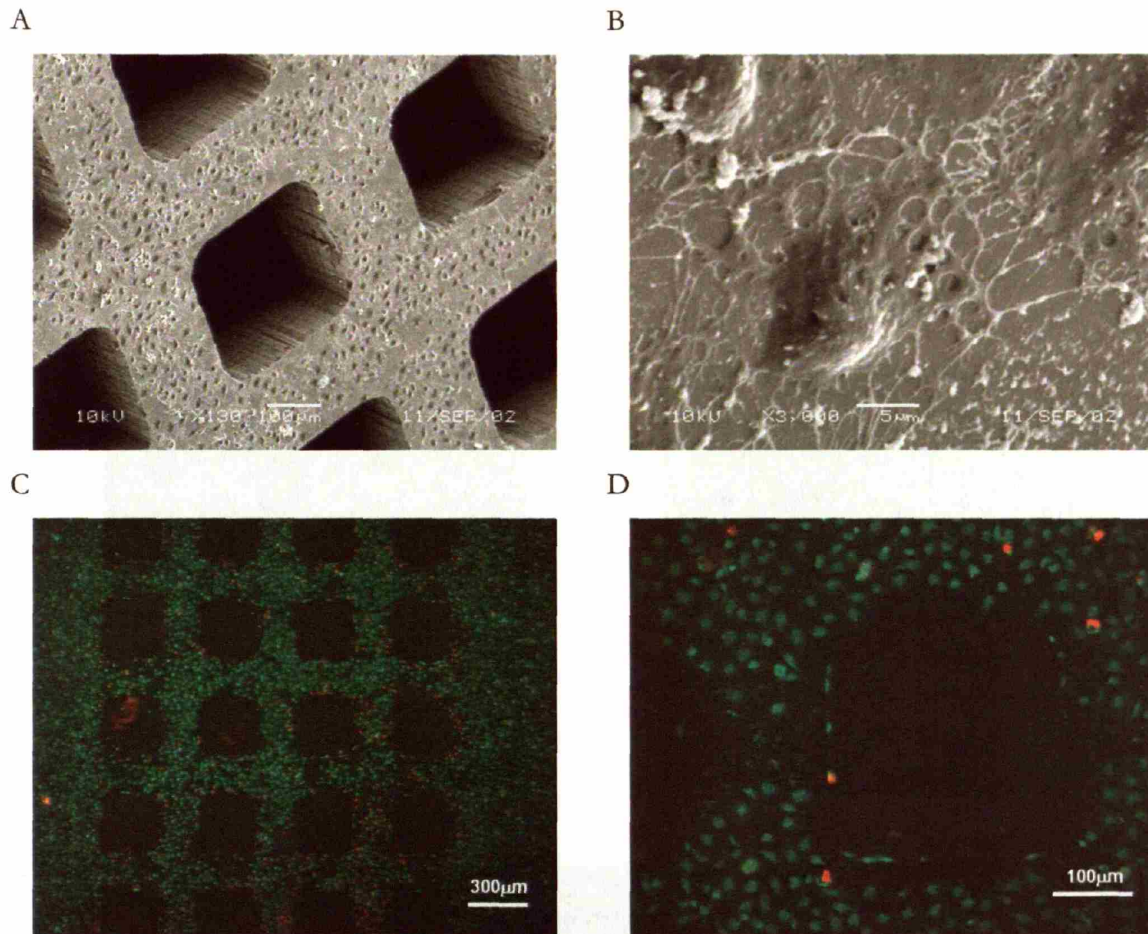


Figure 2.5: Liver endothelial cells adhere to the top surface of silicon scaffold (A, B) SEM images show significant coverage of endothelial cells and consistent morphology of sinusoidal endothelial cells. (C, D) Live/dead stain (green/red) showed that most cells are alive and occasionally a few cells attach to the channel walls.

Incorporation of endothelial cells into the hepatic tissue required a method of identifying endothelial cells among the 3D tissue. As discussed earlier in section 1.7, each methodology had its own limitations. With complications of imaging, absence of endothelial signal may not conclusively determine the absence of endothelial cells. As a preliminary screening method, the generic endothelial marker DiI-labeled acetylated low-density lipoprotein (DiI-AcLDL, Molecular Probes) was used to fluorescently label liver endothelial cells [107].

One-day old hepatocyte spheroids were produced, and those within 100-300 μ m in diameter were seeded into reactors assembled with endothelium-covered scaffolds. Reactors were maintained according to standard procedure (Appendix 4-5) with HEGM medium. Ingrowth of endothelial cells was qualitatively observed daily by noting the presence of DiI fluorescence within channels under a standard epifluorescence microscope. (Figure 2.6)

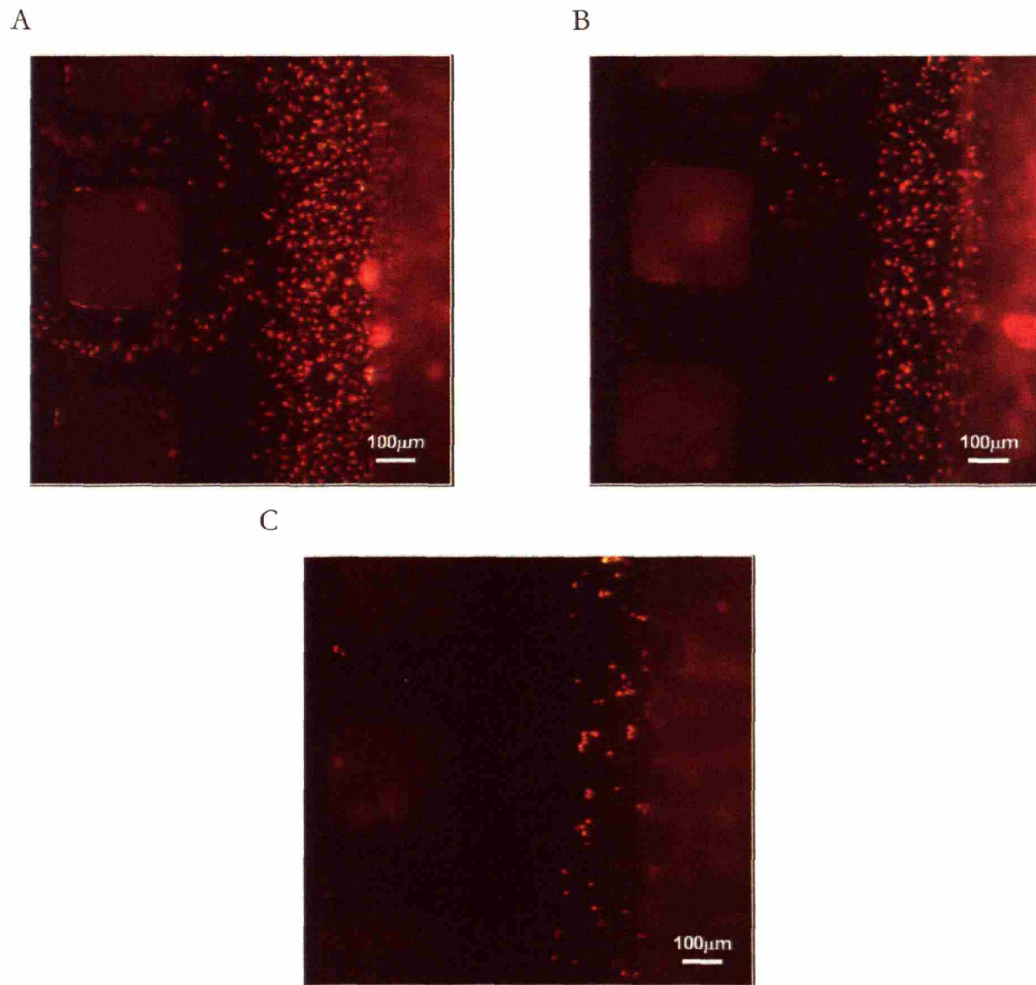


Figure 2.6: co-culture reactor with scaffold top surface covered with liver endothelial cells and channels seeded with hepatocyte spheroids on (A) day 1, (B) day 2, and (C) day 3. Endothelial cells were labeled with DiI-AcLDL (red). Endothelial population was gradually lost over time with no significant presence in channels.

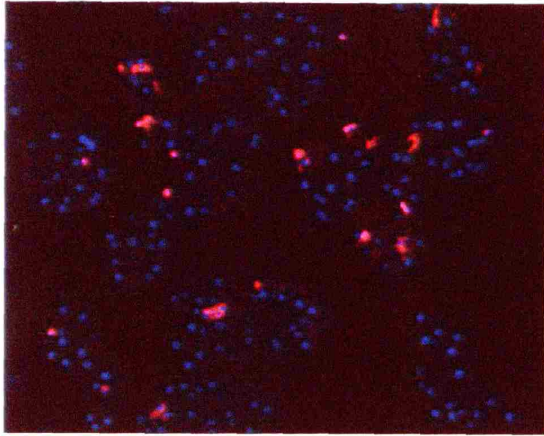
Endothelial cell loss was significant due to trauma from reactor assembly. During the assembly, forceps were used to handle scaffolds and scratched off some cells. Air bubbles generated from opening and closing the reactor body were stressful on the cells because of their high surface tension. During reactor seeding, the 4°C hepatocyte spheroid solution was introduced into 37°C endothelial-covered scaffolds. This temperature difference was probably traumatic to endothelial cells as well. Most of all, axial flow in reactors also flushed away many cells. This was evident in Figure 2.4B, where there were much more cells remaining near the edge of the scaffold due to wall effects near the edge of the flow chamber. After day 3 few endothelial cells remained on the scaffold. Very rarely endothelial cells would be observed inside channels (Figure 2.4C).

2.3.4 Approach 3: Pre-aggregate Liver Endothelial Cells with hepatocytes into spheroids prior to reactor seeding

EGM-2 (Cambrex) was mixed 1:1 (v/v) with HGM (HEGM) and was used in co-culture spinner flasks. Since no direct cell-cell adhesion was expected between these two cell types, the possible incorporation mechanism included random physical entrapment and cell adhesion onto ECM molecules that may be synthesized by endothelial cells or hepatocytes in culture and those already present on cell surface or in EGM-2, which contained 2% fetal bovine serum. This incorporation rate was expected to be low. Therefore, 75×10^6 endothelial cells/flask were used to produce co-culture spheroids.

One-day old spheroids with diameters within 100-300 μm range were processed for immunostaining to confirm the presence of non-parenchymal cells. Co-culture spheroids contained $20 \pm 0.5\%$ SE-1-positive nuclei, while mono-culture spheroids contained $3 \pm 0.1\%$ SE-1-positive nuclei. The addition of endothelial cells in the co-culture group thus yielded a 7-fold increase in sinusoidal endothelial population. (Figure 2.7) Kupffer cell population was also higher in the co-culture spheroids. (Figure 2.8) Occasionally stellate cells were observed. (Figure 2.9)

A



B

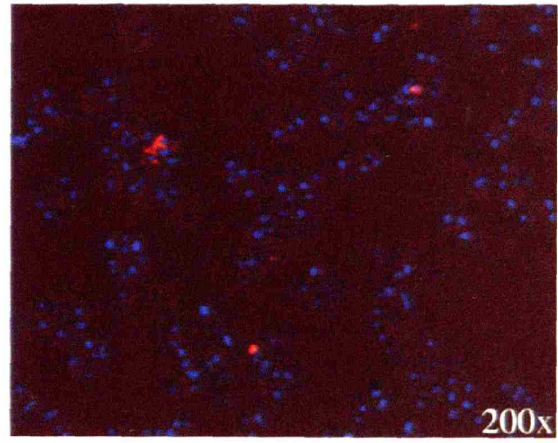


Figure 2.7: Immunohistochemistry on 1-day old co-culture (A) and mono-culture (B) spheroids. Sections were stained with SE-1 (red) and Hoechst nuclear stain (blue)

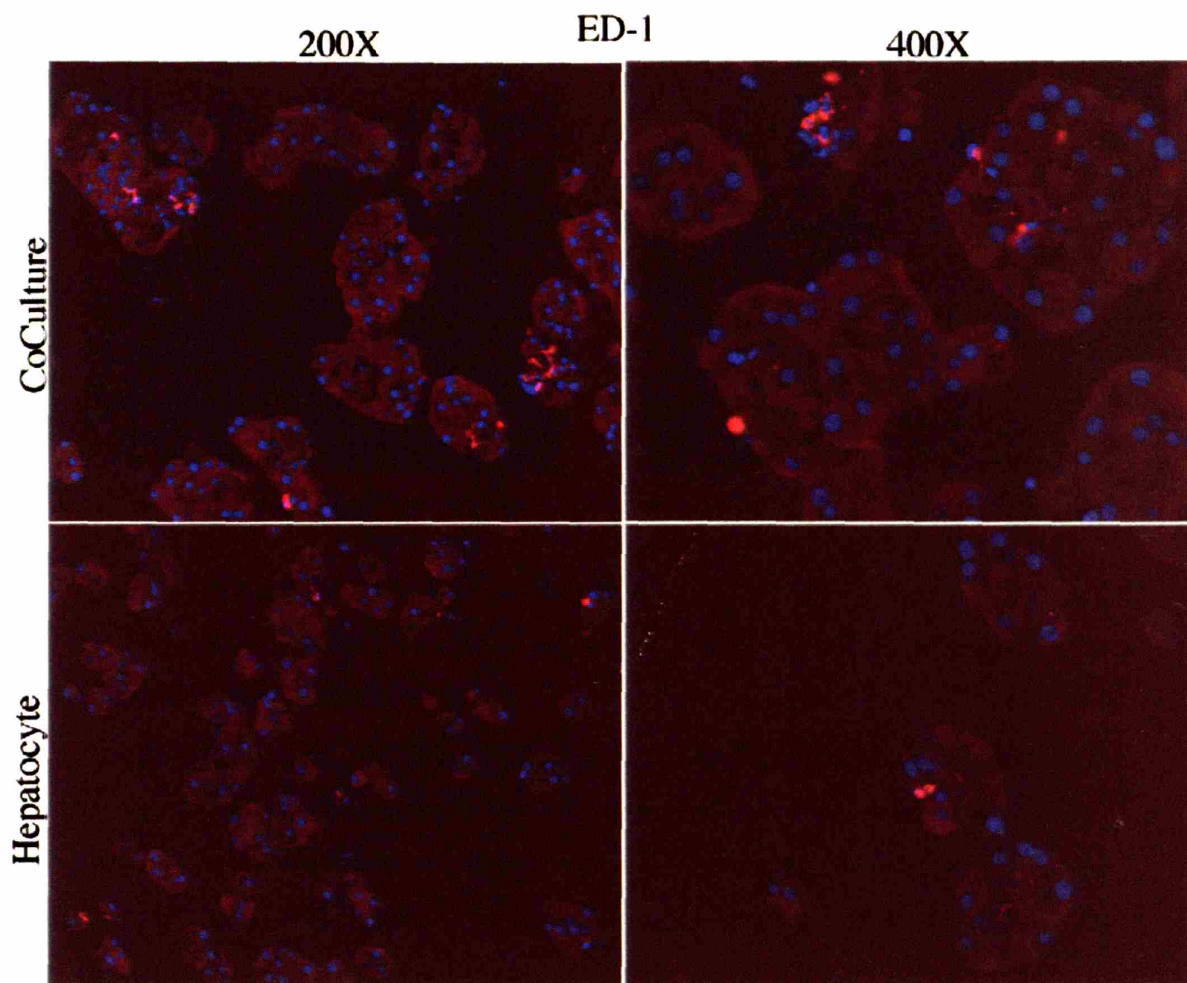


Figure 2.6: ED1 staining (Kupffer cells) on sections of co-culture (upper row) and mono-culture (lower row) spheroids. Red: ED1; blue: Hoechst

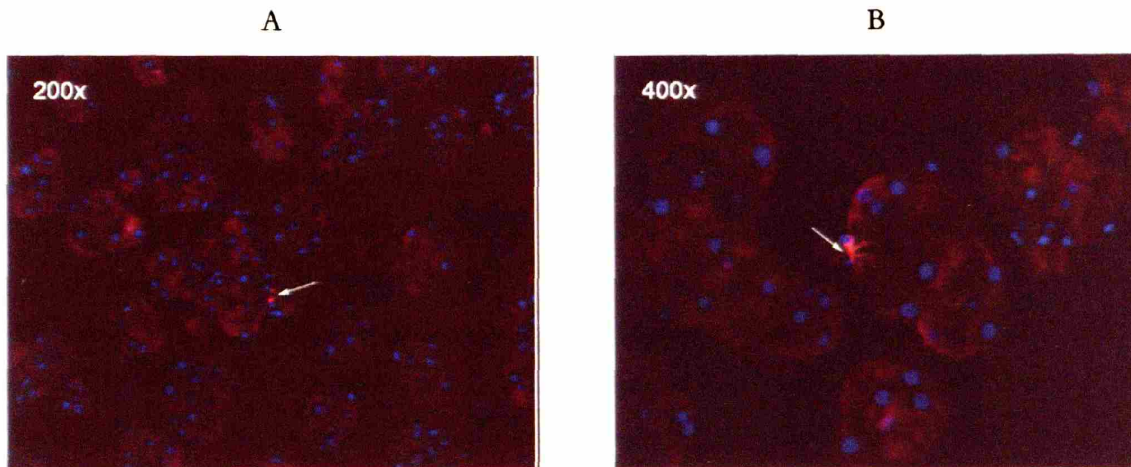


Figure 2.7 Desmin staining (stellate cells) on sections of co-culture spheroids. Red: desmin; blue: Hoechst

2.4 Discussion and conclusion

Primary cell isolations are difficult to achieve 100% purity. For a quantitative co-culture protocol the starting cell population must be well characterized. Previous study calculated the endothelial isolate to contain 87% endothelial cells [106]. Comparing this number to the result shown here ($89.3 \pm 2.5\%$ SE-1+ cells in the isolate), it appears that all of these endothelial cells are from the sinusoids. There is also a population of CD31+ cells, at $8.7 \pm 2.0\%$. DeLeve et al. reported that surface expression of CD31 is a marker for sinusoidal endothelium dedifferentiation [29]. Since these cells were stained without membrane permeabilization, the CD31 expression most likely be on the cell surface. This small percentage of CD31+ cells may be from large vessels, or they may be dedifferentiated sinusoidal endothelium. It is unclear whether SE-1 and CD31 surface expressions are mutually exclusive. However, it is certain that the majority population of the liver endothelial isolate is *sinusoidal in origin*.

In developing a co-culture protocol, approaches 1 and 2 were inspired by observations of liver regeneration events and previous reports on cell self-organization [22, 104]. In approach 1, monolayers of RLMVECs were successfully created on channel walls, but the protocol was not translatable to liver endothelial cells. Liver endothelial cells are difficult to culture and sensitive to culturing conditions [18-21, 29]. It was speculated that the RLMVECs completely filled all the

channels so that many cells had access to the channel walls. Liver endothelial cells have a slightly smaller cell size and could have easily passed through the reactor filter during seeding, leaving no opportunity for cell adhesion. In fact during RLMVECs seeding the resistance pressure on the syringe could be felt before all the cell solution was injected and such pressure was not observed during liver endothelial cells seeding, indicating only RLMVECs caused crowding in the channels. When filters of a smaller pore size were used, the inherent pressure drop across the filter was so high that reactors often started leaking during seeding. No cell adhesion was observed with small-pore filters, and nor was it observed with fibronectin, a commonly used matrix protein for endothelial cells. It is likely that the condition was too harsh for liver endothelial cells, a fragile cells type after being isolated from its native environment, to adhere vertically onto a substrate.

In approach 2, liver endothelial cells readily adhered to the top surface, but the axial flow may have been too strong since most of the cells detached from the surface of the scaffold. Furthermore, no movement of liver endothelial cells into the channels was observed. The survival of liver endothelial cells alone in reactors was difficult to maintain. They may only survive in the presence of hepatocytes in close proximity.

Previously, spheroids were made by culturing only the hepatocyte-enriched fraction at 30×10^6 cells/100 mL HGM in a spinner flask [73, 86, 108]. Cells generally formed loose aggregates after 24 hours and continued to grow in size and compact into spherical shape over time. It was shown that reactors seeded with 3-day old spheroids showed higher albumin secretion rates than those seeded with single cells or 2-day old spheroids [108]. For approach 3, however, 1-day old spheroids were chosen. The rationale behind this chosen time point was two-fold.

First, due to reasons still unknown, the size of spheroids occasionally increased at a much higher rate so that many spheroids of diameters greater than 300 μm formed after only 24 hours. Spheroids with sizes above 300 μm were not appropriate for reactor seeding because they were physically prevented from entering reactor channels. The size of co-culture spheroids always increased faster than mono-culture spheroids based on visual inspection of the culture: as more and bigger spheroids formed, fewer single cells remained in solution, resulting in a less opaque solution; as spheroids grew in size, they became visible to the eye and could be easily identified.

Secondly, 1-, 2-, and 3-day old spheroids made with only enriched hepatocyte fraction were processed for toluidine blue histological stain, and the spheroids at later time points contained higher proportions of dead cells (D. Stolz, personal communication).

Even though liver endothelial cells do not have direct cell-cell contact with hepatocytes *in vivo*, previous reactor cultures have shown the occasional presence of endothelium [86]. It is thought possible to incorporate liver endothelial cells into hepatocyte spheroids, and indeed a 7-fold increase (3% to 20%) in endothelial population was observed.

Based on these findings, approach 3 was chosen as the co-culture protocol because it was the only approach that produced close interactions between hepatocytes and endothelial cells. Even though there may well be optimal conditions for the first two approaches to be successful, in light of the overall goals of this thesis, a standard protocol had to be chosen in order to test these hypotheses. There are also other ideas not yet explored: liver endothelial cells can be seeded after hepatocyte cultures have been established in the reactors; liver endothelial cells and hepatocytes can be seeded together in the form of single-cell suspension into the reactor with or without the addition of ECM synthesized during liver regeneration; carrier beads or gels with liver endothelial cells can be used to enhance cell retention; novel scaffold production methods may print out vascular paths for liver endothelial cells to adhere to before hepatocytes are seeded. Many of these approaches may seem more logical but would require repeated protocol testing and modification. The approach chosen is an engineering compromise that offered a quick solution to combining liver endothelial cells with hepatocytes in the reactor. Additional experiments should also be performed to examine the effect of reducing the number of endothelial cells in the starting cell population because the current protocol uses almost the entire endothelial isolate from one rat liver for one spinner flask culture.

Chapter 3

Testing of Methodologies to Visualize Cell Types and Their Morphology within the 3D Microreactor

3.1 Introduction

One of the aims of this thesis is to visualize the morphological outcome of the endothelial cells in the 3D tissue. Imaging can be roughly divided into two categories: live imaging and end-point immunostaining.

The difficulty of live imaging stems from the inherent colorless nature of cells and the 3D tissue environment, which strongly interferes with the light path in conventional microscopy. Previously it has been shown that two-photon microscopy is able to detect hepatocytes infected by adenovirus carrying the EGFP gene in the 3D microreactor [86]. Therefore it is possible to detect a particular cell type within the 3D tissue if a robust and specific labeling method can be applied. Acetylated low-density lipoprotein (AcLDL) is a commonly used marker for endothelial cells [107]. It can bind to the scavenger receptors on endothelial cells and macrophages and is taken up through endocytosis [107]. But its compatibility with microreactors needed testing. Another approach is to label endothelial cells prior to mixing them with hepatocytes. Cells with intrinsic markers such as those isolated from EGFP-positive rats are useful because no labeling procedure is required, and the fluorescence markers are produced continuously only by live cells. But the signal-to-noise ratio, namely the EGFP endothelial cell fluorescence level versus wild-type hepatocyte autofluorescence, needs to be determined.

The aim to examine the endothelial morphological outcome may have to include visualization tools to look for the fluid paths within the 3D tissue. Previous studies used confocal or multi-photon microscopy coupled with fluorescent dyes to image all fluid space [109-111]. This system presents significant challenges due to the reactor design. The long distance between tissue and the surface of the optical window greatly hampers the efficiency of imaging (Figure 1.3). Furthermore, the depth of the reactor channels (230 μm) and the highly light-scattering nature of hepatic tissue may make such imaging very difficult. Two approaches were examined: fluorescently

labeled carboxylated beads were used to label any negatively-charged surfaces, namely the tissue surface; fluorescently labeled large dextran beads were used to color all space with access to fluid.

Since no primary cell isolation can be 100% pure, the final cell population within the 3D tissue has to be determined with immunostaining using cell-specific markers. The reactor design again poses a challenge because the scaffold material (silicon) cannot be easily cut through without disturbing the tissue integrity. Many plastic scaffold materials and manufacturing methods were considered, including polycarbonate, polyimide, and polystyrene, made with laser machining or injection molding. Based on rudimentary morphological observations, polycarbonate was considered to be the best alternative to silicon (data not shown). Other than the scaffold material, an embedding polymer was needed to provide mechanical support to the tissue and retain its immunogenicity. Technovit8100 has been reported to be such a material [112, 113]. However, the original protocol had to be modified to accommodate the reactor system.

In this chapter, the findings on the practicality of these imaging options are presented. It provides working protocols for experiments using the microreactors, and it also details the limitations of several methods for future improvement.

3.2 Materials and methods

3.2.1 Compatibility of AcLDL with the microreactor

Microreactors were assembled according to standard protocol (Appendix 3). Reactors were primed with HGM at 37°C and 8.5% CO₂ for at least 30 min. After priming, half the reactors were dosed with DiI-labeled acetylated LDL (DiI-LDL, Molecular Probes) at 1 µg/mL medium. The reactors were allowed to operate for 1 hour at 37°C and 8.5% CO₂ before observation under an epifluorescence microscope with the Rhodamine filter.

3.2.2 EGFP-positive Endothelial Cells

Hepatocytes and liver endothelial cells were isolated from wild-type Fischer rats and EGFP-positive Sprague-Dawley rats, respectively, according to standard protocol (Appendix 1). Cells were

seeded into 6-well plates (Falcon) and maintained for 24 hours at 37°C and 5% CO₂. EGM-2 (Cambrex) was used in endothelial cell-only cultures, and HEGM, a 1:1 (v/v) mix of HGM and EGM-2, was used in co-cultures with wild-type hepatocytes. DiI-AcLDL (Molecular Probes) was added to the endothelial-alone culture at 1 µg/mL and allowed to incubate for 4 hours. Cells were observed through the green and red channels of an epifluorescence microscope. (The endothelial-alone experiment was performed by Donna Stolz at University of Pittsburgh Center of Biologic Imaging)

3.2.2 Visualization of Fluid Space within the 3D Tissue Using Two-photon Microscopy

3.2.2.1 Labeling tissue-fluid interface

One-day old co-culture spheroids were made with hepatocytes and liver endothelial cells from wild-type male Fischer rats (see section 2.2.4). Microreactors were assembled and seeded with co-culture spheroids according to standard protocol (Appendix 4-5). The cultures were maintained for 3 days before labeling with fluorescent beads. Medium was replaced with PBS to remove most proteins and charged molecules, and the PBS wash was circulated through the reactors for 15 min. The washing liquid was replaced with fresh PBS dosed with FluoSpheres® carboxylate-modified microspheres (0.02 µm diameter in red, Molecular Probes) at 1:200 or 1:1000 dilutions. The labeling solution also contained 1:40,000 dilution of Sytox Green nuclei stain or 1:4,000 dilution of DiO Vibrant CellTracker (Molecular Probes). The cultures were labeled by recirculating the labeling solution for 15 minutes at 37°C and 8.5% CO₂. The labeling solution was then replaced with 2% paraformaldehyde (EMS) in PBS to fix the tissue for 30 min at room temperature. The cultures were imaged using a multiphoton laser scanning confocal microscope system comprising a titanium-sapphire ultrafast tunable laser system (Coherent Mira Model 900-F), Olympus Fluoview confocal scanning electronics, an Olympus IX70 inverted system microscope, and custom built input-power attenuation and external photomultiplier detection systems. Samples were viewed with a Olympus water-immersion 20X UApo 0.7NA objective. Green fluorescence emission detection utilized a HQ535/50m filter, and red fluorescence emission detection utilized a HQ610/75m emission filter (Chroma, Brattleboro, VT). Images were imported into Metamorph (Molecular Devices) for low-

pass filtering, stack building, and 3D reconstruction. (This work was performed at University of Pittsburgh Center for Biologic Imaging with assistance from Glenn Papworth)

3.2.2.2 Labeling all fluid space

Microreactors containing co-culture spheroids were assembled and maintained as described above for 3 days. The reactor cultures were fixed by recirculating 2% paraformaldehyde (EMS) in PBS in the reactor fluidics for 30 min at room temperature. The residual paraformaldehyde was washed out by fresh PBS exchanges. Fluorescent PBS solution containing 2.5 mg/mL or 1.25 mg/mL FITC-labeled dextran beads (70,000 MW, Molecular Probes) were injected into the upper chamber (axial flow) of the reactors by a syringe while the cross-flow pulls the fluorescent fluid through the tissues in the channels at 40 μ L/min with peristaltic pumps. Passage of labeled dextran was confirmed by visual inspection of the cross-flow fluid as the dextran solution had a visible green hue. All fluidic lines immediate to the reactors were clamped shut to prevent air bubble formation within the reactor chamber. The samples were viewed under the two-photon microscope in the green channel as described above. Images were also processed for low-pass filtering and stack-building in Metamorph. (This work was performed at University of Pittsburgh Center for Biologic Imaging with assistance from Glenn Papworth)

3.2.3 Immunohistochemistry on the Microreactor 3D Tissue

Slivers of liver tissue with at least one dimension less than 5mm were excised from anesthetized wild-type male Fischer rats or EGFP Sprague-Dawley female rats and immediately submerged in 2% paraformaldehyde (EMS) inside a 50 mL conical tube (Falcon). The tube was kept on a nutator at 4°C for 3 hours. Tissue samples were washed overnight in 6.8% sucrose (Sigma-Aldrich) in PBS at 4°C on a nutator. Following the wash they were dehydrated with 100% acetone (Sigma-Aldrich) or 100% ethanol for 1 hr, and embedded in Technovit8100 (EMS) according to manufacturer's protocols. Embedded tissue was cut into 6 μ m-thick sections on a microtome with a dry glass knife. Sections were floated on milli-Q water on a glass slide and dried on a 37°C heat block.

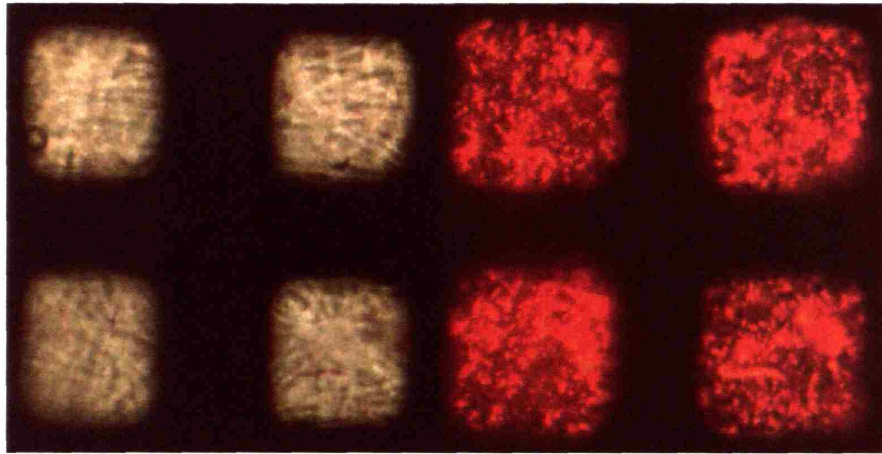
Sections of tissue were stained using protocols in previously published reports [112, 113]. Primary antibodies included SE-1 (IBL America), anti-CD31 (Chemicon), ED-2 (Serotec), and anti-GFAP (Serotec). Fluorescently conjugated secondary antibody was either goat-anti-mouse Cy3 (Jackson ImmunoResearch) or biotin (Jackson ImmunoResearch) followed by a tertiary Cy3-conjugated streptavidin (Jackson ImmunoResearch). Several modifications to the protocol were examined, including dehydration using ethanol or acetone, the necessity of trypsin antigen retrieval, and whether overnight incubation of primary antibody enhances the fluorescence signal. The finalized protocol is described in Appendix 10.

3.3. Results

3.3.1 DiI-AcLDL is trapped in reactor filter

Even though the reactor filter membrane was soaked in 1% BSA in PBS prior to assembly, previous experiments using DiI-AcLDL in the reactor medium suggested possible binding of AcLDL to the filter. When DiI-AcLDL was added to HGM with no cells in the reactor, the filters took up a significant amount of AcLDL. (Figure 3.1)

A



B

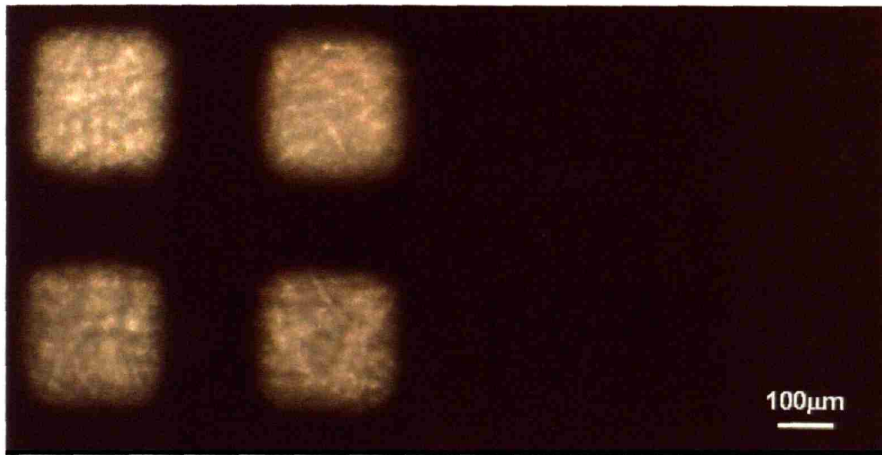


Figure 3.1: Reactors dosed with (A) or without (B) DiI-AcLDL. Transmitted-light pictures of 4 representative channels are shown on the left, and the same focal plane images under rhodamine filter are shown on the right. Red: DiI-AcLDL.

3.3.2 EGFP labeled liver endothelial cells

Liver endothelial cells were isolated from EGFP-positive Sprague-Dawley rats and cultured on 2D plates. Their endothelial phenotype was confirmed by uptake of DiI-AcLDL (Figure 3.2). Their fluorescence level was confirmed to be above wild-type hepatocyte autofluorescence (Figure 3.3).

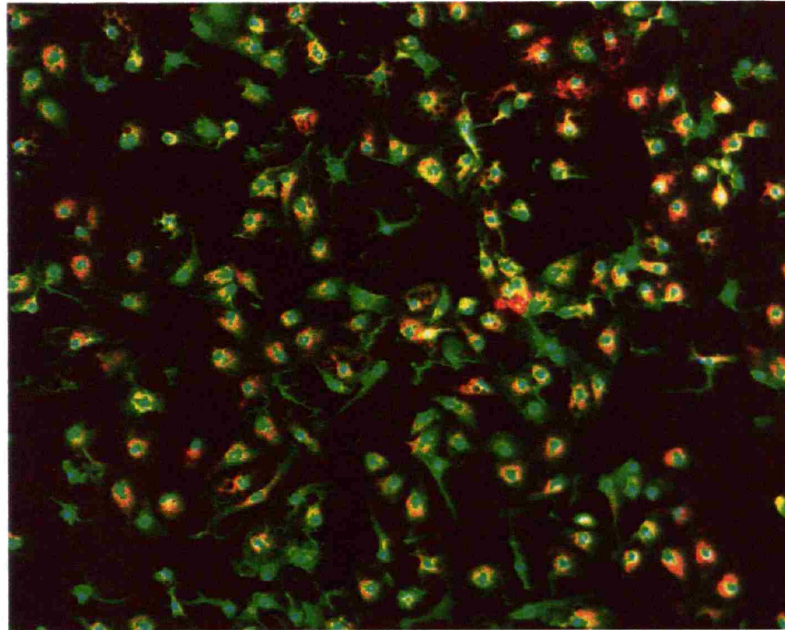


Figure 3.2: 1-day old EGFP liver endothelial cells dosed with DiI-AcLDL. Image is an overlay of the green and red fluorescence channels. Green: EGFP; red: DiI-AcLDL.

A



B

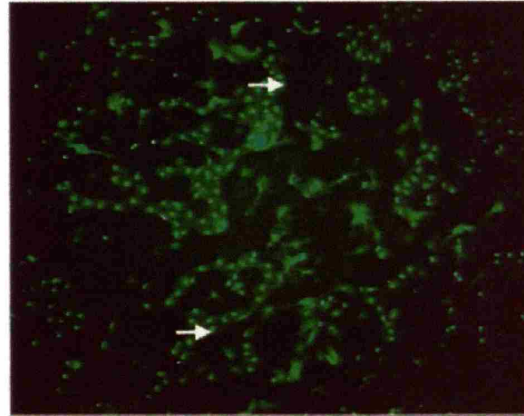


Figure 3.3: Phase contrast (A) and green fluorescence channel (B) images of 1-day old 2D co-culture of wild-type hepatocytes and EGFP-positive liver endothelial cells. Arrows indicate two areas occupied by wild-type hepatocytes which showed minimal background green autofluorescence.

3.3.2 Fluid channel visualization using 2-photon microscopy

3.3.2.1 Fluid-tissue interface

Two concentrations of red carboxylated beads were used, and the cells were labeled green within the nucleus or the cytoplasm to provide contrast. Red beads at lower concentration produced very low fluorescence level (Figure 3.2A). Beads at higher concentration clearly defined the staining area (Figure 3.2B), but the staining pattern is uneven. While some portions of the tissue had extremely bright spots, others may be minimally stained.

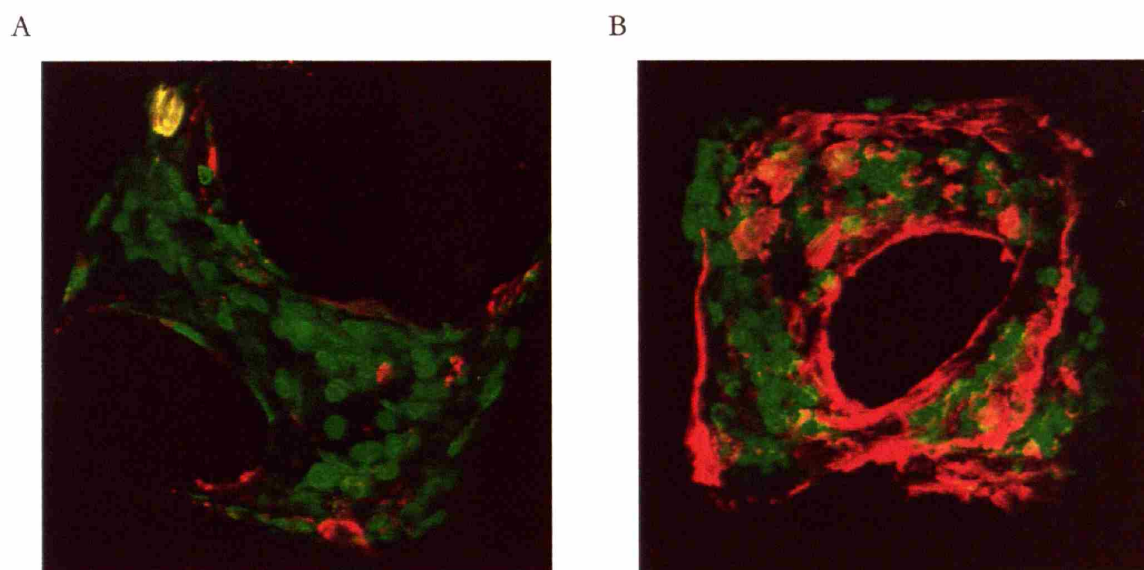


Figure 3.4: Three-day old co-culture reactors were stained with Sytox Green nuclei stain (A) or DiO CellTracker (B) and dosed with red fluorescent carboxylated beads at low (A) or high (B) concentrations. Images are overhead views of a stack of x-y plane sections through the reactor channels. Green: Sytox Green nuclei stain or DiO CellTracker; Red: carboxylated beads

3.3.2.2 Fluid space

Another approach to visualize the fluid space is to fluorescently label the liquid itself [109-111]. The fluid within 3-day old co-culture reactors was dosed with FITC-labeled dextran with an average molecular weight of 70,000, a size that would be excluded by cell membranes and cell-cell junctions [114-116]. Therefore all green fluorescence indicates wherever there is fluid access, and all black space theoretically indicates areas occupied by tissue. Observation of the fluid space with two-

photon microscope revealed great image resolution of this method, as shown by the cell shape in black (Figure 3.5A). However, as the focal plane penetrates deeper past the entire tissue thickness, no fluorescence was observed from the fluid below tissue mass (Figure 3.5B).

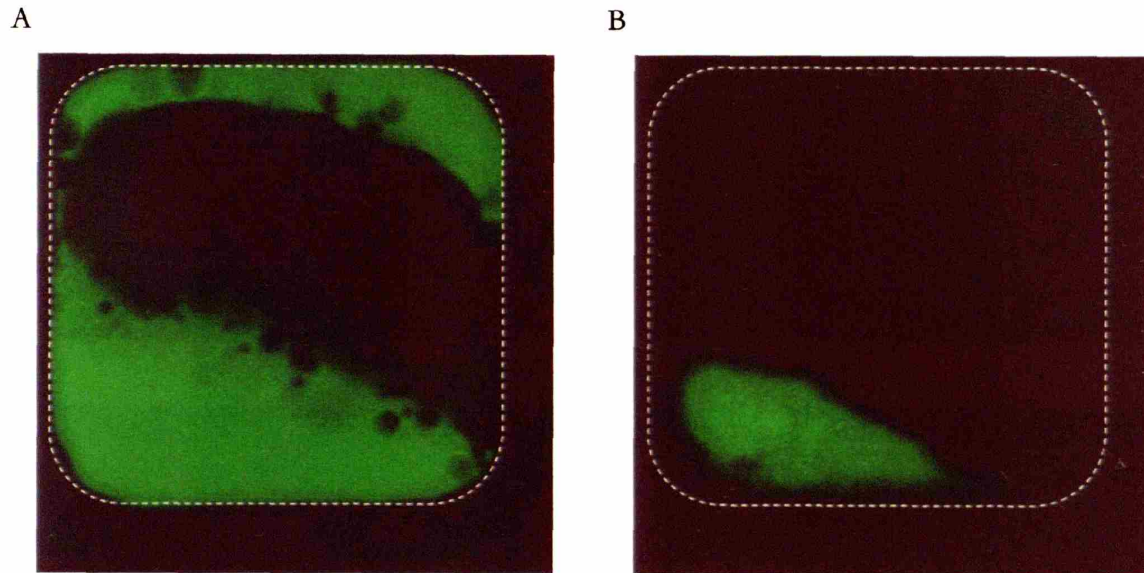


Figure 3.5: x-y plane images of a reactor channel at 54 μm (A) and 267 μm (B) below the top scaffold surface. Dashed white lines indicate channel walls. Fluid space is green from FITC-labeled dextran, and black space indicates tissue mass (A). At the depth of 267 μm , actual focal plane should be at the filter membrane saturated with the fluorescent liquid, only areas where there was no tissue mass above were visible (B).

3.3.3 Immunohistochemistry on liver tissue embedded in Technovit8100

Original technovit8100 protocol recommends tissue dehydration using acetone. However, polycarbonate scaffolds dissolves in acetone, and tissue dehydration has to occur before scaffolds can be removed from embedded tissue. Preliminary staining in liver was successful with acetone dehydration, and ethanol substitution seemed to have no adverse effect on the staining result. All the antibodies tested were able to detect specific cells types in patterns of normal tissue distribution. (Figure 3.6)

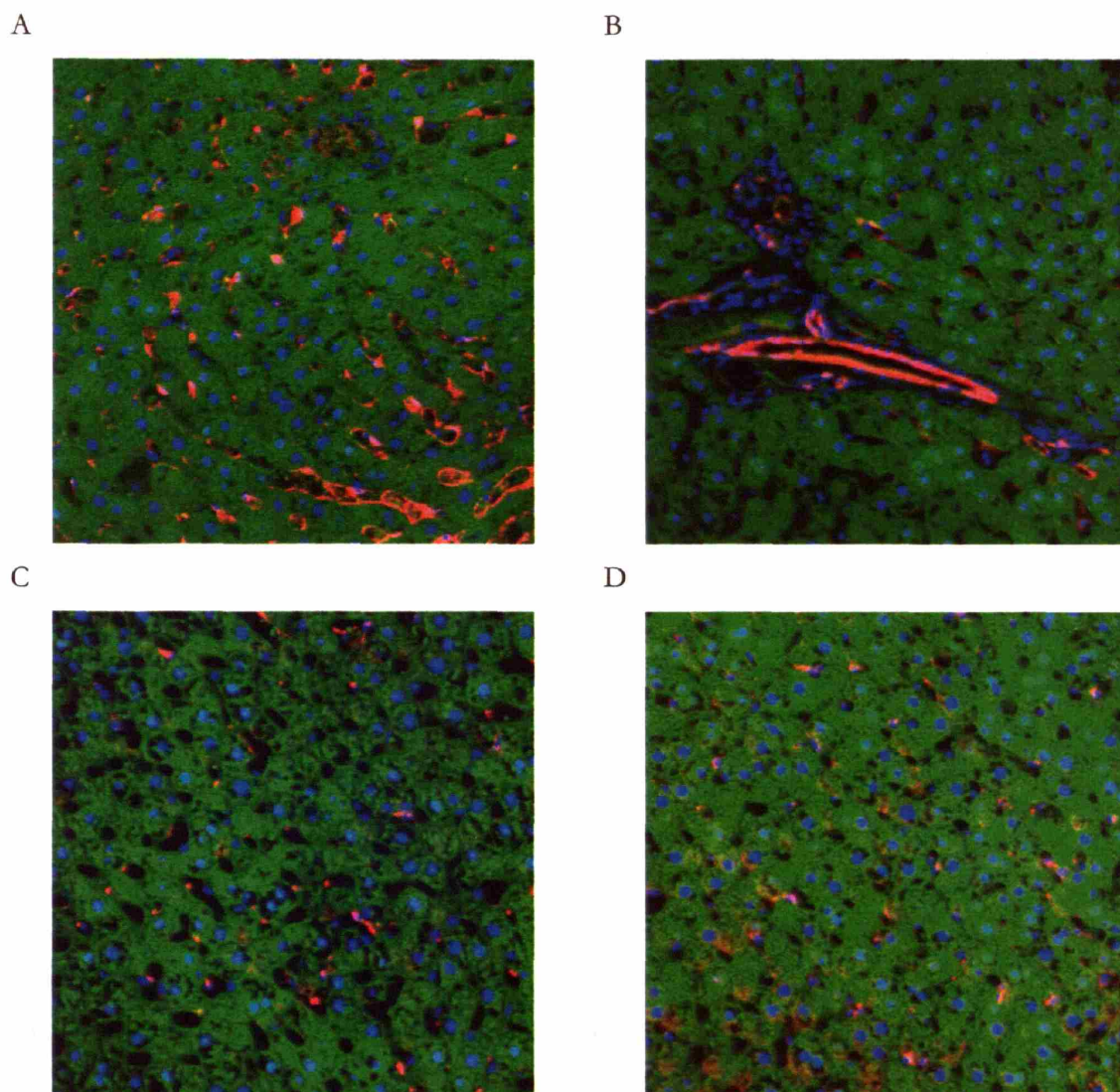
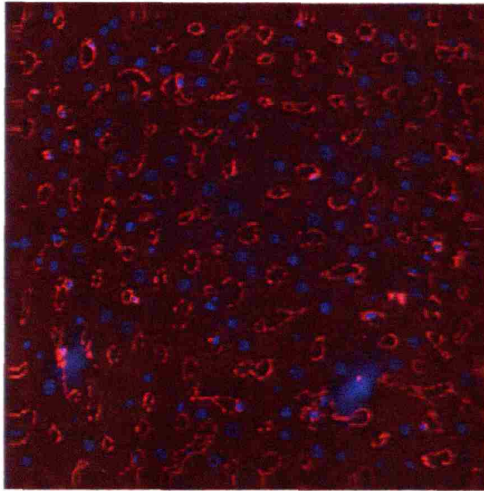


Figure 3.6: Immunostaining of EGFP liver tissue embedded in Technovit8100. Labels included SE-1 (A) for sinusoidal endothelium, CD31 (B) for large-vessel endothelium, ED-2 (C) for Kupffer cells, and GFAP (D) for quiescent stellate cells. Green: EGFP; Red: Cy3 marking of primary antibody; Blue: Hoechst nuclei stain.

Further modification to the protocol included an antigen retrieval step using trypsin. No signal was observed if this step was omitted (data not shown). Primary antibody incubation at 37°C for 2 hours was compared to that at 4°C overnight. It was determined that 2 hours of 37°C incubation produced better staining signals (Figure 3.7).

A



B

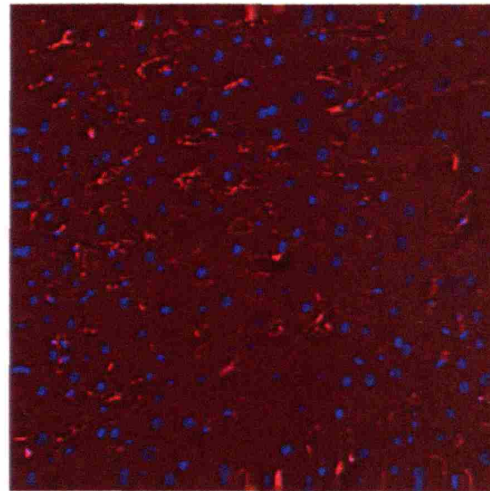


Figure 3.7: Trypsin antigen retrieval was used and 2hr 37°C incubation (A) or overnight 4°C (B) incubation of SE-1 antibody was performed on wild-type Fischer rat liver sections embedded in Technovit8100. The sinusoid staining pattern is shown in red (SE-1) and nuclei in blue (Hoechst).

3.4 Discussion and conclusion

Endothelial cells may be differentiated from hepatocytes by labeling them before they are mixed with hepatocytes, or during the culture using specific targeting agents. The advantage of using AcLDL is that only the live cells can be labeled. However, it has cross-reactivity with macrophages, and it cannot be taken up unless the targeted cells have access to the fluid. Here it is shown that AcLDL can be trapped by reactor filter, greatly lowering its effective concentration. Increasing the dosing concentration can become prohibitively expensive. Alternatively, there are generic dyes (such as CellTracker, Molecular Probes) that react with cytoplasmic enzymes and permanently reside in the cell. However, they may be cytotoxic (J. Moritz, personal communication) and their labeling protocols generally require a long period of time not suitable for freshly isolated endothelial cells, which are quite fragile. Hence the generous gift of EGFP-positive rats from Professor Okabe was an elegant solution. Previously reported GFP rat strain expressed GFP in almost all organs except the liver [117], but the strain developed by Okabe, CZ-004, expresses EGFP protein in all organs including the liver. Those with homozygous EGFP genes do not develop well (M. Okabe, personal communication), but no apparent physical abnormality was observed on rats with heterozygous EGFP genes. Here it is shown that EGFP endothelial cells emit green fluorescence at a level above

the hepatocyte autofluorescence, and their endothelial phenotype appears similar to that of wild-type endothelium.

Fluid-tissue interface could be visualized after it is labeled by charged fluorescent beads, but they tend to aggregate in certain areas and may not stick at all in others. Therefore absence of signal may not necessarily indicate lack of fluid contact. In the second method, fluid space is visualized easily with labeled dextran beads, but the scattering nature of the tissue prevents visualization of great depth. This may be compensated by higher laser power, but currently there is no feedback controls to gradually change the power in response to fluorescence level. Furthermore, higher laser power may reveal fluid ducts below tissue, but it will also generate much brighter fluorescence from areas with no tissue. The photo-multiplier may be over-saturated by the extreme brightness. An ideal fluorophore would be just as bright inside or outside the tissue, an unlikely characteristic.

Since there is no easy way to tease tissue out of the scaffold without damaging its integrity, an embedding material that infiltrates the tissue and hardens is needed to provide mechanical support. However, typical epoxy and resins are hydrophobic and antibodies cannot gain access to the embedded tissue. There are a variety of commercial embedding agents that claim to retain immunogenicity of the tissue, including LR white, LR gold, Technovit 7100, 8100, and 9100. Nevertheless, there are many intricacies in processing samples, and any deviations from the working protocol can lead to absence of signal. Fixation and dehydration chemicals may mask or denature the protein of interest. During embedding, crosslinking polymers may conceal antigen epitopes, and heat released during polymerization may denature proteins. These conditions may vary depending on the antigens and antibodies. Therefore a working protocol should be followed closely. The finalized protocol (Appendix 10) is shown to consistently stain liver tissue for the antibodies tested. For reactor samples, plastic scaffolds may be sectioned easily, but polycarbonate, unlikely Technovit8100, does not expand upon soaking up water. Sections containing both materials will wrinkle due to differential expansion rates. It is recommended that all plastic material be removed for sample re-embedding before sectioning.

In conclusion, additional non-parenchymal cells in microreactors can be identified in real-time *in situ* by their EGFP signals through two-photon microscopy. Specific cell types can be determined by immunohistochemistry as an end-point assay. Labeling endothelial cells with AcLDL

is not compatible with the microreactors, and visualizing the fluid space may require a different strategy.

Chapter 4

Morphological Study on 3D Microperfused Co-cultures of Rat Hepatocytes and Liver Endothelial Cells

4.1 Introduction

Primary hepatocytes rapidly lose most liver-enriched functions when cultured in standard 2D formats, and thus a variety of culture approaches have been developed to restore aspects of cell-cell, cell-matrix, and soluble signaling mechanisms *in vitro* in order to preserve liver function [10, 42]. Co-culture of primary hepatocyte isolates with other liver cell types in 2D, or even fibroblasts or endothelial cells derived from unrelated tissues, can enhance secretion of serum proteins and some metabolic functions [41, 42, 49], as can culture under conditions that foster 3D tissue formation, such as spheroids that can readily be initiated from certain 2D substrates [118-121].

The cellular composition of liver parenchyma includes, by number, ~60% hepatocytes, 19-21% endothelia, 5-8% stellate cells and 10-15% Kupffer cells [1, 36, 122]. Primary liver cell isolates obtained by standard collagenase digestion are relatively depleted of endothelial cells, and are typically further purified to contain 90-95% hepatocytes. Stellate cells that contaminate the hepatocyte-rich fraction, like fibroblasts derived from other tissues, proliferate and secrete abundant matrix under most culture conditions, and can become an appreciable fraction of the total cell number in long-term culture, even under serum-free conditions [79, 123]. In some 3D culture formats, the contaminating NPCs foster organization of sinusoid-like structures [65, 78, 79, 124], though robust presence and organization of endothelia are rarely seen.

In vivo, hepatocytes are generally no more than one cell away from sinusoidal blood, and thus the dimensions of 3D diffusion-controlled cultures are inherently limited to at most a few cell layers by metabolic demands, and may be limited as well by other poorly understood phenomena such as loss of physiological mechanical stresses and cell polarity. In order to address the metabolic demands of liver cells in 3D culture while creating tissue structures of comparable size to the liver

capillary bed, we have developed a microreactor culture system based on a scaffold that fosters organization of primary liver cells into tissue-like units ~ 0.3 mm on each side, with 40-1000 such units per scaffold (Figure 1) [10, 86]. The scaffold is housed in a microreactor system that perfuses all tissue units uniformly with culture medium at controlled flow rates, and allows *in situ* imaging. Many liver-enriched programs of gene expression are maintained at approximately physiological values when the hepatocyte-rich fraction is cultured in this system [10], and endothelia have occasionally been observed lining the surface of vessel-like structures in these cultures [86].

This chapter reports on the morphological and proliferation behavior of endothelia in deliberate co-cultures of rat liver endothelium with hepatocytes maintained for two weeks, using female EGFP-expressing endothelia against a background of unlabeled male hepatocytes.

4.2 Materials and methods

4.2.1 Culture medium

A serum-free “HGM” medium [125] was used with the following modifications [10, 88]: niacinamide (Sigma-Aldrich), 0.305 g/l; glucose (Sigma-Aldrich), 2.25g/l; 1 mM L-glutamine (Sigma-Aldrich); ZnCl₂ (Sigma-Aldrich), 0.0544 mg/l; ZnSO₄·7H₂O (Sigma-Aldrich), 0.0750mg/l; CuSO₄·5H₂O (Sigma-Aldrich), 0.020mg/l; MnSO₄ (Sigma-Aldrich), 0.025mg/l; EGF (Collaborative), 20 ng/mL; and 0 ng/mL HGF. (See Appendix 2) Endothelial Growth Medium (EGM-2 bullet-kit, Cambrex) was mixed with HGM 1:1 (v/v) to create “HEGM” for the initial days of culture.

4.2.2 Cell isolation

Cells were isolated from 150 to 230-g male Fischer rats by a two-step collagenase perfusion [10]. A 25 mL/min flow rate was used for isolation of hepatocytes and separate isolations with a 15 mL/min flow rate were used for isolation of the endothelial cell fraction. Hepatocyte viability was 90–95% (trypan blue, Gibco). The supernatant material from the first two centrifugation steps of the cell isolate was used to isolate endothelial cells [126]. For some experiments, the EGFP-endothelial cell fraction was isolated from 150-250g female EGFP-positive Sprague-Dawley rats, which were bred from EGFP-positive males that were a generous gift of M. Okabe [127, 128]. Endothelial

fractions were 80-90% pure as assessed by analysis by DiI-LDL uptake and immunostaining of 3 replicate isolations plated for 2 hr on collagen I. Cells were fixed in 2% paraformaldehyde (EMS) and stained with anti-GFAP antibodies (Chemicon) and ED-2 antibodies (Serotec) followed by Cy3 secondary goat antibodies (Jackson ImmunoResearch). Nuclei were marked with Hoechst 33342 (Molecular Probes). GFAP- or ED2-positive cells were counted manually in 4 randomly selected areas per well and divided by total nuclei to yield percentages of stellate cells (3%) and Kupffer cells (10%), yielding by difference 87% as endothelial cells [106].

4.2.3 Microreactor seeding and maintenance

Spheroids were formed by seeding 500 mL spinner flasks (Bellco Glass) containing 100 mL of HEGM with 20×10^6 hepatocytes (mono-cultures) or 20×10^6 hepatocytes plus 60×10^6 total cells from the liver endothelial cell fraction (co-cultures) and stirring at 85 rpm for 24 hr. Spheroids were filtered sequentially through 300- and 100- μm nylon meshes (SEFAR), resuspended in 25 mL HEGM, centrifuged at 40g for 2 min, and resuspended in 30 mL HEGM for seeding.

Microreactors (Figure 1.3C) were operated as previously described [86, 88]. (See Appendices 3-5) The system was primed with HEGM (1 hr, 37°C). Spheroids were introduced by syringe and then axial flow was maintained at 0.5mL/min. Crossflow through the scaffold (40 $\mu\text{l}/\text{min}$) was directed toward the filter for the first 24 hours, then the culture medium was changed, an inline double filter of 0.8/0.2 μm size (Pall) was installed on the crossflow line, and the flow direction was permanently reversed to flush debris. The medium and the inline filter were changed every 3 days thereafter. For all cultures, HEGM was used for the first 6 days and HGM thereafter.

4.2.4 2D collagen gel sandwich

Collagen gel sandwiches were prepared in 6-well plates (Falcon) using 600 μl collagen solution (Cohesion) for the lower layer (gelled overnight at 37°C) and 300 μl for the upper layer, which was added 4 hr after cell seeding and allowed to gel for 1 hr before addition of culture medium [10]. (See Appendix 12) Cells were seeded at 50,000 total cells/ cm^2 , (co-cultures comprised a 3:1 mix of endothelial cell fraction:mono-culture fraction). Medium was changed every other day. HEGM was used for the first 6 days, followed by HGM.

4.2.5 SEM and image analysis

Microreactor tissue was processed for SEM imaging according to previously published protocols [129, 130] (see Appendix 6) and viewed under a JEOL JSM-5600 LV scanning electron microscope. Features comprising pores of 5-10 μm in diameter in each image of a single channel were quantified by importing into Metamorph (Universal Imaging). Images were taken from experiments using three separate perfusions with two microreactors in each group per perfusion. A total of 56 images were counted.

4.2.6 *In situ* two-photon microscopy and image analysis

A protocol similar to that described previously was used [86]. The distance between the objective and the microreactor was regulated with a MIPO 500 piezoelectric driver (Piezosystem Jena) with a range of 400 μm . A Zeiss Water Achroplan 20x objective was used to accommodate long working distance between the viewing window and the top of the tissue mass (Fig 1.3C) in order to maximize the viewing area without compromising resolution. A microscope environmental chamber was constructed to maintain cultures in humidified air with 8.5% CO_2 and at 37°C during imaging.

Two microreactors were imaged per experiment. Four channels were randomly selected on day 1 post-seeding from each microreactor and observed on days 2, 6, and 11 post-perfusion. For each channel imaged, the piezo was initially brought to its zero position and the objective was allowed to focus on the microreactor filter. Between scanning each image, the piezo was instructed to move at 3 μm per step in the z-direction, for a total of 61 images per channel. For consistency, all samples were excited by the same laser power at 100 mW before entering the microscope. These images were imported into Metamorph for low-pass filtering noise reduction and image analysis.

In Metamorph, raw image data without filtering were first subjected to a universal threshold to define EGFP-positive objects before morphometry analysis. These data were read by a Matlab v6.5 script file which counted the total number of pixels that were above threshold value. This number was divided by the total number of pixels in each image to yield percent fluorescent pixels.

All images for one sample on one time point were averaged to yield percentage of fluorescent pixels. Perimeter (P), area (A), and centroid position were calculated for all the objects in each image. For each object, metrics associated with tube-like morphology were then calculated. Fiber length (Fl) and fiber breadth (Fb) were calculated by the following definitions: $Fl = \left[P + (P^2 - 16A)^{1/2} \right] / 4$, $Fb = \left[P - (P^2 - 16A)^{1/2} \right] / 4$. Inner radius (Ir) and outer radius (Or) were defined as the distances from an object's centroid to the nearest and farthest point on the perimeter, respectively. Shape factor was calculated as $4\pi A / P^2$. Axial fiber ratio was calculated as Fl / Fb . Radius ratio was calculated as Or / Ir . Each category was averaged over all images of each sample on each day.

4.2.7 RNA and DNA isolation

One mL of Trizol (Invitrogen) was added directly to samples and kept at -80°C until ready for RNA and DNA isolation, which was performed according to manufacturer's protocols. RNA from the aqueous phase was purified using the RNeasy mini kit (Qiagen) according to the manufacturer's instructions. (See Appendix 7) The concentration and quality of purified RNA was determined by assessing the ratio of absorbance at 260nm to 280nm, and only samples with a ratio within the range 1.7-2.1 were used. The RNA was stored at -80°C . The interfacial and chloroform phases remaining after RNA extraction into the aqueous phase were used to isolate genomic DNA using the manufacturer's protocol. (See Appendix 8)

4.2.8 Quantification of EGFP cell percentages in co-cultures

Expression levels of EGFP mRNA per (endothelial) cell determined via RT-PCR (data not shown) were found to be significantly higher *in vitro* than *in vivo*, and thus EGFP mRNA levels were not reliable for quantitative analysis of EGFP cell numbers under different conditions. The fraction of EGFP cells present when female EGFP liver-derived endothelia were cultured with non-fluorescent male Fischer rat-derived hepatocytes was thus determined using the ratio of genomic GAPDH to Y-chromosome (Sry). A calibration curve was constructed by mixing a defined number of cells from the EGFP liver endothelial cell fraction (cultured on tissue culture treated 6-well plates with EGM for one day) with freshly-isolated Fischer hepatocytes to achieve a range of ratios between 0% and 90% female cells. Genomic DNA and RNA were isolated from these samples and

quantitative PCR were performed to obtain ratio of Sry:GAPDH or EGFP:18s, using the SYBR Green kit (Qiagen) according to manufacturer's instructions. Primers (salt-free purity from Qiagen Operon) were: Sry (forward) 5'-GCCTCCTGGAAAAGGGCC-3', (reverse) 5'-GAGAGAGGCACAAGTTGGC-3'; GAPDH (forward) 5'-GTGGTGCAGGATGCATTGCTGA-3', (reverse) 5'-ATGCTGGTGCTGAGTATGTTCG-3'.

4.2.9 Immunohistochemistry

Laser-machined polycarbonate (rather than silicon) scaffolds were used to facilitate histological sectioning. On day 13, microreactors were perfused with 2% paraformaldehyde in PBS for one hour, washed in 6.8% sucrose in PBS overnight and dried in 100% ethanol for 1 hour before embedding in Technovit8100 (EMS). Plastic scaffold pieces were removed under a microtome and embedded tissue samples were re-embedded in Technovit8100. Samples were cut into 4-micron sections and stained [112]. (See Appendix 10) Primary antibodies included mouse-anti-rat SE-1 (IBL America), CD31 (Chemicon), ED2 (Serotec), GFAP (Serotec), and SMA (Sigma). Goat-anti-mouse biotin-conjugated antibodies and streptavidin-conjugated Cy3 were used as secondary and tertiary antibodies (Jackson Immunoresearch).

4.3 Results

4.3.1 Co-culture with endothelium alters tissue surface morphology

SEM images of mono-cultures maintained 3 days in perfusion culture (Figure 4.1) showed cell-cell contact and large ($>10\ \mu\text{m}$) fluid duct structures, corresponding to previous findings [86]. Both mono-cultures and co-cultures showed cell surface microvilli typical of hepatocytes, and both cultures exhibited numerous small pore structures ranging 5-10 μm in diameter, similar to the average diameter of sinusoids in liver (Figure 2). These tiny pore structures appearing on the surface were about 3 times more numerous in endothelial co-cultures than in mono-cultures ($n_{\text{microvessel}} = 19.5 \pm 2.1$ per channel for co-cultures and $n_{\text{microvessel}} = 7.3 \pm 5.4$ per channel for mono-cultures (mean \pm SD)). Occasionally (i.e., about one in 10 channels), a smoothly-wrinkled cell, distinctly different in

appearance from hepatocytes, is observed around the opening of one of these tiny vessel-like structures (Figure 4.1D).

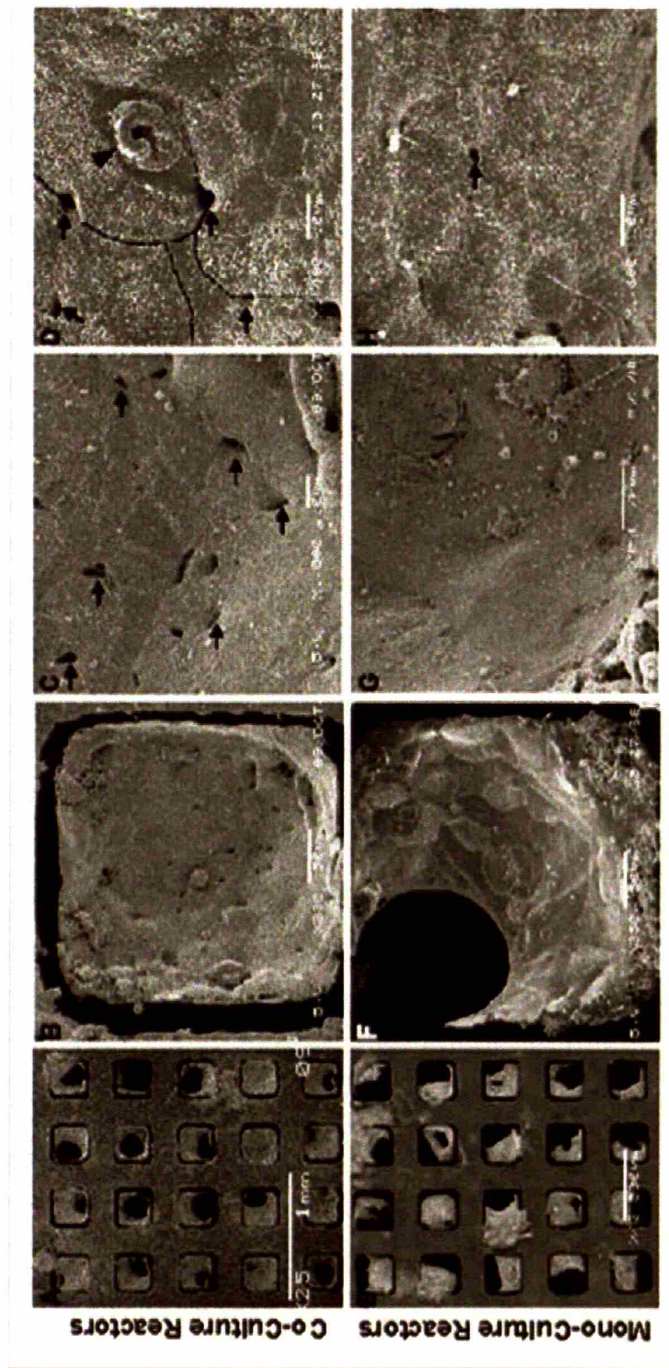


Figure 4.1: SEM images of 3-day old bioreactor cultures. Tissue structure in both mono-culture (A-D) and co-culture (E-H) groups showed hepatocyte microvilli and cell-cell junctions. In co-culture many more pore openings (arrows) were observed. Occasionally a smooth cell type is observed around the pore openings (arrowhead in D).

4.3.2 The endothelial cell fraction proliferates and forms 3D networks in 3D perfusion culture, but is lost in 2D culture.

We speculated that the 5-10 μm pore structures seen in SEM images might reflect organization of endothelial cells present in the cultures into microvessel-like structures. We thus sought to follow the spatial organization of endothelial cells in co-cultures over the typical 2-week culture period by capturing sequential images of endothelial cells in 3D culture. We found that the level of green fluorescence expressed by primary endothelia derived from EGFP rats was much brighter than the autofluorescence from wild-type (Fischer rat) hepatocytes (Figure 4.2), thus allowing a high signal-to-noise ratio in 3D imaging experiments.

We have found previously that confocal imaging causes photodamage to hepatocytes and has a relatively poor depth of penetration in 3D tissue. For live, non-invasive imaging, we thus used multi-photon microscopy, which uses longer-wavelength excitation light that penetrates more deeply and excites only a tiny volume, preserving tissue viability [86, 102]. Penetration depth is particularly critical here, as the continuous perfusion of the tissue requires a distance of several hundred microns between the objective and the tissue (Figure 1.3C), and hepatic tissue is strongly scattering.

Sequential 3-D images of EGFP cells in microreactor culture revealed an evolution of organization from an initial dispersed state to networks of microvessel-like structures over approximately a week. We first made several qualitative observations. On day 2 post-perfusion the spheroids were attached to the scaffolds, and the EGFP cells had a mostly rounded morphology and were distributed seemingly randomly among the cell aggregates. By day 6 we observed that a substantial fraction of the EGFP cells were more elongated, and in some cases appeared to be tube-like. The number of EGFP cells also appeared greater at day 6 compared to day 2. On day 11 we could clearly observe network and cord-like structures and an apparent increase in EGFP cell numbers (Figure 4.2).

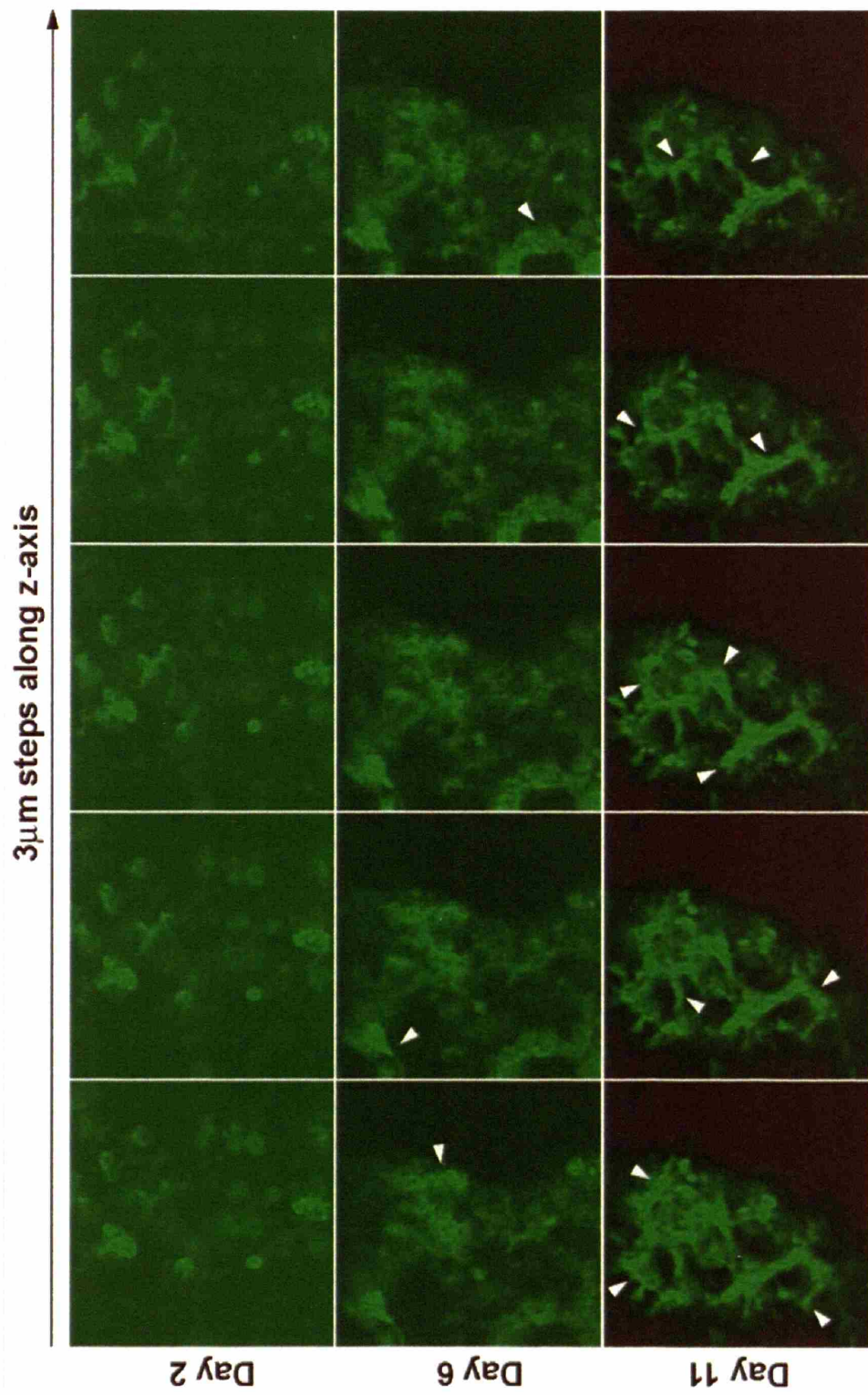
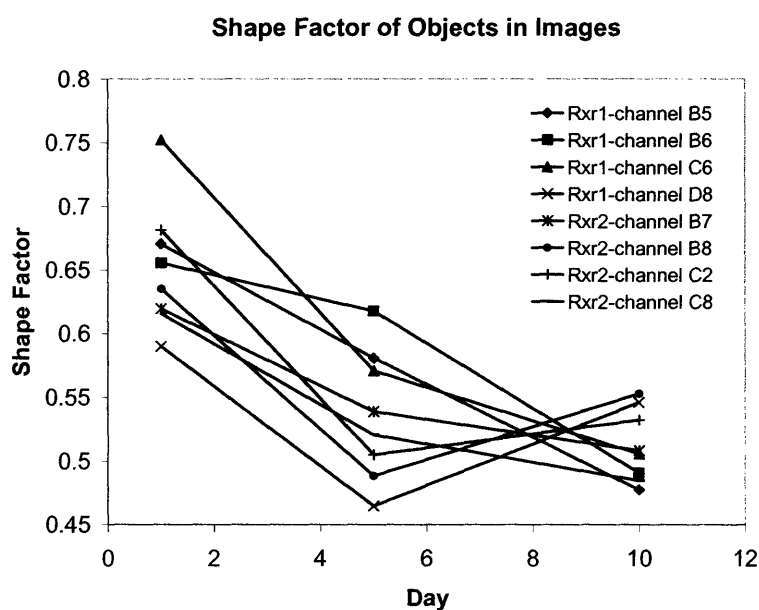


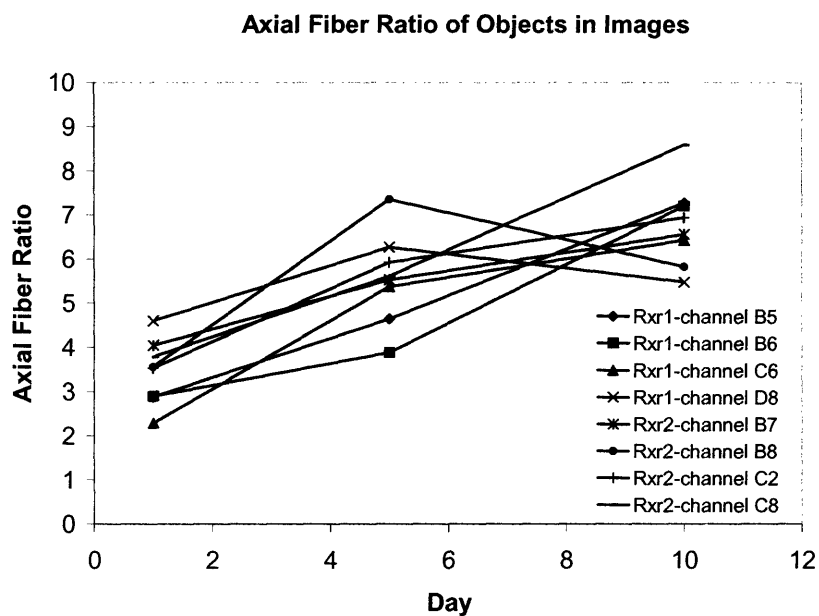
Figure 4.2: A reactor channel observed on day 2, 6, and 11 post-perfusion. Image x-y plane sections are shown here from left to right in 3 μm intervals. Arrowheads indicate tube formations.

In order to assess changes in cell number and organization quantitatively, fluorescent pixel counting and morphometry analysis were applied to all the images (i.e., to each section within an optical stack for each channel and each reactor and each time point). Three metrics, which each compare facets of the longest/shortest dimension of the object, were used to assess changes in the cell morphology. The shape factor indicated the degree of rounding (0 = absolutely flat; 1 = perfectly round). The axial fiber ratio presumed the shape to be a fiber and assessed the degree of elongation by comparing the length to width [131]. Radius ratio was a similar representation of this elongated cell shape. By each of these metrics, the shape of the EGFP cells became more elongated over time in culture, as indicated by the decreases in shape factor and increases in axial fiber ratio and radius ratio (Figure 4.3A-C).

A



B



C

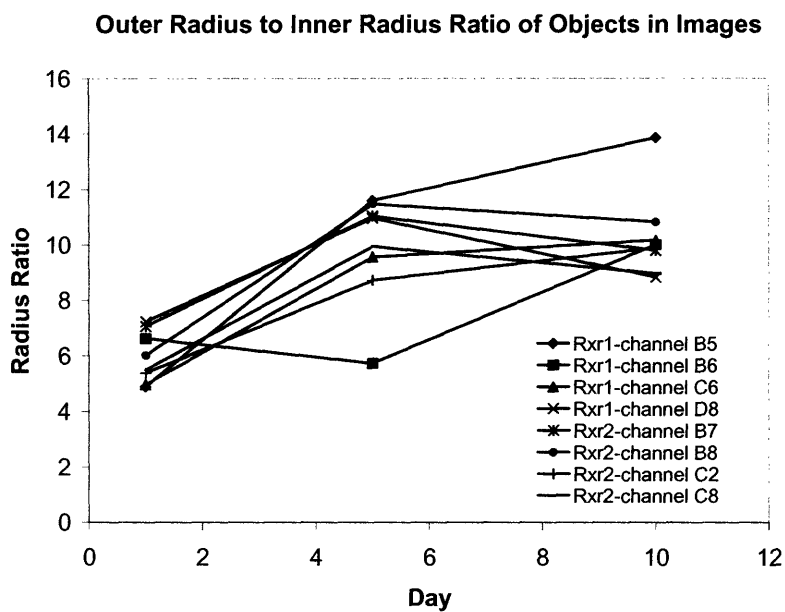


Figure 4.3: Morphometry analysis defined cell elongation using three parameters: shape factor (A), axial fiber ratio (B), and radius ratio (C). All three parameters indicated that cells became more elongated over time.

Parallel to the two-photon experiment, mono- and co-cultures were prepared in a 2D collagen gel sandwich (CGS) system, using identical culture medium and the same starting cell populations. These cultures were observed with an epifluorescence microscope on the same days as the microreactor multi-photon experiment (Figure 4.4). On day 2 there were many EGFP cells scattered around hepatocyte islands (Figure 4.4A). Many of these cells attached to outer perimeter of hepatocyte islands, similar to what was reported in Matrigel co-cultures [65]. By day 6, fewer EGFP cells were seen (Figure 4.4B-C) and the EGFP cells were almost absent by day 11 (Figure 4.4D). Judging from cell morphology, some of the surviving EGFP cells are stellate cells, which showed dendritic cell processes (Figure 4.4C). The morphology of hepatocytes in 2D collagen gel sandwich mono-cultures (Figure 4.4E-H) was similar to the hepatocyte morphology in 2D endothelial co-cultures. Cells with the morphology of stellate cells were also observed in mono-cultures at longer times (Figure 4.4G). Overall the EGFP cell population was not well-maintained in 2D co-cultures, and no microvessel structures were seen. These primary endothelial cells also could not survive alone without the hepatocytes in the bioreactors (data not shown), although microreactor culture fostered attachment and survival of rat lung microvessel endothelial cells on vertical channel walls over 2 days.

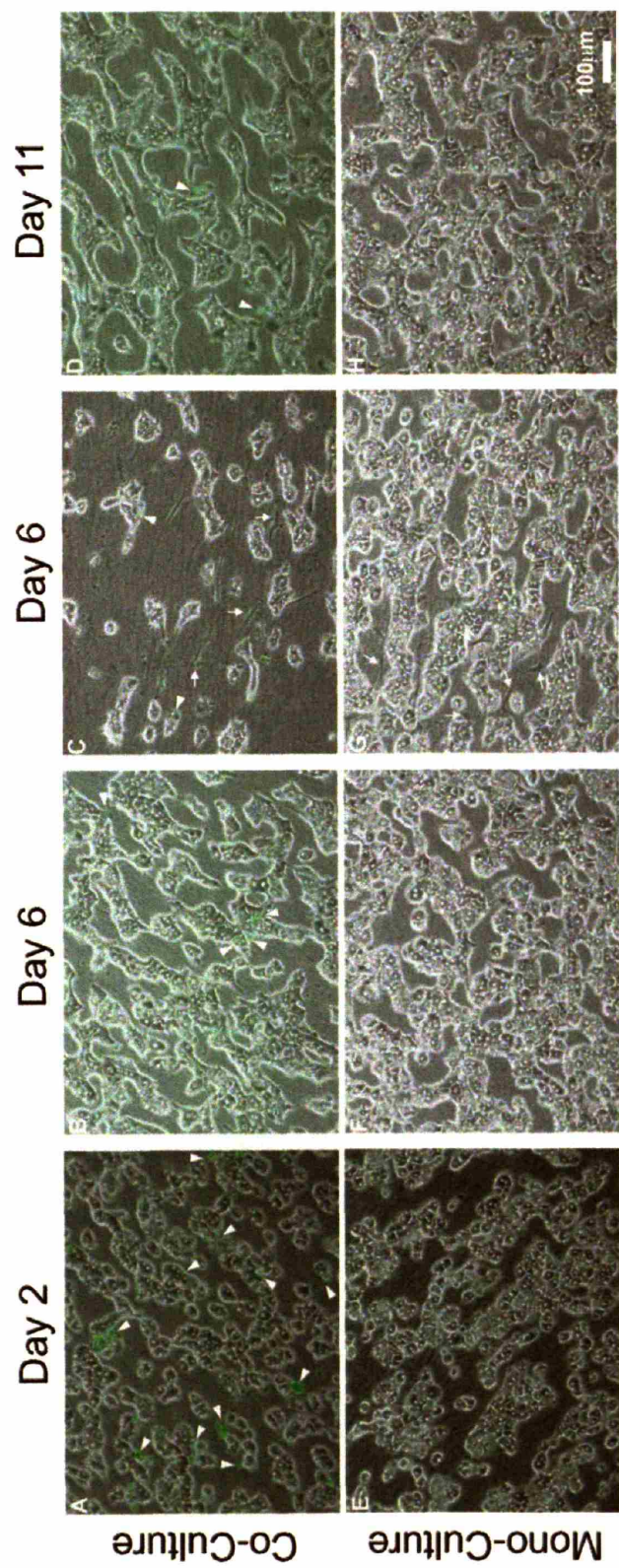
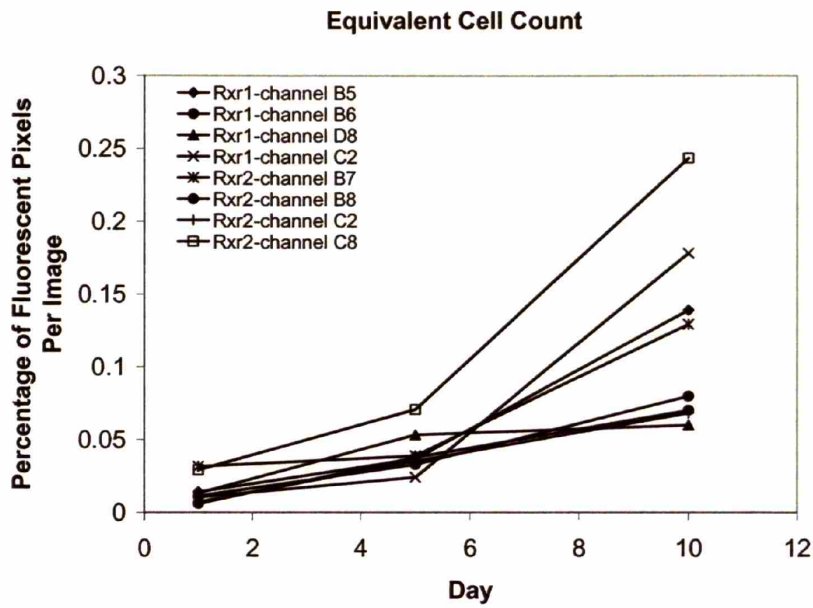


Figure 4.4: Co-culture (A-D) or mono-culture (E-H) in 2D collagen gel sandwich. Many EGFP-positive cells (arrowheads) were seen on day 2 post-perfusion in the co-culture but their presence decreased as time went on. On day 6 cells with stellate morphology (arrows) were occasionally observed in both groups, regardless of EGFP expression. On day 11 very few EGFP cells remained.

4.3.3 Quantification of EGFP-positive population

Since only the EGFP cells emitted green fluorescence above a threshold level, the percentage of fluorescent pixels per image was used as a surrogate measure of cell number. The pixel count confirmed that the number of EGFP cells increased over 10 days of perfused microreactor culture (Figure 4.5A). We compared the changes in numbers of EGFP cells over time in 2D and 3D cultures using quantitative PCR analysis of genomic DNA using the ratio of Sry to GADPH (genomic). The percentage of EGFP cells in 3D microreactor culture, as measured by %female cells, increased from an initial level of 7% to 12% over 11 days in culture while control mono-cultures had no EGFP (female) cells (Figure 4.5B), a finding consistent with the results obtained from image analysis in 3D and epifluorescence in 2D. Thus, 3D perfused microreactor culture fosters retention and proliferation of the EGFP non-parenchymal fraction, as well as organization of these cells into network structures within the parenchymal tissue, while the 2D collagen gel sandwich culture does not support any of these behaviors of the endothelial fraction-derived non-parenchymal cells.

A



B

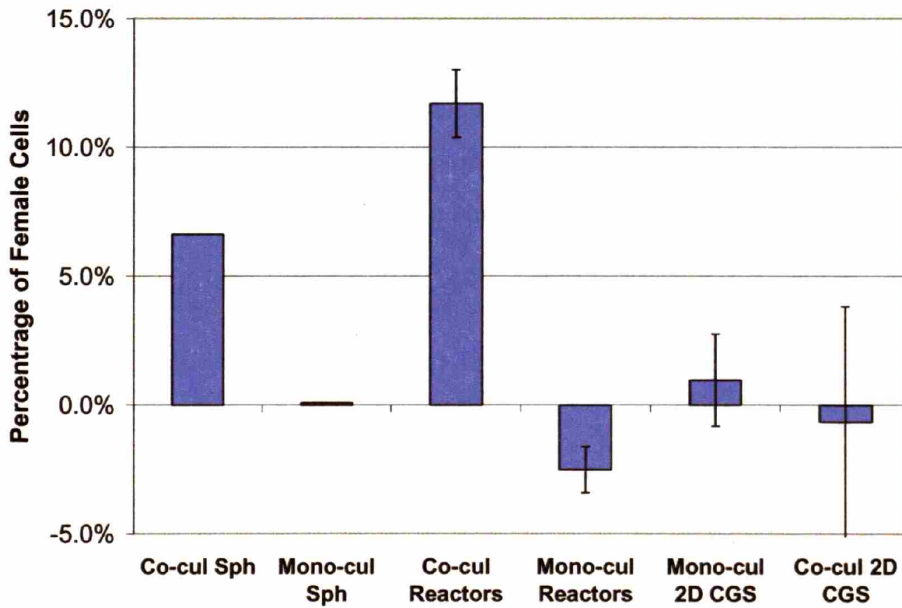


Figure 4.5: Pixel analysis (A) showed that over time EGFP cell number increased in the co-culture bioreactor. Percentage of female cells determined by quantitative PCR on ratio of genomic Sry and GAPDH DNA (B).

4.3.4 Immunohistochemical identification of endothelial cells in microreactor culture

The initial endothelial cell fraction derived from the EGFP liver was ~85% pure. We thus sought to establish by immunostaining that endothelial cells were indeed strongly present at day 11, as proliferation of stellate cells and death of the endothelia could possibly have been responsible for the networks observed. Using the SE-1 antibody against sinusoidal endothelial cells (SE-1), we found that sinusoidal endothelial cells were present throughout the interior of the tissue in the endothelial co-culture, but largely absent in mono-culture (Figure 4.6A-B). Large vessel endothelia, revealed by anti CD-31 staining, were present in the co-culture at tissue-fluid interface, but no evidence of such endothelia was seen in the mono-culture (Figure 4.6C-D). Thus, both sinusoidal and large vessel endothelial cells were present in the co-cultures and located in physiologically-appropriate regions of the tissue (i.e., small vessel within the tissue and large vessel at the tissue interface with the fluid). The EGFP signal does not seem to consistently survive through the processes necessary for tissue embedding, and in several areas did not co-localize with red antibody staining. It is especially a problem for small cells such as sinusoidal endothelial cells. In fact, embedded EGFP liver tissue as positive controls showed mainly green fluorescence in hepatocytes, while the non-parenchymal cells rarely showed enough signals indicating co-localization (data not shown). Furthermore, some surviving non-parenchymal cells from the WT hepatocyte-enriched fraction may contribute to the staining without emitting any green fluorescence.

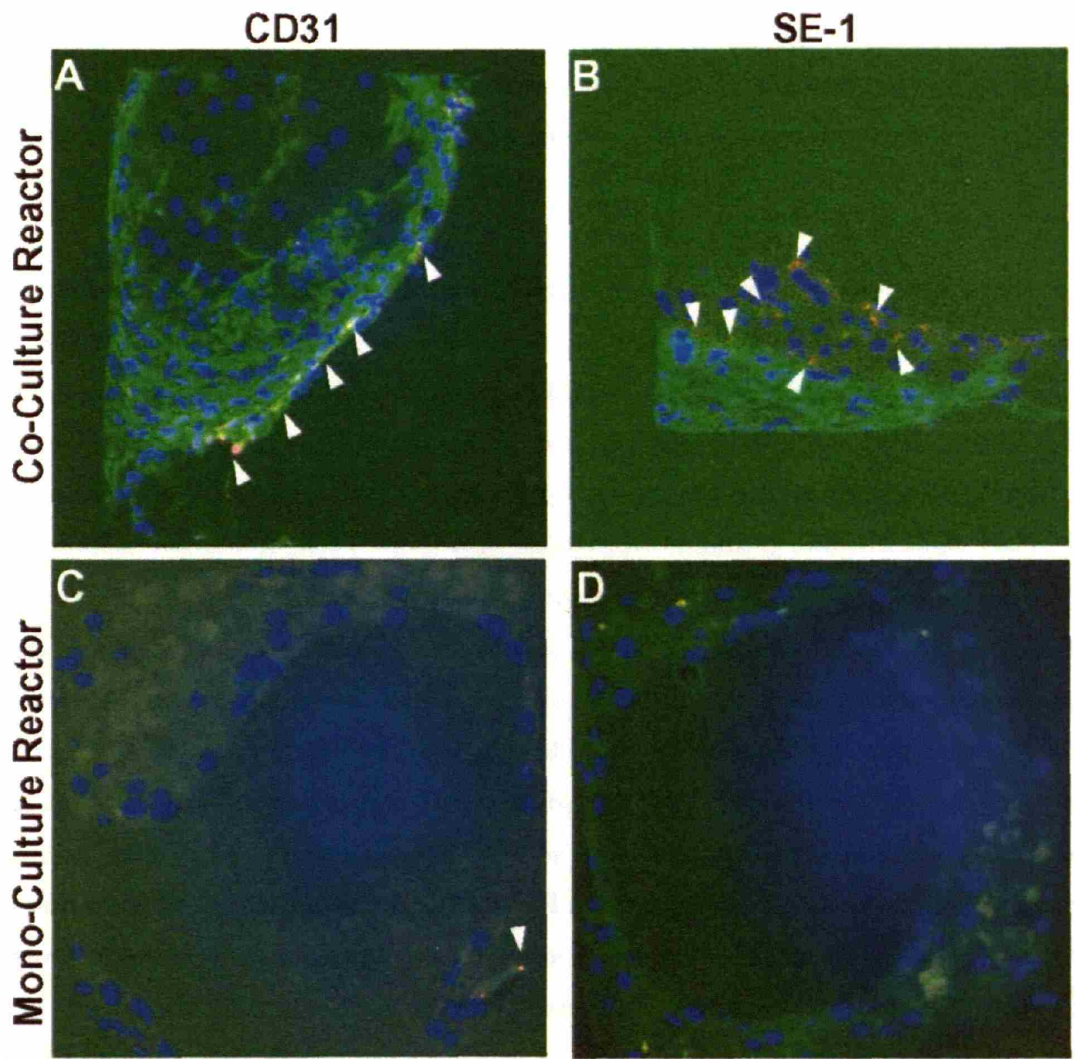


Figure 4.6: Immunohistochemistry of CD31 (A,C) and SE-1 (B, D) on co-culture (A-B) and mono-culture (C-D) bioreactor tissue. Blue: Hoechst nuclei stain; Green: EGFP; Red: CD31 or SE-1 antibody.

4.4 Discussion

Sinusoidal endothelia in liver play a key role in hepatic physiology and pathophysiology [11]. Their survival in culture is generally poor and their distinctive phenotype -- characterized in part by fenestrations, expression of (in rats) the specific marker SE-1, and low or absent CD31 expression --

is labile [18, 29, 49, 126]. In serum free, hormonally-defined medium, purified rat SEC plated on extracellular matrix survive less than a week, even when plated at high cell density, and lose most fenestrae within a few days [18, 126]. Addition of hepatocyte-conditioned medium to SEC culture modestly improves survival but stimulates overgrowth by stellate cells after about a week of culture [18].

Liver-derived endothelial cells have been observed in cultures of rat and porcine primary hepatocytes maintained for several weeks in culture formats that foster 3D tissue formation, although whether these cells represent phenotypically normal sinusoidal endothelia or endogenous large vessel endothelia that are also present in the initial cell isolate is not known, as SE-1 was not used to delineate populations [78, 79, 124]. Here, we supplemented the standard hepatocyte isolate with a purified fraction of EGFP+ liver endothelial cells comprising primarily sinusoidal endothelia to give an approximate initial endothelial cell composition of 7% by number. The antibody SE-1 is a specific marker of rat liver sinusoidal endothelia, and we found that SE-1+ cells were abundantly present throughout the interior of the tissue mass after 13 days of culture. To our knowledge, this is the first report of retention of the SE-1 sinusoidal marker for two weeks accompanied by formation of an apparent microvessel network; SE-1 staining has been previously reported as a rare event in long-term culture and not accompanied by tube formation [132]. Most endothelia express the adhesion molecule CD31 (platelet endothelial cell adhesion molecule) at cell-cell junctions, where it facilitates leukocyte trafficking. Normal liver sinusoidal endothelia express relatively low levels of CD31, though strong expression in liver microvessels is observed in cirrhosis and other diseased states and purified liver SEC upregulate CD31 expression on their surfaces in culture in a VEGF-dependent manner [29]. Our cultures contained CD31+ endothelia at the interface of bulk fluid flow with the tissue, but rarely were CD31+ cells seen inside the tissue mass. The source of these cells may be surviving large vessel endothelia, or sinusoidal endothelia induced to express CD31 due to the local environment present at the fluid-tissue interface. Previous report of long-term 3D hepatocyte culture also found endothelium to be at the fluid-tissue interface [78, 79].

Most endothelia can form tubes and vessel-like structures in culture, at least transiently, under appropriate matrix conditions. Rat liver SEC form tubes within hours when cultured on matrigel [65, 133] and can form tubes in laminin and collagen gels [133, 134]. When primary rat hepatocytes are added to tubes formed on matrigel from human dermal microvessel or umbilical

vein endothelia, or rat liver-derived endothelia, the hepatocytes migrate to the vessel structures, and the dermal microvessel and umbilical vein endothelia persist in long term culture (presumably due to stabilization of vessel structure by fibroblasts present in the primary cell isolates) [65], consistent with other observations that endothelial cells from many tissues can be induced to form stable microvessel networks in the presence of fibroblasts [135, 136]; however, the vessels formed by liver-derived endothelia in the study by Yaakov et al. collapse and disappear within about a week [65]. Most primary liver cell isolates contain stellate cells, which can proliferate robustly in culture, and we suspect that the stellate cells present in our cultures contribute to maintenance of sinusoidal endothelial cell viability and phenotype under our particular culture conditions. We also observed more robust behavior of endothelia from other tissues in our cultures -- rat lung microvessel endothelial cells migrated out of channels and proliferated rapidly in co-culture with hepatocytes in the bioreactors (data not shown), in sharp contrast to the moderate proliferation we observed for the sinusoidal endothelia.

Our culture method differs from previous methods in at least two ways that may be important for stabilization of the connective tissue components – localized perfusion flow, and 3D mechanical support of the tissue structure. Flow across pulmonary microvessel endothelial cells cultured on collagen gels is associated with enhanced tube formation of cells growing into the gel [137] and slow interstitial perfusion has been reported to induce organization of endothelial cells into microvessel networks in a VEGF-dependend manner [95]. We are currently evaluating whether the microvessel-like networks we observe are functionally perfused.

Organization of the dispersed endothelia into vessel-like structures required about a week, a time scale comparable to that required for endothelia to invade avascular hepatocyte islands following partial hepatectomy [138] and far longer than is typically required for endothelial tube formation on matrigel. We observe some proliferation of the endothelial cell fraction during the process of network formation. We thus speculate that the process has some features of angiogenesis, which involves sprouting of endothelial microvessels accompanied by endothelial proliferation, and can occur *in vitro* under some conditions, including isolated endothelia forming networks in matrix gels [139] or growing into tumor spheroids [140]. During liver regeneration, hypoxic hepatocyte islands increase VEGF production [96], an important survival factor for primary liver endothelial cells [20, 22] and an angiogenesis signal for endothelial cells in general [141, 142]. Oxygen gradients

are predicted to exist in our cultures, and although we indeed find upregulation of hypoxia-inducible genes at the 3-day time point if the cultures are maintained without perfusion [88], no such induction has been observed under the culture conditions used here.

In conclusion, we report spontaneous formation of microvessel-like networks in an *in vitro* 3D perfusion culture system comprising co-cultures of rat hepatocytes and liver endothelial cells over a 2-week culture system. The formation of microvessel networks is consistent with enhancement of endothelial-specific genes as revealed by global gene expression profiling (see next chapter). This culture system may prove useful in analysis of chronic pathophysiological behaviors *in vitro*, and is currently being adapted to multi-well format [10, 143].

Chapter 5

Effects of rat liver endothelia on Gene Expression in 3D Perfusion Hepatocyte Co-culture

5.1 Introduction

Liver physiology and pathophysiology are governed in large part by an interwoven set of interactions between hepatocytes and non-parenchymal cells (NPCs), which include stellate cells, Kupffer cells, and endothelial cells. When hepatocytes are isolated from liver and placed in culture, they usually rapidly lose liver-specific functions such as cytochrome P450 (CYP) expression [10]. This phenomenon has been attributed, in part, to loss of cell-cell, cell-matrix, and soluble signals that are a normal part of the heterotypic cell milieu *in vivo*. Accordingly, improvements in some hepatocyte functions *in vitro* are observed when hepatocytes are deliberately co-cultured with other cell types [41, 46, 61, 144-146] even when the cells are not of liver origin [147-149].

Improvements in hepatocyte function *in vitro* are also often reported in various 3D culture configurations initiated with primary hepatocyte isolates that are not deliberate co-cultures [51, 84, 108, 150-152]. Hepatocyte populations prepared by standard collagenase perfusion protocols typically contain a few percent NPCs, and most NPC types are often observed histologically in 3D cultures [78, 79, 86, 123], suggesting that 3D culture may foster heterotypic cell interactions in ways that may stabilize hepatocyte phenotype.

Endothelial cells, which comprise about 19-21% of all liver cells [1], play a crucial role in liver functions ranging from development [153] to protection of liver during stress [23]. They are the second largest cell population in liver, but may be preferentially lost during liver cell isolation procedures due to their close contact with perfusion flow. In culture, sinusoidal endothelia typically lose their characteristic fenestrations within days and fail to survive more than about a week [18, 126].

We found that when EGFP+ rat liver-derived endothelia are co-cultured with primary (unlabelled) hepatocytes in 3D microreactor culture system that includes localized culture medium flow through the tissue (Fig 1), the EGFP-labeled cells proliferate moderately and organize into networks of microvessel-like structures, as observed by multi-photon microscopy over a period of 2 weeks. Further, cells within these tissue-like structures stain positive for the rat sinusoidal endothelial cell-specific marker SE-1 [30]. In contrast, when the same starting cell populations were maintained in 2D culture, no evidence of endothelia was found at 2 weeks.

At least two questions arise from these previous studies. First is the comparative fate in the 3D culture of endothelial cells, and other non-parenchymal cells, that are present in the standard hepatocyte isolates and the EGFP+ cells added in deliberate co-cultures. Cells positive for pan-endothelial markers have been observed in long-term 3D cultures prepared from standard hepatocyte isolates [78, 79] and cells with endothelial morphology have likewise been observed occasionally in previous experiments with the 3D microperfused system, but retention of sinusoidal endothelia has not been well-characterized [86]. Second is whether the sustained presence of endothelial cells in deliberate co-cultures significantly influences hepatocyte function compared to cultures prepared from standard hepatocyte isolate (“mono-culture”), which contains ~5% total NPC of all types and relatively few endothelia. Here, we address these questions with a combination of immunohistochemistry and global transcriptional profiling.

5.2 Materials and Methods

5.2.1 Cell Isolation and Culture

A serum-free hepatocyte growth medium (HGM) [125] was used with the following modifications [10, 88]: 0.305 g/l niacinamide; 2.25g/l glucose; 1 mM L-glutamine; 0.0544 mg/l ZnCl₂; 0.0750mg/l ZnSO₄·7H₂O; 0.020mg/l CuSO₄·5H₂O; 0.025mg/l MnSO₄; 20 ng/ml EGF (Collaborative, Bedford, MA); and 0 ng/ml HGF. (See Appendix 2) Endothelial growth medium (EGM-2, Cambrex, Walkersville, MD) was mixed with HGM 1:1 (v/v) to create “HEGM.”

A two-step collagenase perfusion procedure [10] was performed on 150-230g male Fischer and female EGFP+ Sprague-Dawley rats for wild-type (WT) hepatocyte and EGFP+ endothelial

cell isolations, respectively. EGFP⁺ rats were bred from EGFP⁺ males that were a generous gift of M. Okabe [127, 128]. Animals were treated according to protocols approved by the MIT Committee of Animal Care. Flow rates at 25 and 15 mL/min were used for separate isolations of the hepatocyte and the endothelial cell fractions, respectively. Hepatocyte viability was 90–95% (trypan blue, Gibco, Carlsbad, CA). The supernatant from the first two centrifugation steps of the cell isolate was used to isolate endothelial cells [126]. Endothelial fractions' purity was assessed by immunostaining of 3 replicate isolations plated for 2 hours on collagen I. Cells were fixed in 2% paraformaldehyde (EMS, Hatfield, PA) and stained with anti-GFAP (Chemicon, Temecula, CA) and ED-2 antibodies (Serotec, Oxford, UK) followed by Cy3 secondary antibodies (Jackson ImmunoResearch, West Grove, PA). Nuclei were marked with Hoechst 33342 (Molecular Probes, Carlsbad, CA). GFAP- or ED2-positive cells were counted in 4 randomly selected areas per well and divided by total nuclei to yield percentages of stellate cells (3%) and Kupffer cells (10%), yielding by difference 87% as endothelial cells [106].

5.2.2 Microreactor seeding and maintenance

Spheroids were formed in 500 mL spinner flasks (Bellco, Vineland, NJ) containing 100 mL of HEGM with 20×10^6 hepatocytes (mono-cultures) or 20×10^6 hepatocytes plus 60×10^6 total cells from the liver endothelial cell fraction (co-cultures) and stirring at 85 rpm for 24 hours. Spheroids were filtered sequentially through 300- and 100- μm nylon meshes (SEFAR, Depew, NY) and cultured in microreactors (Fig 1) as previously described [86, 88]. (See Appendices 3-5) HEGM was used for the first 6 days, followed by HGM.

5.2.3 2D Collagen Gel Sandwich (CGS)

CGSs were prepared in 6-well plates using 600 μl collagen solution (Angiotech, Palo Alto, CA) for the lower layer (gelled overnight at 37°C) and 300 μl for the upper layer, which was added 4 hours after cell seeding and allowed to gel for 1 hour before addition of culture medium[10]. (See Appendix 12) Cells were seeded at 50,000 total cells/ cm^2 , (co-cultures comprised of a 3:1 mix of endothelial cell fraction:mono-culture fraction). Medium was changed every other day. HEGM was used for the first 6 days, followed by HGM.

5.2.4 RNA Isolation

One mL of Trizol (Invitrogen, Carlsbad, CA) was added directly to samples and stored at -80°C until ready for RNA isolation, performed according to manufacturer's protocols. RNA from the aqueous phase was purified using the RNeasy mini kit (Qiagen, Valencia, CA). (See Appendix 7) The concentration and quality of purified RNA were determined by its absorbance at 260nm and 280nm, and only samples with a 260nm:280nm ratio within 1.7-2.1 were used. The remaining phases after RNA extraction were used to isolate genomic DNA using the manufacturer's protocol. (See Appendix 8)

5.2.5 Immunohistochemistry

Laser-machined polycarbonate (rather than silicon) scaffolds were used to facilitate histological sectioning. On day 13, microreactors were perfused with 2% paraformaldehyde in PBS for one hour, washed in 6.8% sucrose in PBS overnight and dried in 100% ethanol for 1 hour before embedding in Technovit8100 (EMS). Plastic scaffold pieces were removed under a microtome and embedded tissue samples were re-embedded in Technovit8100. Samples were cut into 4-micron sections and stained [112]. Primary antibodies included SE-1 (IBL America, Minneapolis, MN), CD31 (Chemicon), ED2 (Serotec), GFAP (Serotec), and SMA (Sigma). Biotin-conjugated antibodies and streptavidin-conjugated Cy3 were used as secondary and tertiary antibodies (Jackson ImmunoResearch). (See Appendix 10)

5.2.6 Global Transcriptional Profiling and Analysis of Expression Data

For all samples, 50ng of total RNA was amplified to at least 20 µg and labeled according to the Affymetrix Small Sample Labeling Protocol vII. Samples include: 3 mono-culture microreactors, 3 co-culture microreactors, mono-culture CGS (pooled from 6 replicates), and co-culture CGS (pooled from 6 replicates), all on 13-day post-perfusion, WT hepatocyte-enriched fraction, EGFP+ endothelial cell fraction, and *in vivo* WT liver slice. The microarray experiment was carried out with GeneChip® Rat Genome 230 2.0 arrays (Affymetrix, Santa Clara, CA) according to the standard protocol described in Affymetrix Genechip Expression Analysis Technical Manual.

Data analysis was performed in Spotfire and Microsoft Excel. Gene ontology mapping was performed on the Fatigo website (<http://www.fatigo.org>). An endothelial cell-enriched gene set was defined as the probesets that were expressed more than 2-fold higher in the EGFP endothelial cell fraction relative to *in vivo* liver and the hepatocyte-enriched fraction.

5.3 Results

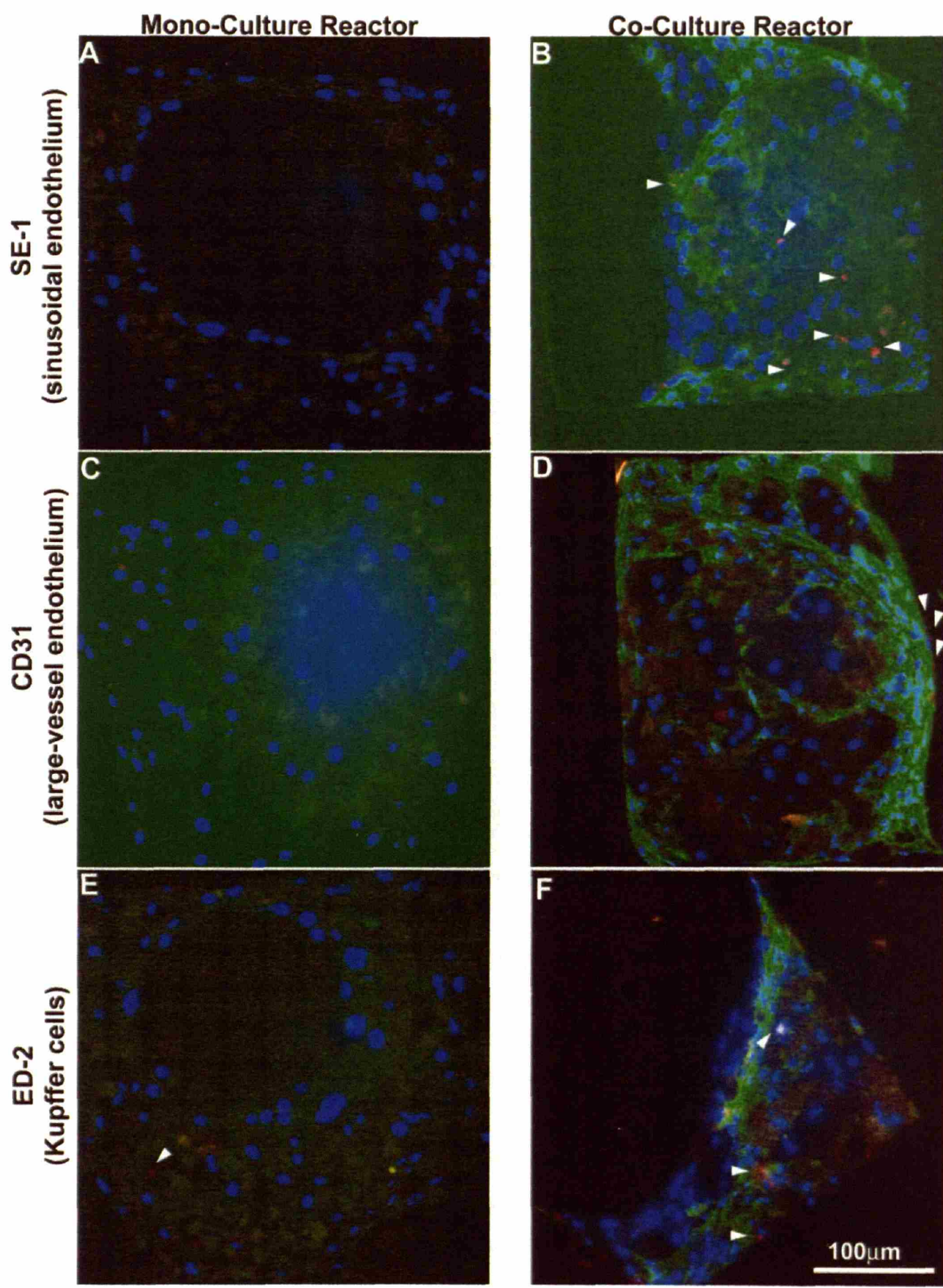
5.3.1 Immunohistochemical Identification of Non-Parenchymal Cells in Microreactor Culture

Standard protocols for isolating rat liver hepatocytes result in a cell population that comprises ~ 95% hepatocytes. Under some *in vitro* culture conditions, the small fraction of NPCs initially present in such isolations can proliferate to become a much more substantial fraction of the total cells present, and ICAM-1+ and factor-VIII+ endothelia have been observed weeks after culture initiation [78, 79]. The presence of cells stained positive for the specific rat sinusoidal endothelial marker SE-1 after more than a week of culture has only rarely been reported [132].

We have previously found that in co-cultures comprising an endothelial fraction derived from EGFP-expressing liver mixed with unlabelled primary hepatocytes and maintained in a microperfused 3D culture format, the EGFP+ cells, initially present at 7% by number, persist and proliferate to constitute ~12% of total cells by day 13, and form a network as observed by *in situ* multi-photon microscopy. The initial endothelial cell fraction derived from the EGFP+ liver was ~85% pure, and thus the observation of persistent EGFP+ cells could reflect a dynamic state wherein endothelia die off and are replaced by proliferation of the contaminating NPCs.

We thus performed qualitative immunohistochemistry to assess the distribution of key NPC types in the 3D endothelial co-cultures, and to compare the tissue structure to that of mono-cultures in 3D, a configuration where we have occasionally observed cells with endothelial morphology lining vessel-like structures [86]. Immunohistochemistry was performed on microreactor tissue using antibodies against rat sinusoidal endothelial cells (SE-1), Kupffer cells (ED2), quiescent stellate cells (anti-GFAP), and activated stellate cells (anti-SMA). The pan-endothelial marker CD31, which stains

sinusoidal endothelia at best weakly but stains large vessels in liver strongly, was also used as a general endothelial marker.



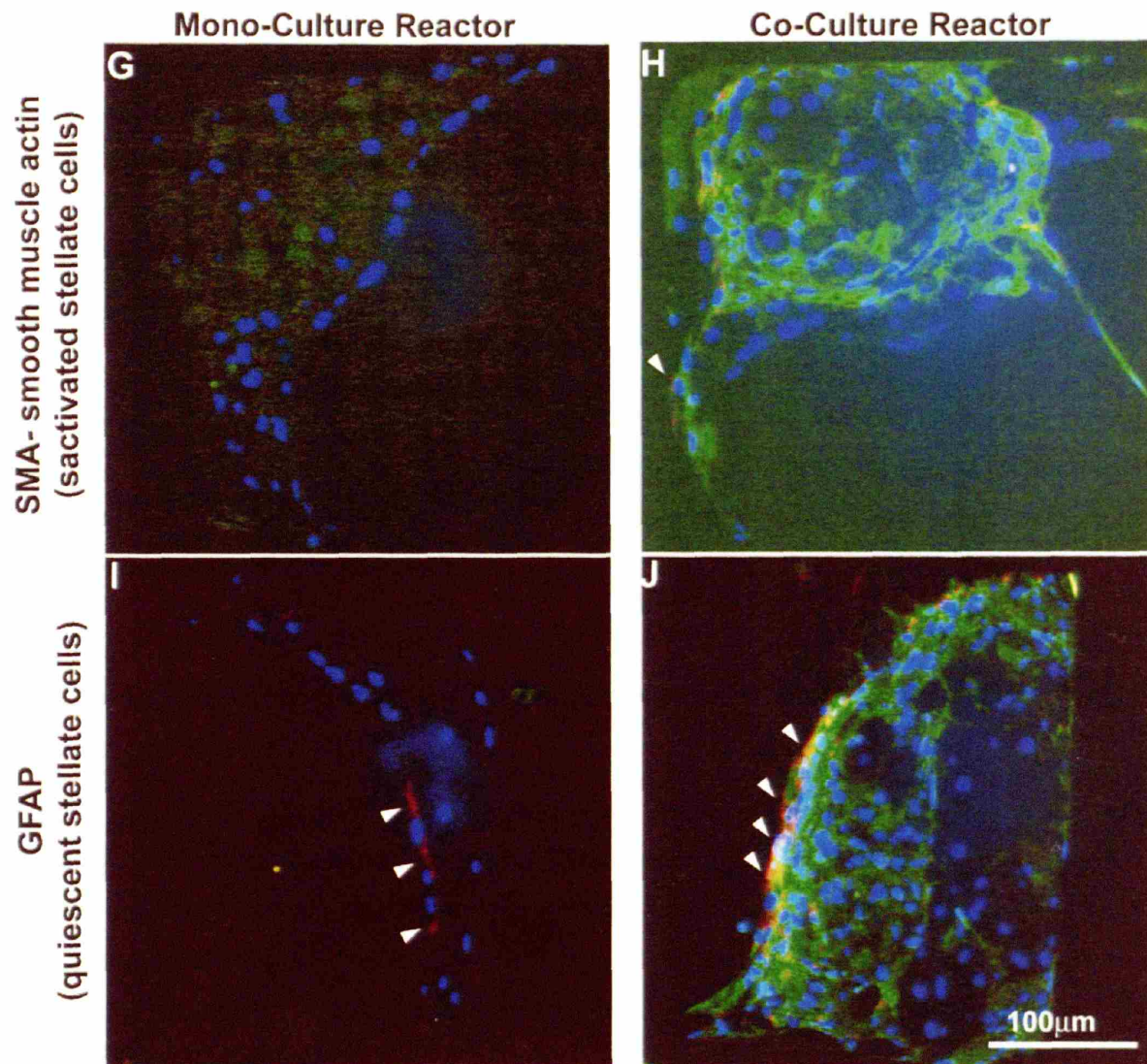


Figure 5.1: Immunohistochemistry of mono-culture (A, C, E, G, I) and co-culture (B, D, F, H, J) microreactor tissue. Sections were stained with antibody SE-1 for sinusoidal endothelial cells (A-B), anti-CD31 for large-vessel endothelial cells (C-D), ED2 for kupffer cells (E-F), anti-SMA for activated stellate cells (G-H), and GFAP for quiescent stellate cells (I-J). Blue: Hoechst nuclei stain; green: EGFP; red: antibody stain. Arrowheads indicate positive antibody staining.

Sinusoidal endothelial cells were present throughout the interior of the tissue in the endothelial co-culture, but largely absent in mono-culture (Figure 6.1A-B). Endothelia expressing the general marker CD31 were present in co-cultures at tissue-fluid interface, but such endothelia were not seen in the mono-culture (Figure 6.1C-D). Kupffer cells were present in both groups but were

present in larger numbers in the co-culture (Figure 6.1E-F). Activated stellate cells were absent from the tissue, but were seen as rare cells along the walls of the channels (Figure 6.1G-H). Quiescent stellate cells stained strongly in both groups at fluid-tissue interface (Figure 6.1I-J). Thus, while the EGFP signal in the co-cultures had a contribution from stellate cells and Kupffer cells, both sinusoidal and large vessel endothelial cells were present in the co-cultures and located in physiologically-appropriate regions of the tissue (i.e., small vessel within the tissue and large vessel at the tissue interface with the fluid).

The EGFP signal does not seem to consistently survive through embedding process, especially in small cells such as sinusoidal endothelia. Indeed, embedded and stained control EGFP liver tissue showed green fluorescence mainly in hepatocytes, while NPCs rarely showed co-localization of EGFP with immunostaining.

5.3.2 Endothelial Cells Contribute to Gene Expression in 3D Cultures but not in 2D Cultures

Global gene expression analysis was used to assess whether the presence of sinusoidal endothelial cells within the tissue structures in 3D microreactor co-cultures altered gene expression compared to mono-cultures. We plotted the differential gene expression fold-change levels of co-culture over mono-culture (Figure 5.2). There are 157 probesets with robust (>4-fold) increased expression (Robust-3D) in co-cultures compared to mono-cultures at the 13-day time point (Fig 5.2A), while 583 probesets exhibited moderate (>2-fold) increased expression (Moderate-3D). These results are in strong contrast to the behavior of co-cultures and mono-cultures maintained in 2D CGS culture for 13 days, where only 2 probesets are differentially expressed at the 4-fold level between co-culture and mono-culture, and both are decreased in the co-culture (Fig 5.2B). These results are consistent with the visual observation that EGFP-expressing cells are lost from the 2D co-cultures by day 11. Gene Ontology analysis of the 157 probesets within Robust-3D showed that significant ontological processes include cell-cell communication, morphogenesis, organ development, and cell differentiation (Table 5.1).

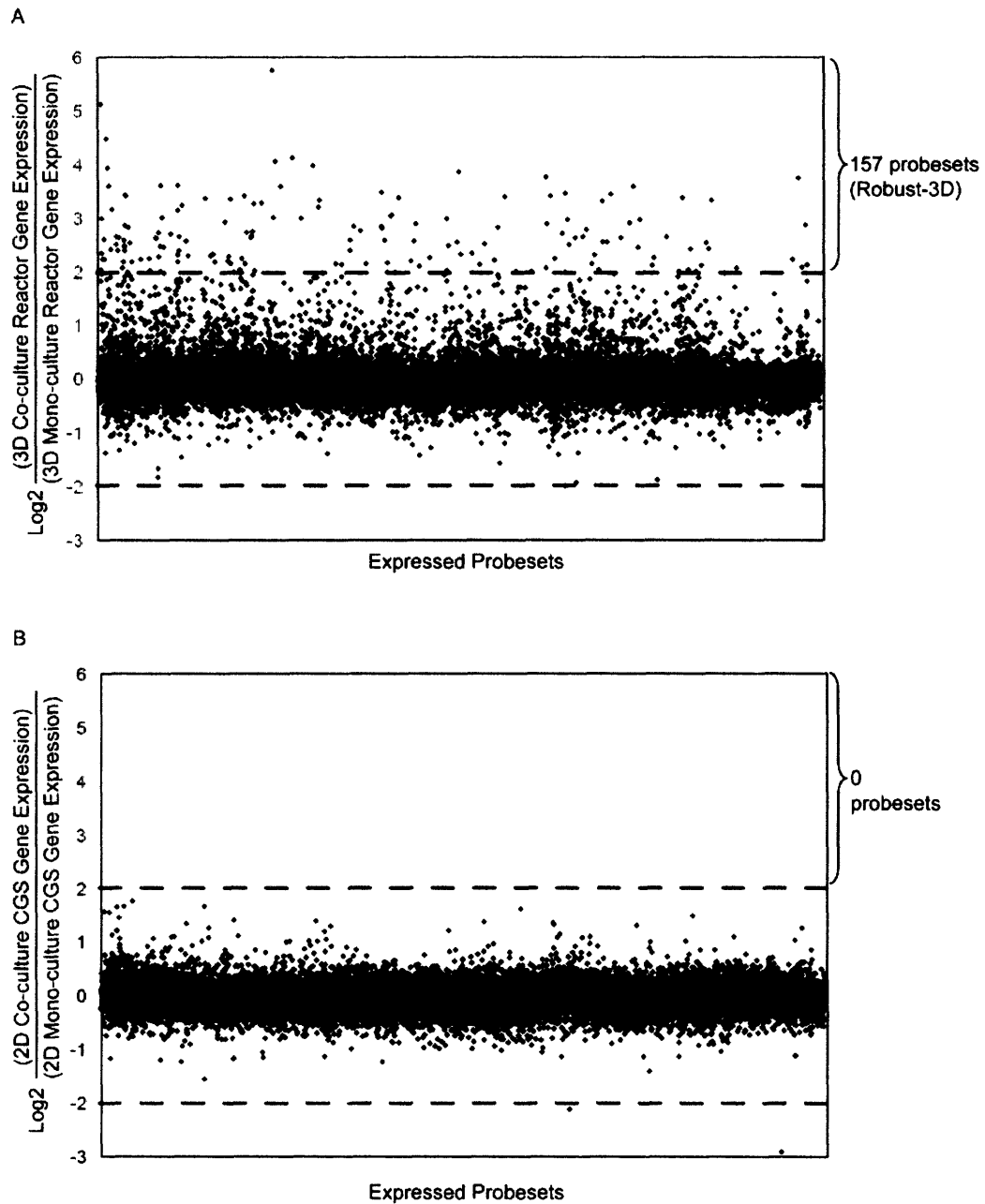


Figure 5.2: Comparison of global gene expression profiles in co-cultures vs. mono-cultures for 3D culture (A) and 2D culture (B). Differential gene expression fold-change levels of co-cultures over mono-cultures are plotted. The points around $y=0$ indicate similar gene expression levels between co- and mono-cultures. Points within the dashed lines ($-2 < y < +2$) deviate at most 4-fold in expression levels between the culture conditions. Points outside the dashed lines deviate more than 4-fold in expression levels between the two culture conditions.

Gene Ontology Category	Probesets			
Cell Communication	Cxcr4	Cspg2	Calcr1	Col11a1
	Gja5	Fcgr3	Ptpro	Tnc
	Lgals1	Prkcb1	Ccl2	Trpc6
	Ccr1	Rgs10	Col3a1	Col1a2
	Il18	Vcam1	Col5a2	Hck
	Emb	Spp1	Gpnmb	Il1r2
	C5r1			
Morphogenesis	Cxcr4	Col11a1	Gja5	Ptpro
	Mgl1	Sla	Ccr1	Tagln
	Bhlhb3	Ptn	Col3a1	Il18
	Mgp	Col5a2	Spp1	Gpnmb
	Actg2			
Organ Development	Cxcr4	Col11a1	Gja5	Ptpro
	Sla	Ccr1	Tagln	Bhlhb3
	Ptn	Col3a1	Il18	Mgp
	Col5a2	Spp1	Gpnmb	Actg2
Cell Differentiation	Sla	Lgals1	Ccr1	Spp1
	Gpnmb			

Table 5.1: Significant gene ontology categories in Robust-3D

5.3.3 Most Genes with Higher Expression Levels in 3D Co-culture than Mono-culture are Endothelia-associated Genes

To assess whether the differentially expressed genes may arise from the endothelial population, we generated a database of genes enriched in endothelium by performing global transcriptional profiling of the freshly-isolated endothelial fraction and comparing that profile to the profiles of liver and freshly isolated hepatocytes, designating as “endothelial specific” those probesets with increased expression in both reference data sets, as each reference has the potential for artifacts. The process of cell isolation causes changes in expression levels of ~5% of hepatocyte probesets (> 2-fold increase or decrease compared to liver, data not shown). Comparison to the

unperturbed *in vivo* tissue is confounded by the presence of endothelia in liver tissue (~20% by number), which causes the apparent increased expression to be lower than the true value compared to hepatocytes.

The effect of endothelial presence in liver as a reference can be seen quite easily mathematically if we assume that hepatocytes and other non-endothelial cells contain the mRNA of interest at basal level x_0 copies per cell, and that endothelial cells contain $\alpha_{\text{true}} x_0$ copies where α_{true} is the true level of increased expression. The observed value of increased expression then, for a given value β_{endo} representing the fraction of liver mRNA arising from endothelia, is $\alpha_{\text{obs}} = \alpha_{\text{true}} / [(1 - \beta_{\text{endo}}) + \beta_{\text{endo}} \alpha_{\text{true}}]$. As the value of α_{true} becomes very large, the value of α_{obs} reaches an asymptote of $1/\beta_{\text{endo}}$. As long as the value of α_{true} is relatively small this effect is modest; for example, if endothelial cells contribute 5% of the mRNA in the liver homogenate (they are <5% of liver volume), a gene with 4-fold higher expression in endothelial cells relative to hepatocytes (and other liver cells) will appear to be expressed 3.6-fold higher; a gene with 10-fold higher expression will appear to be expressed 6.9-fold higher.

For endothelial cells relative to liver (endo/liver), 4650 probesets were expressed at least 2-fold higher in the endothelial fraction compared to liver, and of these, 1826 were expressed at least 4-fold higher, from a total of 28464 expressed probesets. For the endothelial fraction to the hepatocyte-enriched fraction (endo/hep), 4353 probesets were expressed at least 2-fold higher and 1985 at 4-fold higher in the endothelial fraction relative to the hepatocyte-enriched fraction. We found significant overlap between these two data sets: 3688 probesets with expression levels >2 for endo/liver and endo/hep (Moderate-endothelial set) and 1534 probesets with expression levels >4 for both criteria (Robust-endothelial set) (Figure 5.3).

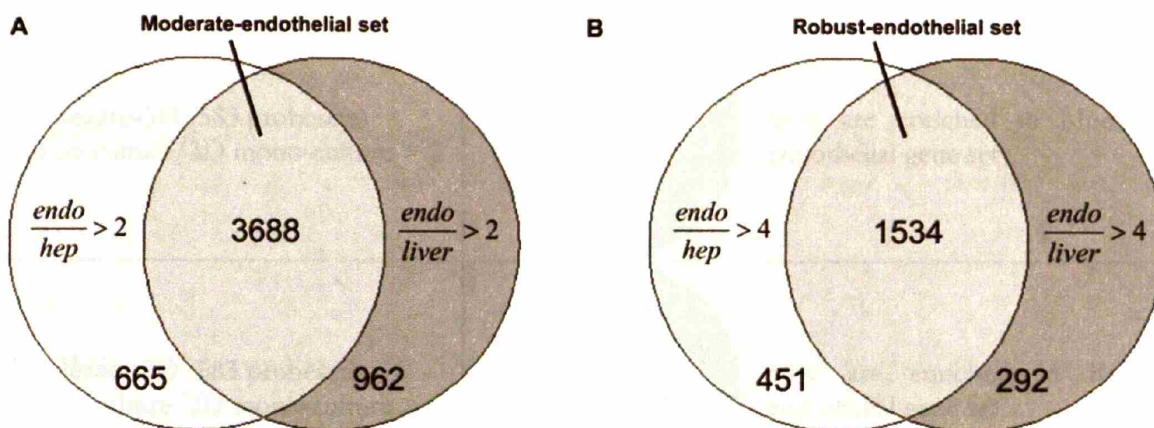
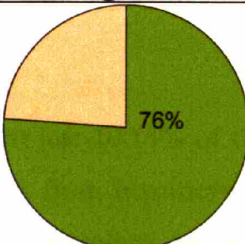
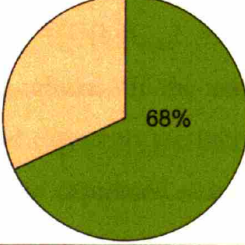


Figure 5.3: Endothelial gene sets were derived from comparison against liver, the hepatocyte fraction, and the intersecting group. The gene sets are defined by 2-fold (A) and 4-fold (B) higher expression levels in the endothelial isolate over the comparison group.

We found that 76% probesets within Robust-3D were included in the Robust-endothelial set, and 68% in the Moderate-endothelial set (Fig 5.4). If the criteria are relaxed to include probesets expressed at least 2-fold higher in co-culture compared to mono-culture, we found 68% within Moderate-3D was included in Moderate-endothelial set, and 56% in the Robust-endothelial set. The reverse look-up of this analysis found 21% of the Robust-endothelial set included in Moderate-3D, and 11% of the Moderate-endothelial set in Moderate 3D (Figure 5.4).

Designated Gene Set	Percentage
Robust-3D (157 probesets) 3D co-culture/3D mono-culture > 4	 <p>76% are enriched in Moderate-endothelial gene set</p>
Robust-3D (157 probesets) 3D co-culture/3D mono-culture > 4	 <p>68% are enriched in Robust-endothelial gene set</p>

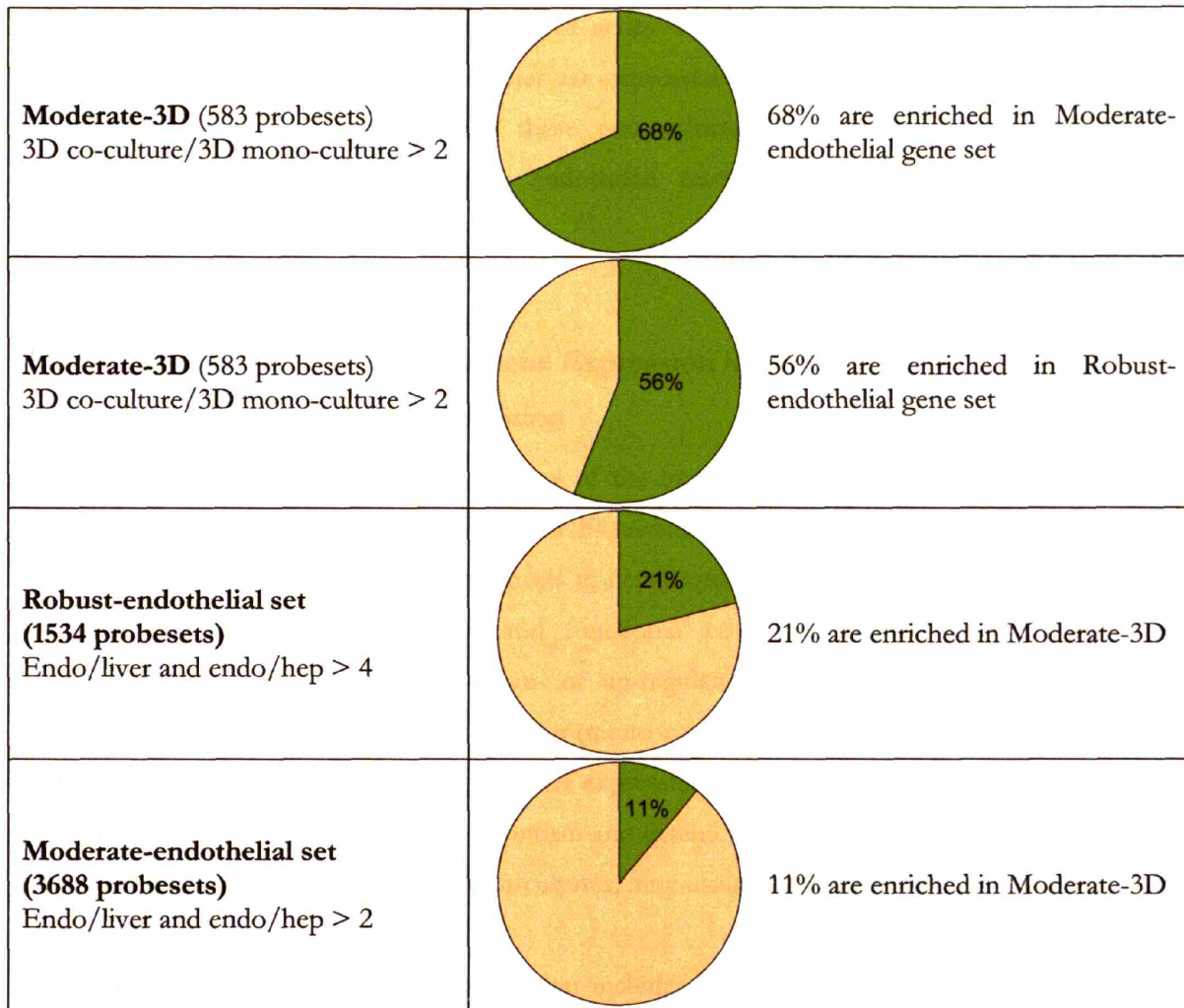


Figure 5.4: Test for overlap of probesets between the endothelial sets and Moderate-3D and Robust-3D.

Because endothelial cells represent just 10-15% of the total cell number in the co-culture, endothelial mRNA is diluted with mRNA from hepatocytes and other cells. Thus, the apparent upregulation in co-culture compared to mono-culture for an endothelial gene with expression level $\alpha_{\text{true}} \times_0$ compared to hepatocytes is $\alpha_{\text{obs}} = (1 - \beta_{\text{endo}}) + \beta_{\text{endo}} \alpha_{\text{true}}$, presuming endothelial cells contribute ~0% of the mRNA in mono-culture. If the endothelial cells contribute 5-10% of the total message level in co-culture we would expect to see increased expression levels in co-culture at the 2-fold level only for those genes that are expressed at least 10-20-fold higher in endothelial cells compared to hepatocytes.

In summary, the high concordance of genes with higher expression levels in co-culture compared to mono-culture with genes that are expressed in endothelial cells supports both the immunohistochemistry data comparing these two cultures, as well as previous studies that demonstrate that the EGFP-expressing endothelial fraction persists, proliferates, and forms networks in the 3D perfused cultures.

5.3.4 Liver-Enriched Metabolism Gene Expression is Preferentially Maintained in 3D Regardless of Endothelial Cell Addition

We have previously found that many of the important transcription factors that regulate programs of liver-enriched genes, including HNF4, as well as many drug metabolizing enzymes (e.g., CYP3A) are maintained at physiological levels in hepatocyte mono-cultures in the microreactor, as assessed by RT-PCR, western blots, and functional assays for metabolism, although some metabolism genes were significantly down- or up-regulated compared to *in vivo* [10]. Further, microreactor culture of the hepatocyte fraction (mono-culture) was far more effective than 2D CGS culture in maintaining hepatocyte specific gene expression when a select set of genes was analyzed by PCR and functional assays [10]. We confirm and extend these previous results in comparing 2D CGS cultures to 3D perfused microreactor cultures, here using global transcriptional profiling.

When we plot the subset of genes that includes hepatocyte-enriched transcription factors, nuclear receptors, CYPs, and phase II metabolism genes (124 probesets) as a comparison of expression levels in 3D microreactor culture to levels in 2D CGS culture, we found that all substantial expression differences were due to lower expression levels in 2D, with 25% of these probesets expressed moderately lower (2-fold, all red and green data points) and 12% with robust decrease (4-fold, all red data points) (Figure 5.5A). The solid 45-degree line shows zero gene expression difference. Greater expression difference between the culture conditions translates to greater deviation from this line. To truly compare the culture method's ability to maintain physiological liver-enriched transcription, we defined quadrant I, where gene expression is maintained in 2D (within 4-fold of *in vivo* liver) but not in 3D, and quadrant II, where gene expression is maintained in 3D (within 4-fold of *in vivo* liver) but not in 2D (Figure 5.5A). In quadrant I, 2 genes representing 1.6% of the metabolism gene set were better maintained in 2D.

However, in quadrant II, 17 genes representing 14% of the metabolism gene set have greatly decreased expression levels in 2D (Figure 5.5A)

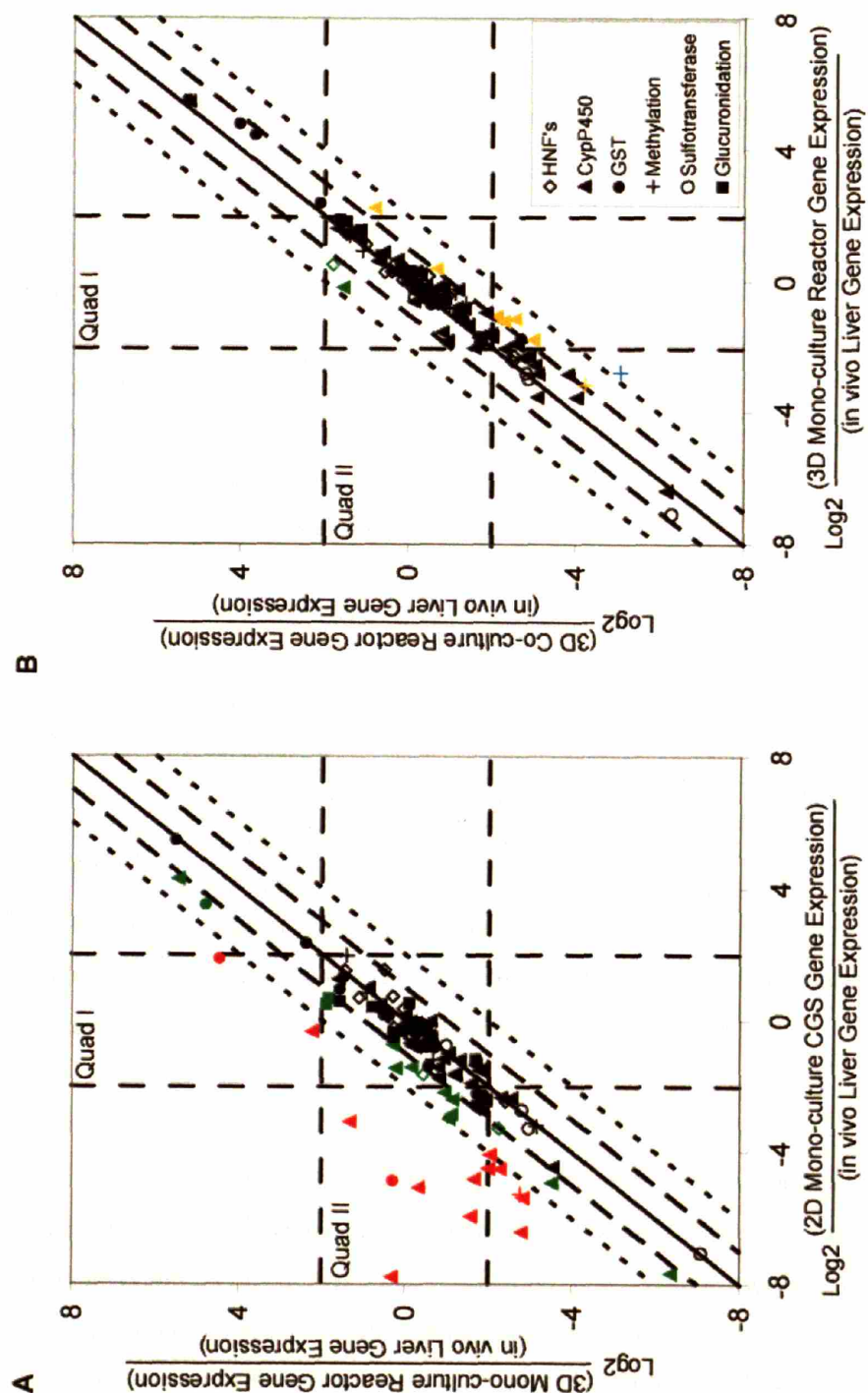


Figure 5: Important metabolic genes and liver-enriched nuclear factors were selected, and their gene expression in 2D mono-cultures (A) and 3D co-culture (B) plotted against those in 3D mono-culture after all expression levels are normalized to *in vivo* liver. Solid line indicates $x=y$ relationship. Area within dashed lines indicates $-1 < x-y < 1$, and area within dotted lines indicates $-2 < x-y < 2$. Data points for which $x-y > -2$ are colored in red, and for which $-1 > x-y > -2$ are colored in green, $2 > x-y > 1$ in orange, and $x-y > 2$ in blue. Between 2D and 3D mono-cultures, all the differentially expressed genes have lower expression values in 2D, where 25% are moderately lower (green and red points) and 12% are substantially lower (red). Only one probeset is robustly expressed lower in 3D co-culture than 3D mono-culture (blue and orange points) and 12% are moderately lower (orange). To truly compare these values against *in vivo* liver, quadrant I and quadrant II are defined by the lines $x=2$, $x=-2$, $y=2$, and $y=-2$. We found that 14% of these genes, particularly several CYPs, were greatly down-regulated in 2D mono-culture and maintained in the 3D mono-culture, shown in quadrant II, while only 1.6% is maintained in 2D but not in 3D, shown in quadrant I.

Interestingly, when we compare the phenotype of 3D co-cultures to 3D mono-cultures (and both relative to *in vivo*), using this same gene subset of hepatocyte-enriched genes, we find that only one of these genes (representing less than 1%) showed substantial differences (blue point in Figure 5.5B). Probesets with more than 2-fold lower expression levels in 3D co-cultures than mono-cultures are listed in Table 5.2.

Unigene ID	Gene Title	Gene Symbol	$\log_2 \frac{3D_{mono} - culture}{3D_{co} - culture}$
Rn.10870	Cytochrome P450, subfamily IIC (mephenytoin 4-hydroxylase)	Cyp2c	1.01
Rn.91355	cytochrome P450, family 2, subfamily d, polypeptide 26	Cyp2d26	1.06
Rn.11142	glycine N-methyltransferase	Gnmt	1.07
Rn.44992	CYP2J4	Cyp2j4	1.08
Rn.32106	cytochrome P450, family 2, subfamily d, polypeptide 13	Cyp2d13	1.08
Rn.91314	cytochrome P450, family 2, subfamily j, polypeptide 9	Cyp2j9	1.22
Rn.2184	arachidonic acid epoxygenase	Cyp2c23	1.42
Rn.10172	cytochrome P450, family 17, subfamily a, polypeptide 1	Cyp17a1	1.44
Rn.11406	betaine-homocysteine methyltransferase	Bhmt	2.31

Table 5.2 Key liver transcription and metabolism enzyme probesets with a least 2-fold lower expression difference in 3D co-culture than 3D mono-culture.

It is apparent that substantially more genes are differentially expressed in the 2D-3D comparison than 3D mono- and co-culture comparison. Many of these genes may be regulated by specific components in the culture medium (e.g., insulin regulation of CYP2E1) and that the relatively small number of NPCs present in the mono-cultures may be sufficient to maintain most hepatocyte-specific functions when cells are cultured in a perfused, 3D microreactor format. Even though there are few genes with substantial expression differences between 3D co- and mono-culture, most of the probesets with moderate expression differences are expressed higher in mono-

culture. In fact, out of the total 124 probesets, 99 (80%) fall below the x-y line (expressed higher in mono-culture, Figure 5.5B). We suspect this overall lower expression in co-culture is the result of hepatocyte-specific genes diluted by NPC contributions toward the total RNA. Because hepatocytes likely contain higher amounts of total RNA per cell than NPCs and they comprise the majority of the cell population in the cultures, this dilution effect is not as significant as in the case of endothelial-specific gene set.

5.4 Discussion

Relative to endothelia from many other tissues, liver-derived endothelia generally do not adapt well to *in vitro* culture [18, 65, 126]. Sinusoidal endothelia rarely survive more than about a week, and within a few days lose fenestrations, upregulate the general endothelial marker CD31, and lose expression of the specific marker SE-1 [18, 29, 49, 126]. Although SE-1 positive cells are rarely reported in long term culture [132], some culture formats that foster 3D tissue formation reported survival of liver-derived cells that stain positive for pan-endothelial markers for periods up to weeks [65, 78, 79, 124].

Because survival and function of endothelia are regulated by many factors in the microenvironment, including both bulk and interstitial fluid flow [95], we reasoned that co-cultures maintained in a microenvironment that fosters 3D tissue organization, coupled with localized flow through the tissue, may provide appropriate cues for longer term survival of liver sinusoidal endothelia. We have observed that a purified fraction of EGFP+ liver endothelial cells persists and proliferates over of 13 days in perfused co-culture with hepatocytes.

However, because isolation of EGFP+ endothelial cells results in a population of 80-90% purity, it is possible that the SE-1+ cells observed in immunohistochemical analysis of the tissue represent only a fraction of surviving EGFP+ cells, and that stellate cells or other NPCs proliferated and overwhelmed the endothelial cells. Global gene expression profiling revealed that 157 probesets were more highly expressed in the co-cultures relative to the mono-cultures, and that most of these genes are endothelial-associated based on our analysis of freshly-isolated rat liver endothelia. We did not generate a separate data set for other NPC fractions present in the cultures, and it is possible that the gene set we identify as endothelial-specific – a set that represents 16% of the total probesets

expressed in the liver tissue – overlaps some with genes highly expressed in Kupffer cells or stellate cells, and that these overlap genes may be among those appearing in the Robust-3D set. Further, some genes are likely up-regulated in the endothelia during isolation (which takes over 2 hours) and return to more basal levels during culture; the compromise between purity of endothelial cells and potential mRNA changes during purification is always present [154]. However, immunohistochemical analysis revealed that 3D cultures initiated with either the hepatocyte fraction or the hepatocyte fraction supplemented with the EGFP+ endothelial fraction contained Kupffer cells and quiescent stellate cells in numbers that were not remarkably different, but only the cultures initiated with the EGFP+ endothelial cell fraction contained endothelial cells. Thus, we would not expect significant differences in the level of expression of stellate and Kupffer cell genes, unless they are differentially regulated by endothelia.

Some probesets within the Robust-3D set are likely related to phenomena involved in liver tissue morphogenesis and angiogenesis. Many genes highly expressed in co-culture are matrix proteins or related to matrix degradation -- including collagen, pro-collagen, tenascin, lumican, chondroitin sulfate proteoglycan, and metalloproteinase MMP2 and MMP12 -- and thus may be related to events critical in the extracellular matrix remodeling associated with angiogenesis during liver regeneration [98, 138]. In fact extracellular matrix and proteases are two major functional classes of genes upregulated during endothelial tube formation [155]. Perhaps the most compelling connection to liver angiogenesis is the upregulation of neuropilin 1, a receptor for VEGF that can be upregulated by VEGF during angiogenesis [156]. Its expression can be induced by bFGF and in turn enhance cell migration in response to VEGF through VEGFR2 signaling [157]. Neuropilin mRNA level has also been shown to be upregulated in liver sinusoidal endothelial cell *in vitro* culture under shear stress [158]. The stronger expression of these genes in the endothelial co-culture reinforces the observation of endothelial tube formation in the culture and its analogy to liver regeneration and angiogenesis. In addition, pleiotrophin, a protein implicated as a hepatocyte mitogen during liver regeneration, is also expressed higher in the co-culture and suggests liver regeneration processes [159].

A somewhat surprising finding is that addition of endothelia did not appear to alter the expression of a broad set of genes typically associated with hepatic-specific function. In 2D culture formats, co-culture with endothelial cells [65, 146, 148], liver epithelial cells [41, 144, 145], fibroblasts

and other cells [42, 149] can remarkably enhance many liver functions including secretion of serum proteins, synthesis of urea, and activity of enzymes involved in biotransformation of drugs and xenobiotics, over their corresponding performance in cultures initiated with standard hepatocyte isolates. Further, 3D spheroid co-culture with primary stellate cells can likewise enhance function at long times (2+ weeks) although appears to depress function at initial culture stages (<10 days) [61]. However, because 3D culture also enhances these same liver-specific functions, and fosters persistence of a range of liver cell types in culture [78, 79, 86, 124, 160], it is possible that many 3D cultures formats effectively foster survival and function of most non-parenchymal cells present in the initial cell isolate, and thus the heterotypic cell interactions necessary for maintaining hepatocyte phenotype, in a manner that does not spontaneously occur in 2D culture. Thus, for studies that primarily focus on hepatocyte behavior, 3D cultures of primary hepatocyte isolates may offer sufficient phenotypic response even though the numbers of several NPCs are sub-physiological.

However, the presence of NPC at more physiological levels may be critical to achieve appropriate physiological responses to certain stimuli *in vitro*. For example, additional rat liver NPCs on top of a CGS culture of hepatocytes do not alter basal levels of hepatocyte function compared to cultures without the added NPCs, but the co-cultures show a marked difference in response to lipopolysaccharide stimulation [46]. Because endothelia are essential players in many pathophysiological behaviors of liver, such as responses to toxins and tumor cell invasion, culture models that foster long-term retention of endothelia *in vitro* are potentially an important tool for mechanistic investigations.

Chapter 6

Gene Expression Profile Comparison to Liver Regeneration and Stellate Cell-specific Gene Sets

6.1 Introduction

Liver regeneration is a complex event that involves precise timing and interplay among cell types, growth factors, cytokines, and matrix proteins changes. Hepatocytes are the first cell type to rapidly proliferate, followed by stellate cells, Kupffer cells, and then endothelial cells [97]. Liver mass is almost completely recovered after one week post-partial hepatectomy (PHx) [100], but the proliferation of endothelial cells and Kupffer cells seems to extend beyond this time point [97]. During liver regeneration the process of restoring normal liver tissue architecture mimics events of angiogenesis where endothelial cells organize into blood vessels. Upon observation of probable endothelial tube formation in the co-culture reactors, it is natural to ponder the similarity between liver regeneration and this tissue morphogenesis. Since the difference between 3D co- and mono-culture is the addition of an EGFP endothelial cell fraction, the later time points of liver regeneration will be more reflective of changes in the endothelium. The RNA from reactor cultures was extracted on the 13th day post-perfusion, so the gene expression patterns in reactor cultures are more likely to resemble the later parts of the liver regeneration rather than the early and immediate gene changes, which have been the focus of most gene expression profile studies on liver regeneration [161, 162]. This raises two questions: Are there common sets of genes that are turned on? Is there a particular time point during liver regeneration that is repeated on day 13 of *in vitro* reactor culture?

In chapter 5, an endothelial-specific gene set was defined by comparing the gene expression levels in the primary endothelial isolate against the primary hepatocyte fraction and *in vivo* liver. We found that only a small subset of these genes was expressed substantially higher in the 3D co-culture compared to mono-culture. One possible explanation is that contaminating stellate cells in the primary endothelial isolate contribute toward the endothelia-specific gene set. These stellate-specific genes may not exhibit any difference in their expression levels between 3D co- and mono-culture

because both maintained some population of GFAP⁺ stellate cells. If the true stellate-specific genes can be identified by comparing gene expression profiles of primary stellate cells and all other primary cell isolations, we will have a much more stringent cell-specific gene set of each cell type in the liver.

This chapter describes the gene expression profiling on primary stellate cell isolate and partial hepatectomy samples, and how these gene sets intersect with the previously defined gene sets.

6.2 Materials and Methods

6.2.1 Preparation of liver regeneration tissue samples

Partial hepatectomy (PHx) was performed on male Fischer 344 rats with weights around 200g, and liver samples were collected at 48 hour, 72 hour, 1 week, and 2 weeks post-surgery. Samples were flash frozen in liquid nitrogen and stored at -80°C until ready for RNA isolation. (This work was performed by Mark Ross and Donna Stolz at University of Pittsburgh. Samples were shipped overnight to MIT on dry ice before RNA isolation was performed.)

6.2.2 RNA extraction from PHx samples

About 1cm³ of each liver sample was mixed with 10 mL of Trizol (Invitrogen) and homogenized with an Ultra-Turrax T25 Basic homogenizer (IKA) at 24,000 rpm/min. A 1 mL aliquot of the homogenate was used for RNA extraction with the RNeasy mini kit (Qiagen). Detailed protocol is described in Appendix 7.

6.2.3 Preparation of primary stellate isolate

A two-step collagenase perfusion was performed on 150-230g male Fischer rats [10]. The supernatant from the first two 50g centrifugation cycles contained NPCs. NPCs were centrifuged at 350g for 5 min, re-suspended with HBSS buffer (Gibco), and then spun down again at 350g for 5 min. NPCs were then re-suspended in 8 mL of 11.5% optiprep (v/v in HBSS) (Sigma-Aldrich) in 15 mL centrifuge tubes. Four mL of HBSS was carefully placed on the top of the 11.5% Optiprep layer without disturbing the interface between HBSS and Optiprep. The layered solutions were spun at 350g for 20 min with the lowest brake setting. Cells at the interface between HBSS and Optiprep were collected. The collection of cells was mixed with 10 mL of stellate medium, DMEM (Gibco)

with 10% fetal bovine serum (Sigma-Aldrich), and spun down again at 350g for 5 min. Cell pellets were re-suspended in 10 mL of stellate medium. Their concentration and viability were determined by trypan blue exclusion test (Gibco). All procedures were performed at 4°C.

Eight-well glass-bottom Nuncwell (Falcon) chamber slides were coated with 200 µL of type I collagen (BD Biosciences) at 100 µg/mL in PBS for 5 min at room temperature. It was then aspirated and the slides were dried for 2 hours at room temperature. Each well received ~7,500 HSCs in 200 µL of stellate medium. Cells were cultured at 37°C and 5% CO₂.

One-day old HSC cultures were fixed in 2% paraformaldehyde (EMS) in PBS (Gibco) for 20 min at room temperature and washed several times in PBS. The Nuncwell walls were removed, and a coverslip was applied onto each slide with a drop of Fluoromount (EMS). Samples were then imaged under phase contrast and epifluorescence with the DAPI filter for retinoic acid autofluorescence. (Stellate cell isolation, culturing, and imaging were all carried out by Albert Weng)

6.2.4 RNA extraction from primary stellate cells

Two million stellate cells were spun down at 350g for 10 min. After the supernatant was removed, 1 mL of Trizol was added to the cell pellet and well mixed. The mixture was stored in -80°C until ready for RNA isolation. RNA was extracted and purified with the RNeasy mini kit (Qiagen) according to protocol listed in Appendix 7.

6.2.5 Gene expression profiling

Fifty ng of total RNA of the stellate cell samples was amplified to at least 20 µg and labeled according to the Affymetrix Small Sample Labeling Protocol vII. The microarray experiment was carried out with GeneChip® Rat Genome 230 2.0 arrays (Affymetrix, Santa Clara, CA) according to the standard protocol described in Affymetrix Genechip Expression Analysis Technical Manual. Data analysis was performed in Spotfire and Microsoft Excel.

6.3 Results

6.3.1 Stellate cells gene set

There were several confounding factors in interpreting the stellate cell gene set. Stellate cells are a heterogeneous cell population, and typical markers such as desmin and GFAP each tends to stain only a sub-population of this cell type. But these two markers may not be mutually exclusive, and it is unclear whether all HSC populations can be identified with these two markers alone. Therefore it is difficult to determine the purity of this isolation. Primary stellate cells contain oil droplets that store retinoic acid, whose autofluorescence is also another definitive marker for stellate cells. However, retinoic acid is not ubiquitously present in stellate cells. Figure 6.1A shows a typical 1-day old culture of primary stellate cell isolate under phase contrast, while Figure 6.1B shows its corresponding retinoic acid autofluorescence image. It is apparent that only a fraction of all the cells shows retinoic acid autofluorescence. Stellate cells can also be identified by their stellate morphology (black arrow, Figure 6.1A), but all cells in this isolate do not have the same stellate morphology. Figure 6.1A shows a variety of different cell shapes in the HSC isolate. Previous immunostaining data identified ~30% of all cells in this isolation to be GFAP+ (A. Weng, personal communication) while flow cytometry identified at most ~12% are GFAP+ (B. Cosgrove, personal communication). Therefore the purity of this cell population is not clear.

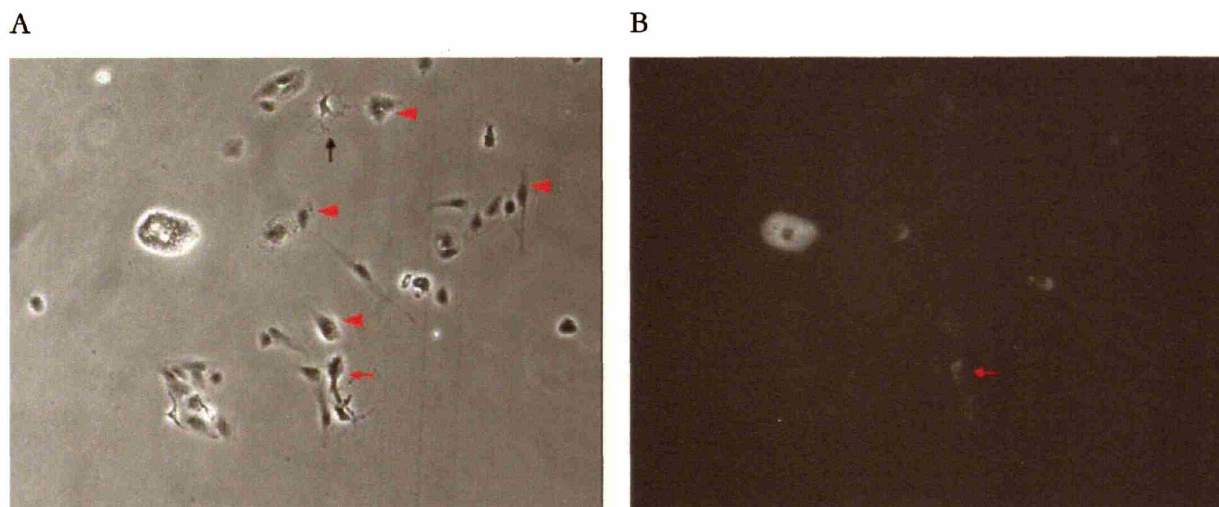


Figure 6.1: Phase contrast (A) and DAPI fluorescence (B) images of 1-day old primary stellate cell isolate. Black arrow points out a classic stellate-shaped cell. Red arrows in both images point to a cell that is RA+. Red arrowheads point out cell with different morphologies.

Three primary isolations were used to extract RNA, but only one sample was successfully amplified to the necessary amount for the microarray experiment. The microarray output was also confounded by its high actin and gapdh 3'/5' ratio, which is an indication of RNA degradation.

Due to the reasons mentioned above, the data generated from stellate cell samples were considered unreliable.

6.3.2 Liver regeneration Gene set

All PHx liver samples were normalized to the average of control groups of livers with sham operation. Of the total 31,099 probesets, 21,878 appeared present. By comparing with the control samples, those probesets with more than 2-fold higher expression values at each time point were selected. Using this criteria, there were 803 more highly expressed probesets for the 48hr (48hr-set), 547 for the 72hr (72hr-set), 103 for the one-week (1wk-set), and 60 for the two-week (2wk-set) time points. The numbers and percentages of overlapping probesets between each of these liver regeneration set and Moderate-3D are shown in Figure 6.2. There is a higher percentage of probesets within Moderate-3D that intersect with 48hr-set and 72hr-set than the later time points, but these probesets constitute only small percentages of the PHx sets.

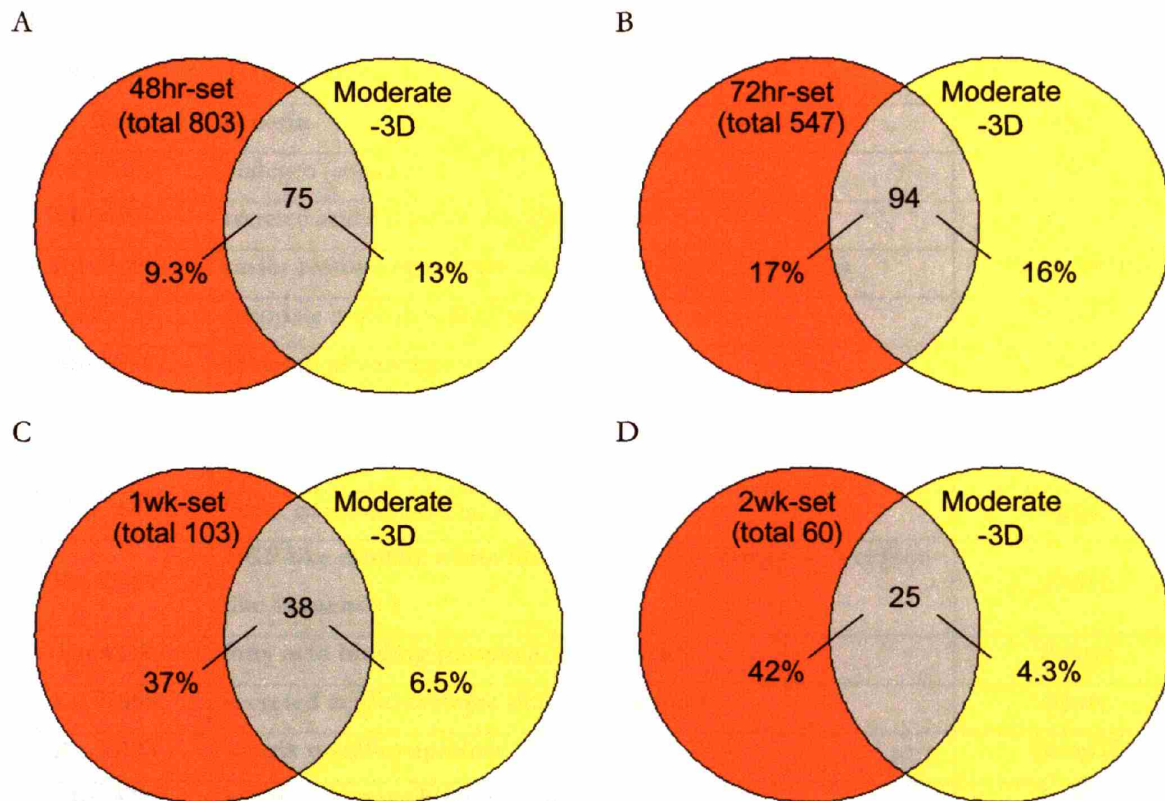


Figure 6.2: Venn diagrams showing how many probesets are shared between the Moderate-3D set (583 probesets) and four liver regeneration gene sets, as well as their percentages with respect to each set.

Nearly half of the probesets within the 2wk-set are included in the Moderate-3D set. These probesets are listed in Table 6.1. Half of these probesets are within the Robust-3D set (marked in bold font) and many are either matrix proteins or a metalloprotease.

Unigene ID	Gene Description	Gene Symbol
Rn.954	Transcribed locus	---
Rn.106103	decorin	Dcn
Rn.105658	Nidogen (entactin)	Nid
Rn.98989	secreted acidic cysteine rich glycoprotein	Sparc
Rn.35809	major histocompatibility complex, class II, DM alpha	RGD:735053
Rn.25736	guanylate nucleotide binding protein 2	Gbp2
Rn.8871	secreted phosphoprotein 1	Spp1
Rn.31988	CD53 antigen	Cd53
Rn.12759	fibrillin 1	Fbn1
Rn.764	lectin, galactose binding, soluble 3	Lgals3
Rn.43404	EGF-like module containing, mucin-like, hormone receptor-like sequence 1	Emr1
Rn.4258	fatty acid binding protein 4, adipocyte	Fabp4
Rn.98989	secreted acidic cysteine rich glycoprotein	Sparc
Rn.33193	matrix metalloproteinase 12	Mmp12
Rn.57	lectin, galactose binding, soluble 1	Lgals1
Rn.2875	collagen, type V, alpha 2	Col5a2
Rn.53801	procollagen, type IV, alpha 1 (predicted)	Col4a1_predicted
Rn.116386	Transcribed locus	---
Rn.53801	procollagen, type IV, alpha 1 (predicted)	Col4a1_predicted
Rn.3247	collagen, type III, alpha 1	Col3a1
Rn.124802	cyclin B2 (predicted)	Ccnb2_predicted
Rn.107239	procollagen, type I, alpha 2	Col1a2
Rn.2953	collagen, type 1, alpha 1	Col1a1
Rn.107239	procollagen, type I, alpha 2	Col1a2
Rn.107220	cyclin-dependent kinase inhibitor 3 (predicted)	Cdkn3_predicted

Table 6.1 List of probesets within the intersection of the Moderate-3D and 2wk-set. Bold font indicate the probeset is included in the Robust-3D set.

The intersection between liver regeneration and endothelial-specific gene sets was also compared, shown in Figure 6.3. At least a third of all probesets within liver regeneration gene sets are included in the Moderate-endothelial set.

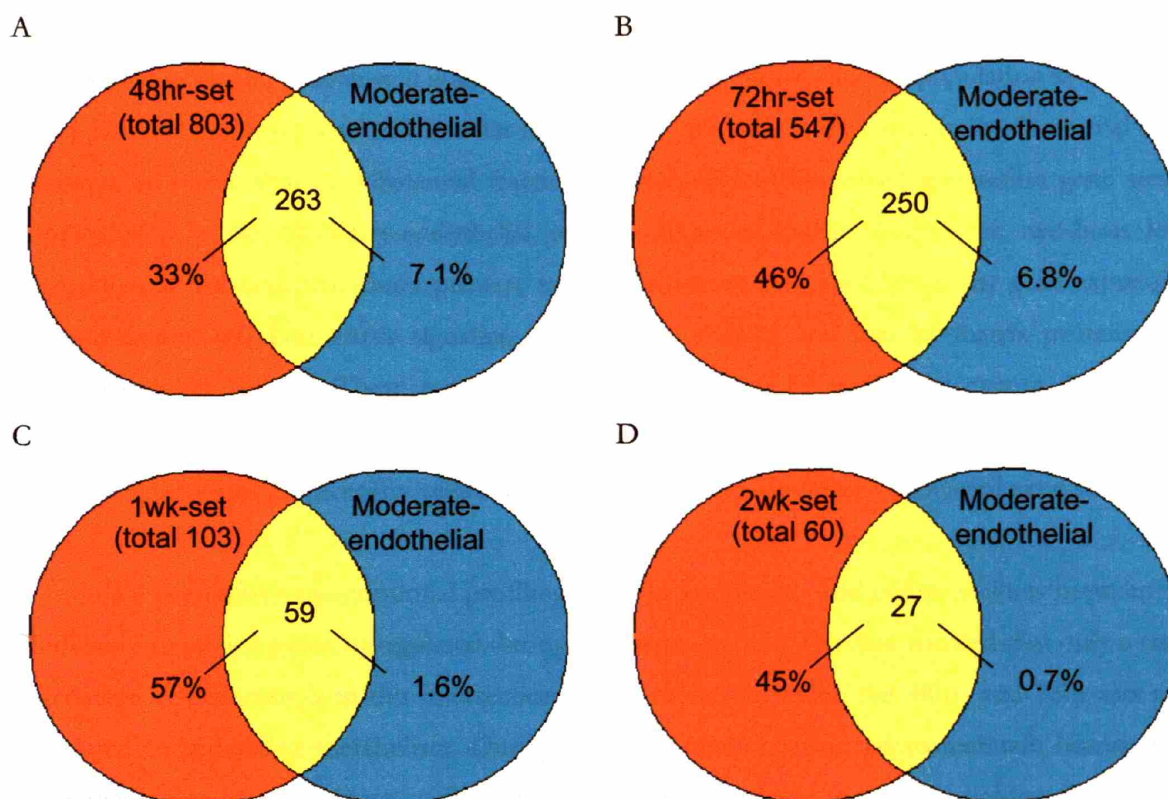


Figure 6.3: Venn diagrams showing how many probesets are shared between the Moderate-endothelial set (3688 probesets) and four liver regeneration gene sets, as well as their percentages with respect to each set.

6.4 Discussion and Conclusion

Molecular events in liver regeneration can be detected as soon as one minute after PHx is performed [163]. To date Many studies detail the molecular mechanisms of inducing hepatocyte replication, such as IL-6, TNF- α , and HGF signaling (for a review see [100]), as well as the immediate early genes induced soon after the surgery [162]. The hugely invested interest in hepatocytes' behavior stems from their unique ability in maintaining homeostasis while undergoing proliferation. Though rarely discussed, it is also convenient that hepatocytes most likely make up major contribution toward liver's total RNA such that many gene expression changes observed on liver as a whole can be attributed to hepatocytes. The dilution effect on total RNA isolated from livers composed of different cell populations should be considered carefully when NPCs are the focus of study. Hepatocytes' proliferation peaks at 24 hours, followed by stellate and Kupffer cells at

~48 hours. At around 48 and 72 hours, endothelial cells are just starting their slower and steady proliferation program. Therefore it is safe to assume that the endothelial cell population at 48 and 72 hours post-PHx represents a much smaller fraction of all the cells in liver than in liver's normal state. However, in our analysis, a substantial fraction of probesets within liver regeneration gene sets is also included in the Moderate-endothelial set. As discussed earlier, during the two-hour long perfusion and isolation procedures primary endothelial isolate may have had many gene expression changes caused by shear stress signaling, temperature change, and loss of matrix proteins and possibly integrin binding. These environmental cues may not be unlike the events during liver regeneration in which cells perform matrix remodeling and migrate. Furthermore, there may be a moderate contribution of Kupffer cells and stellate cells to the Moderate-endothelial gene set.

We performed transcriptional profiling on PHx samples to find commonalities between the Moderate-3D set and genes upregulated during liver regeneration. The data showed that only a small percentage of probesets is in this intersection. Many probesets within the 48hr- and 72hr-sets may be related to hepatocyte metabolism. During liver regeneration, liver has to maintain homeostasis while recovering its mass. Many of the early genes are upregulated to satisfy heightened metabolic demand among hepatocytes. In the reactor the culture medium supplies ample nutrients and less metabolic wastes. Also qualitative observation on reactor tissue showed no substantial change in tissue size (data not shown), suggesting little hepatocyte proliferation activity. The lack of metabolic demand and hepatocyte proliferation may explain why a large number of probesets within 48hr- and 72hr-sets do not intersect with the Moderate 3D set. Nevertheless, our previous speculation on matrix remodeling was validated as expressions of many of the related probesets were recapitulated during liver regeneration at the 2 week time point. Direct comparison, however, is difficult, since the cell composition and culture conditions are different among the PHx and reactor samples. Furthermore, the reactor samples were collected only at one time point. We can only speculate that the Moderate-3D set ought to be most similar to the 2wk-set because the two-photon micrographs showed formation of EGFP networks by day 11 of reactor cultures. A parallel temporal study of the tissue morphogenesis evolution in the reactor culture using immunohistochemistry and transcriptional profiling would help elucidate the similarities and differences between liver regeneration and *in vitro* reactor liver culture.

While gene expression profiling has been widely used to study liver regeneration, most reports focused on the early time points, with maximum of 7 days post-PHx [161, 162, 164-169]. No report has gone as far as 2 weeks. Liver mass almost fully recovers after 5-7 days, and most reports do not examine the later time points because at this point hepatocytes have finished replication and returned to physiological numbers. Our analysis suggests that liver gene transcription activity is still dynamic at 1- and 2-week post-PHx. Even though liver mass has recovered, liver tissue may still be undergoing matrix remodeling. At day 3-4, hepatocytes are grouped in avascularized islands; at day 7 endothelial cells start to invade these islands. Therefore at one week they are actively invading and remodeling the tissue structure. The presence of matrix remodeling genes is especially intriguing. Regeneration occurs when liver responds to acute injury, but cirrhosis occurs during chronic injury. It has been suggested that different ECM deposition has a large role in determining the outcome of these two very different responses [138]. Perhaps the events of matrix remodeling during the later periods of liver regeneration can shed some light on this topic.

A precaution on interpreting the data is that the normalization for liver regeneration gene sets may not be ideal. Since liver cell population changes throughout the regeneration period, any cell-specific gene will be represented in the total RNA pool differently depending on the normalization methods. For example, if an endothelial cell-specific transcript has a constant number of copies per cell regardless of environmental changes, its expression level would appear to be down-regulated at 48-hour post-PHx when the data is normalized to liver in its normal state. The interpretation of down-regulation due to environmental cues or population dilution effects can be very difficult to make unless one has strict confidence in how a particular mRNA transcript is controlled. Therefore global trends of a large group of probesets probably have more predictability than an individual probeset. To avoid the dilution effects, the samples must be generated from pure cell populations. For example, each liver cell type during liver regeneration can be isolated and purified using the conventional perfusion technique. In fact, highly pure liver endothelial cells during liver regeneration have been used to generate transcriptional profiling data (D. Stolz, personal communication). However, this method may still suffer from the compromise between cell purity and effects on gene expression caused by isolation procedures. Laser Capture Microdissection (LCM) appears to be an excellent tool for this application. This technique can parse out cells within tissue composed of heterogeneous cell populations for cell-specific DNA, RNA, or protein extractions [170]. However, the tiny amount of RNA generated with this technique needs to be amplified for

more than one cycle for microarray experiments. The effects of amplification may need to be examined [171].

In conclusion, the comparison of probesets upregulated after PHx and those within the Moderate-3D showed small overlap during the early liver regeneration time points, but matrix remodeling seems to be a late liver regeneration program recapitulated in the 3D co-culture reactor. Many endothelial-specific probesets seemed highly expressed during liver regeneration at the selected time points. However, gene expression data generated from mixed cell population is difficult to interpret, and the use of more pure cell population samples may prove more useful in the long-run.

Chapter 7

Conclusions and Future Recommendations

7.1 Summary and Conclusions

Current *in vitro* liver cultures still cannot adequately represent all physiological liver behaviors, which may require a system containing a mixture of all liver cell types arranged in appropriate tissue architecture. This dissertation set out to create and characterize a co-culture of hepatocytes and liver derived endothelial cells in a 3D perfused microreactor. Incorporation of liver endothelia with hepatocytes into spheroids was demonstrated with immunohistochemistry. Morphology study using SEM showed that these co-culture spheroids in microreactors evolved into tissue structures with significantly higher numbers of pore-like structures in sizes close to *in vivo* sinusoids compared to mono-cultures. This led us to employ endothelia isolated from EGFP+ rats in order to follow the morphological outcome of these endothelial cells. Two-photon microscopy revealed that over the period of two weeks the EGFP+ cells proliferated moderately and organized into microvessel-like structures. By mixing endothelial cells from female rats and hepatocytes from male rats, we were also able to quantify the population of female cells in the co-culture reactor by performing quantitative PCR on the genomic DNA. The DNA quantification agreed with the two-photon microscopy data that these EGFP+ female cells proliferated to constitute ~12% of the total population in the microreactors. Interestingly parallel 2D collagen gel sandwich cultures could not maintain the survival of these cells. This was in line with our hypothesis that the 3D environment with fluid flow provides a more accommodating condition for endothelial cell survival and morphogenesis.

Since all cells were obtained through primary isolations, neither the hepatocyte fraction nor the endothelial fraction was completely pure. Hence we performed immunohistochemistry on microreactor tissue to identify all non-parenchymal cells. We indeed found specific sinusoidal endothelial marker (SE-1) present throughout the co-culture tissue, as well as large-vessel endothelial marker (CD31) on the fluid-tissue interface, both physiological relevant locations. Interestingly, Kupffer cells and quiescent stellate cells were identified in both 3D co-cultures and mono-cultures. We then used transcriptional profiling to explore functional differences among all the culture conditions. Maintenance of endothelia in 3D but not in 2D was clearly demonstrated by the

comparison of co-cultures against mono-cultures where there is no significant gene expression difference in 2D. Genes that were differentially expressed between 3D co-cultures and mono-cultures were found to be largely endothelia-specific. Corresponding to our observation on microvessel structure formation, the 3D co-cultures expressed a subgroup of matrix remodeling genes higher than 3D mono-culture, which seems to be also upregulated during the later time point of liver regeneration. Using a list of genes for hepatocyte transcription factors and liver metabolism proteins, we confirmed our previous findings that microreactors maintained hepatic functions better than 2D cultures at the gene expression level. Surprisingly, these genes showed little expression difference between the 3D cultures. Because the 3D mono-culture in fact contained some non-parenchymal cells, we believe that their presence contributes to the hepatic function enhancement and additional endothelial cells do not amplify this effect.

From this study we conclude that the 3D perfused microreactor is better than 2D at maintaining the liver endothelial fraction and promoting their network morphogenesis. The 3D format also fosters retention of other liver non-parenchymal cells, whose presence likely contributed to maintaining liver functions in 3D.

7.2 Future Recommendations

On the way to reach the conclusions mentioned above, this dissertation established important tools for studying 3D cultures containing mixed cell populations. The 3D format presents many challenges in distinguishing cell types, and conventional imaging techniques have to be adapted. With a successful immunohistochemistry protocol, the 3D tissue can now be tested for specific cellular components. We still know very little about the temporal population changes and ECM deposition within the reactor tissue. A comprehensive temporal study of cell type and ECM staining would help us understand the dynamic changes in the reactor, such as proliferation and cell adhesion.

The demonstration of EGFP network formation raises the question whether these structures are indeed functional blood vessels conducive to fluid flow. Several *in situ* imaging techniques proved unsuccessful at conclusively determining this feature. An alternative technique using charged silica beads to label tissue surfaces for TEM observation is being explored. This 3D hepatocyte-

endothelia co-culture may also prove useful for studies involving liver endothelium, such as cancer metastasis and reperfusion ischemia.

References

1. Arias, I.M. and J.L. Boyer, *The Liver: biology and pathobiology*. 4th ed. 2001, Philadelphia: Lippincott Williams & Wilkins. xvi, 1064 p., [16] p. of plates.
2. Leevy, C.M. and T. Kiernan, *The hepatic circulation and portal hypertension*. Clin Gastroenterol, 1975. 4(2): p. 381-94.
3. Ochoa, E.R. and J.P. Vacanti, *An overview of the pathology and approaches to tissue engineering*. Ann N Y Acad Sci, 2002. 979: p. 10-26; discussion 35-8.
4. Wack, K.E., M.A. Ross, V. Zegarra, L.R. Sysko, S.C. Watkins, and D.B. Stolz, *Sinusoidal ultrastructure evaluated during the revascularization of regenerating rat liver*. Hepatology, 2001. 33(2): p. 363-78.
5. Junqueira, L.C.U. and J. Carneiro, *Basic histology: text & atlas*. 10th ed. 2003, New York: Lange Medical Books, McGraw-Hill, Medical Pub. Division. viii, 515 p.
6. Wake, K., *Structure of the Hepatic Sinusoid*. Cells of the hepatic sinusoid: proceedings of the International Symposium on Cells of the Hepatic Sinusoid, ed. D.K. E Wisse, K Wake (eds). Vol. 5. 1995, Leiden, The Netherlands: Kupffer Cell Foundation. 241-246.
7. LeCluyse, E.L., P.L. Bullock, A. Parkinson, and J.H. Hochman, *Cultured rat hepatocytes*. Pharm Biotechnol, 1996. 8: p. 121-59.
8. LeCluyse, E.L., P.L. Bullock, and A. Parkinson, *Strategies for restoration and maintenance of normal hepatic structure and function in long-term cultures of rat hepatocytes*. Advanced Drug Delivery Reviews, 1996. 22(1-2): p. 133-186.
9. Bhatia, S.N., U.J. Balis, M.L. Yarmush, and M. Toner, *Effect of cell-cell interactions in preservation of cellular phenotype: cocultivation of hepatocytes and nonparenchymal cells*. Faseb J, 1999. 13(14): p. 1883-900.
10. Sivaraman, A., J.K. Leach, S. Townsend, T. Iida, B.J. Hogan, R. Fry, L. Samson, S.R. Tannenbaum, and L.G. Griffith, *A microscale in vitro physiological model of the liver: predictive screens for drug metabolism and enzyme induction*. Current Drug Metabolism, 2005. 6: p. 569-592.
11. Tanikawa, K. and T. Ueno, *Liver diseases and hepatic sinusoidal cells*. 1999, Tokyo; New York: Springer. xii, 348 p.
12. Braet, F. and E. Wisse, *Structural and functional aspects of liver sinusoidal endothelial cell fenestrae: a review*. Comp Hepatol, 2002. 1(1): p. 1.

13. Kmiec, Z., *Cooperation of liver cells in health and disease*. 2001, Berlin; New York: Springer. xiii, 151 p.
14. Smedsrod, B., *Clearance function of scavenger endothelial cells*. *Comp Hepatol*, 2004. **3 Suppl 1**: p. S22.
15. Rieder, H., K.H. Meyer zum Buschenfelde, and G. Ramadori, *Functional spectrum of sinusoidal endothelial liver cells. Filtration, endocytosis, synthetic capacities and intercellular communication*. *J Hepatol*, 1992. **15**(1-2): p. 237-50.
16. Weigel, J.A., R.C. Raymond, and P.H. Weigel, *The hyaluronan receptor for endocytosis (HARE) is not CD44 or CD54 (ICAM-1)*. *Biochem Biophys Res Commun*, 2002. **294**(4): p. 918-22.
17. Laurent, T.C. and J.R. Fraser, *Hyaluronan*. *Faseb J*, 1992. **6**(7): p. 2397-404.
18. Krause, P., P.M. Markus, P. Schwartz, K. Unthan-Fechner, S. Pestel, J. Fandrey, and I. Probst, *Hepatocyte-supported serum-free culture of rat liver sinusoidal endothelial cells*. *J Hepatol*, 2000. **32**(5): p. 718-26.
19. Enomoto, K., Y. Nishikawa, Y. Omori, T. Tokairin, M. Yoshida, N. Ohi, T. Nishimura, Y. Yamamoto, and Q. Li, *Cell biology and pathology of liver sinusoidal endothelial cells*. *Med Electron Microsc*, 2004. **37**(4): p. 208-15.
20. Zhang, Y., K. Ikejima, H. Honda, T. Kitamura, Y. Takei, and N. Sato, *Glycine prevents apoptosis of rat sinusoidal endothelial cells caused by deprivation of vascular endothelial growth factor*. *Hepatology*, 2000. **32**(3): p. 542-6.
21. Samarasinghe, D.A., *Culture of sinusoidal endothelial cells from rat liver*. *J Gastroenterol Hepatol*, 1998. **13**(8): p. 851-4.
22. Ross, M.A., C.M. Sander, T.B. Kleeb, S.C. Watkins, and D.B. Stolz, *Spatiotemporal expression of angiogenesis growth factor receptors during the revascularization of regenerating rat liver*. *Hepatology*, 2001. **34**(6): p. 1135-48.
23. LeCouter, J., D.R. Moritz, B. Li, G.L. Phillips, X.H. Liang, H.P. Gerber, K.J. Hillan, and N. Ferrara, *Angiogenesis-independent endothelial protection of liver: role of VEGFR-1*. *Science*, 2003. **299**(5608): p. 890-3.
24. Davidson, A.J. and L.I. Zon, *Biomedicine. Love, honor, and protect (your liver)*. *Science*, 2003. **299**(5608): p. 835-7.
25. Scoazec, J.Y. and G. Feldmann, *The cell adhesion molecules of hepatic sinusoidal endothelial cells*. *J Hepatol*, 1994. **20**(2): p. 296-300.

26. Scoazec, J.Y. and G. Feldmann, *In situ immunophenotyping study of endothelial cells of the human hepatic sinusoid: results and functional implications*. Hepatology, 1991. **14**(5): p. 789-97.
27. Neubauer, K., T. Wilfling, A. Ritzel, and G. Ramadori, *Platelet-endothelial cell adhesion molecule-1 gene expression in liver sinusoidal endothelial cells during liver injury and repair*. J Hepatol, 2000. **32**(6): p. 921-32.
28. Liu, L., J.C. Tsai, and W.C. Aird, *Egr-1 gene is induced by the systemic administration of the vascular endothelial growth factor and the epidermal growth factor*. Blood, 2000. **96**(5): p. 1772-81.
29. DeLeve, L.D., X. Wang, L. Hu, M.K. McCuskey, and R.S. McCuskey, *Rat liver sinusoidal endothelial cell phenotype is maintained by paracrine and autocrine regulation*. Am J Physiol Gastrointest Liver Physiol, 2004. **287**(4): p. G757-63.
30. Ohmura, T., K. Enomoto, H. Satoh, N. Sawada, and M. Mori, *Establishment of a novel monoclonal antibody, SE-1, which specifically reacts with rat hepatic sinusoidal endothelial cells*. J Histochem Cytochem, 1993. **41**(8): p. 1253-7.
31. Tokairin, T., Y. Nishikawa, Y. Doi, H. Watanabe, T. Yoshioka, M. Su, Y. Omori, and K. Enomoto, *A highly specific isolation of rat sinusoidal endothelial cells by the immunomagnetic bead method using SE-1 monoclonal antibody*. J Hepatol, 2002. **36**(6): p. 725-33.
32. Wisse, E., *Observations on the fine structure and peroxidase cytochemistry of normal rat liver Kupffer cells*. J Ultrastruct Res, 1974. **46**(3): p. 393-426.
33. Wisse, E., *Kupffer cell reactions in rat liver under various conditions as observed in the electron microscope*. J Ultrastruct Res, 1974. **46**(3): p. 499-520.
34. Naito, M., G. Hasegawa, Y. Ebe, and T. Yamamoto, *Differentiation and function of Kupffer cells*. Med Electron Microsc, 2004. **37**(1): p. 16-28.
35. Sato, M., S. Suzuki, and H. Senoo, *Hepatic stellate cells: unique characteristics in cell biology and phenotype*. Cell Struct Funct, 2003. **28**(2): p. 105-12.
36. Geerts, A., *History, heterogeneity, developmental biology, and functions of quiescent hepatic stellate cells*. Semin Liver Dis, 2001. **21**(3): p. 311-35.
37. Kanno, N., G. LeSage, S. Glaser, D. Alvaro, and G. Alpini, *Functional heterogeneity of the intrahepatic biliary epithelium*. Hepatology, 2000. **31**(3): p. 555-61.
38. Marzioni, M., S.S. Glaser, H. Francis, J.L. Phinizy, G. LeSage, and G. Alpini, *Functional heterogeneity of cholangiocytes*. Semin Liver Dis, 2002. **22**(3): p. 227-40.
39. Lazaridis, K.N., M. Strazzabosco, and N.F. Larusso, *The cholangiopathies: disorders of biliary epithelia*. Gastroenterology, 2004. **127**(5): p. 1565-77.

40. Nakatani, K., K. Kaneda, S. Seki, and Y. Nakajima, *Pit cells as liver-associated natural killer cells: morphology and function*. Med Electron Microsc, 2004. **37**(1): p. 29-36.
41. Guguen-Guillouzo, C., B. Clement, G. Baffet, C. Beaumont, E. Morel-Chany, D. Glaise, and A. Guillouzo, *Maintenance and reversibility of active albumin secretion by adult rat hepatocytes co-cultured with another liver epithelial cell type*. Exp Cell Res, 1983. **143**(1): p. 47-54.
42. Chia, S.M., P.C. Lin, and H. Yu, *TGF-beta1 regulation in hepatocyte-NIH3T3 co-culture is important for the enhanced hepatocyte function in 3D microenvironment*. Biotechnol Bioeng, 2005. **89**(5): p. 565-73.
43. Bhatia, S.N., U.J. Balis, M.L. Yarmush, and M. Toner, *Microfabrication of hepatocyte/fibroblast co-cultures: role of homotypic cell interactions*. Biotechnol Prog, 1998. **14**(3): p. 378-87.
44. Singhvi, R., A. Kumar, G.P. Lopez, G.N. Stephanopoulos, D.I. Wang, G.M. Whitesides, and D.E. Ingber, *Engineering cell shape and function*. Science, 1994. **264**(5159): p. 696-8.
45. Hirose, M., M. Yamato, O.H. Kwon, M. Harimoto, A. Kushida, T. Shimizu, A. Kikuchi, and T. Okano, *Temperature-Responsive surface for novel co-culture systems of hepatocytes with endothelial cells: 2-D patterned and double layered co-cultures*. Yonsei Med J, 2000. **41**(6): p. 803-13.
46. Bader, A., E. Knop, A. Kern, K. Boker, N. Fruhauf, O. Crome, H. Esselmann, C. Pape, G. Kempka, and K.F. Sewing, *3-D coculture of hepatic sinusoidal cells with primary hepatocytes-design of an organotypical model*. Exp Cell Res, 1996. **226**(1): p. 223-33.
47. Pollok, J.M., D. Kluth, R.A. Cusick, H. Lee, H. Utsunomiya, P.X. Ma, R. Langer, C.E. Broelsch, and J.P. Vacanti, *Formation of spheroidal aggregates of hepatocytes on biodegradable polymers under continuous-flow bioreactor conditions*. Eur J Pediatr Surg, 1998. **8**(4): p. 195-9.
48. Talamini, M.A., M.P. McCluskey, T.G. Buchman, and A. De Maio, *Expression of alpha2-macroglobulin by the interaction between hepatocytes and endothelial cells in coculture*. Am J Physiol, 1998. **275**(1 Pt 2): p. R203-11.
49. Mitaka, T., F. Sato, T. Mizuguchi, T. Yokono, and Y. Mochizuki, *Reconstruction of hepatic organoid by rat small hepatocytes and hepatic nonparenchymal cells*. Hepatology, 1999. **29**(1): p. 111-25.
50. Ries, K., P. Krause, M. Solsbacher, P. Schwartz, K. Unthan-Fechner, B. Christ, P.M. Markus, and I. Probst, *Elevated expression of hormone-regulated rat hepatocyte functions in a new serum-free hepatocyte-stromal cell coculture model*. In Vitro Cell Dev Biol Anim, 2000. **36**(8): p. 502-12.
51. Ranucci, C.S., A. Kumar, S.P. Batra, and P.V. Moghe, *Control of hepatocyte function on collagen foams: sizing matrix pores toward selective induction of 2-D and 3-D cellular morphogenesis*. Biomaterials, 2000. **21**(8): p. 783-93.

52. Hoebe, K.H., R.F. Witkamp, J. Fink-Gremmels, A.S. Van Miert, and M. Monshouwer, *Direct cell-to-cell contact between Kupffer cells and hepatocytes augments endotoxin-induced hepatic injury*. Am J Physiol Gastrointest Liver Physiol, 2001. **280**(4): p. G720-8.
53. Washizu, J., F. Berthiaume, Y. Mokuno, R.G. Tompkins, M. Toner, and M.L. Yarmush, *Long-term maintenance of cytochrome P450 activities by rat hepatocyte/3T3 cell co-cultures in heparinized human plasma*. Tissue Eng, 2001. **7**(6): p. 691-703.
54. Takai, K.K., S. Hattori, and S. Irie, *Type V collagen distribution in liver is reconstructed in coculture system of hepatocytes and stellate cells; the possible functions of type V collagen in liver under normal and pathological conditions*. Cell Struct Funct, 2001. **26**(5): p. 289-302.
55. Brieva, T.A. and P.V. Moghe, *Functional engineering of hepatocytes via heterocellular presentation of a homoadhesive molecule, E-cadherin*. Biotechnol Bioeng, 2001. **76**(4): p. 295-302.
56. Bhandari, R.N., L.A. Riccalton, A.L. Lewis, J.R. Fry, A.H. Hammond, S.J. Tendler, and K.M. Shakesheff, *Liver tissue engineering: a role for co-culture systems in modifying hepatocyte function and viability*. Tissue Eng, 2001. **7**(3): p. 345-57.
57. Gregory, P.G., C.K. Connolly, B.E. Gillis, and S.J. Sullivan, *The effect of coculture with nonparenchymal cells on porcine hepatocyte function*. Cell Transplant, 2001. **10**(8): p. 731-8.
58. Uyama, N., Y. Shimahara, N. Kawada, S. Seki, H. Okuyama, Y. Iimuro, and Y. Yamaoka, *Regulation of cultured rat hepatocyte proliferation by stellate cells*. J Hepatol, 2002. **36**(5): p. 590-9.
59. Harimoto, M., M. Yamato, M. Hirose, C. Takahashi, Y. Isoi, A. Kikuchi, and T. Okano, *Novel approach for achieving double-layered cell sheets co-culture: overlaying endothelial cell sheets onto monolayer hepatocytes utilizing temperature-responsive culture dishes*. J Biomed Mater Res, 2002. **62**(3): p. 464-70.
60. Arnaud, A., L. Fontana, A.J. Angulo, A. Gil, and J.M. Lopez-Pedrosa, *Proliferation, functionality, and extracellular matrix production of hepatocytes and a liver stellate cell line: a comparison between single cultures and cocultures*. Dig Dis Sci, 2003. **48**(7): p. 1406-13.
61. Riccalton-Banks, L., C. Liew, R. Bhandari, J. Fry, and K. Shakesheff, *Long-term culture of functional liver tissue: three-dimensional coculture of primary hepatocytes and stellate cells*. Tissue Eng, 2003. **9**(3): p. 401-10.
62. Miura, K., H. Nagai, Y. Ueno, T. Goto, K. Mikami, K. Nakane, K. Yoneyama, D. Watanabe, K. Terada, T. Sugiyama, K. Imai, H. Senoo, and S. Watanabe, *Epimorphin is involved in differentiation of rat hepatic stem-like cells through cell-cell contact*. Biochem Biophys Res Commun, 2003. **311**(2): p. 415-23.

63. Kudryavtseva, E.I. and N.V. Engelhardt, *Requirement of 3D extracellular network for maintenance of mature hepatocyte morphology and suppression of alpha-fetoprotein synthesis in vitro*. Immunol Lett, 2003. **90**(1): p. 25-31.
64. Sunman, J.A., R.L. Hawke, E.L. LeCluyse, and A.D. Kashuba, *Kupffer cell-mediated IL-2 suppression of CYP3A activity in human hepatocytes*. Drug Metab Dispos, 2004. **32**(3): p. 359-63.
65. Yaakov, N., R.E. Schwartz, W. Hu, C.M. Verfaillie, and D.J. Odde, *Endothelium-mediated Hepatocyte Recruitment in the Establishment of Liver-like Tissue In Vitro*. In review, 2005.
66. Auth, M.K., D. Woitaschek, M. Beste, T. Schreiter, H.S. Kim, E. Oppermann, R.E. Joplin, U. Baumann, P. Hilgard, S. Nadalin, B.H. Markus, and R.A. Blaheta, *Preservation of the synthetic and metabolic capacity of isolated human hepatocytes by coculture with human biliary epithelial cells*. Liver Transpl, 2005. **11**(4): p. 410-9.
67. Tsuda, Y., A. Kikuchi, M. Yamato, A. Nakao, Y. Sakurai, M. Umezū, and T. Okano, *The use of patterned dual thermoresponsive surfaces for the collective recovery as co-cultured cell sheets*. Biomaterials, 2005. **26**(14): p. 1885-93.
68. De Bartolo, L., G. Jarosch-Von Schweder, A. Haverich, and A. Bader, *A novel full-scale flat membrane bioreactor utilizing porcine hepatocytes: cell viability and tissue-specific functions*. Biotechnol Prog, 2000. **16**(1): p. 102-8.
69. Tilles, A.W., H. Baskaran, P. Roy, M.L. Yarmush, and M. Toner, *Effects of oxygenation and flow on the viability and function of rat hepatocytes cocultured in a microchannel flat-plate bioreactor*. Biotechnol Bioeng, 2001. **73**(5): p. 379-89.
70. Allen, J.W. and S.N. Bhatia, *Formation of steady-state oxygen gradients in vitro: application to liver zonation*. Biotechnol Bioeng, 2003. **82**(3): p. 253-62.
71. Kan, P., H. Miyoshi, and N. Ohshima, *Perfusion of medium with supplemented growth factors changes metabolic activities and cell morphology of hepatocyte-nonparenchymal cell coculture*. Tissue Eng, 2004. **10**(9-10): p. 1297-307.
72. Ito, A., Y. Takizawa, H. Honda, K. Hata, H. Kagami, M. Ueda, and T. Kobayashi, *Tissue engineering using magnetite nanoparticles and magnetic force: heterotypic layers of cocultured hepatocytes and endothelial cells*. Tissue Eng, 2004. **10**(5-6): p. 833-40.
73. Wu, F., J. Friend, C. Hsiao, M. Zilliox, W. Ko, F. Cerra, and W. Hu, *Efficient assembly of rat hepatocyte spheroids for tissue engineering applications*. BIOTECHNOLOGY AND BIOENGINEERING, 1996. **50**(4): p. 404-415.

74. Peshwa, M.V., F.J. Wu, H.L. Sharp, F.B. Cerra, and W.S. Hu, *Mechanistics of formation and ultrastructural evaluation of hepatocyte spheroids*. In *Vitro Cell Dev Biol Anim*, 1996. **32**(4): p. 197-203.
75. Jauregui, H.O., *Liver*, in *Principles of Tissue Engineering*, R.P. Lanza, R. Langer, and J.P. Vacanti, Editors. 2000, Academic Press: New York.
76. Gerlach, J.C., *Long-term liver cell cultures in bioreactors and possible application for liver support*. *Cell Biol Toxicol*, 1997. **13**(4-5): p. 349-55.
77. Gerlach, J.C., K. Kloppel, C. Muller, N. Schnoy, M.D. Smith, and P. Neuhaus, *Hepatocyte aggregate culture technique for bioreactors in hybrid liver support systems*. *Int J Artif Organs*, 1993. **16**(12): p. 843-6.
78. Michalopoulos, G.K., W.C. Bowen, V.F. Zajac, D. Beer-Stolz, S. Watkins, V. Kostrubsky, and S.C. Strom, *Morphogenetic events in mixed cultures of rat hepatocytes and nonparenchymal cells maintained in biological matrices in the presence of hepatocyte growth factor and epidermal growth factor*. *Hepatology*, 1999. **29**(1): p. 90-100.
79. Michalopoulos, G.K., W.C. Bowen, K. Mule, and D.B. Stolz, *Histological organization in hepatocyte organoid cultures*. *Am J Pathol*, 2001. **159**(5): p. 1877-87.
80. Naughton, B.A., B. Sibanda, J.P. Weintraub, J. San Roman, and V. Kamali, *A stereotypic, transplantable liver tissue-culture system*. *Appl Biochem Biotechnol*, 1995. **54**(1-3): p. 65-91.
81. Kaihara, S., S. Kim, B.S. Kim, D.J. Mooney, K. Tanaka, and J.P. Vacanti, *Survival and function of rat hepatocytes cocultured with nonparenchymal cells or sinusoidal endothelial cells on biodegradable polymers under flow conditions*. *J Pediatr Surg*, 2000. **35**(9): p. 1287-90.
82. Kim, S.S., H. Utsunomiya, J.A. Koski, B.M. Wu, M.J. Cima, J. Sohn, K. Mukai, L.G. Griffith, and J.P. Vacanti, *Survival and function of hepatocytes on a novel three-dimensional synthetic biodegradable polymer scaffold with an intrinsic network of channels*. *Ann Surg*, 1998. **228**(1): p. 8-13.
83. Yamada, K., M. Kamihira, R. Hamamoto, and S. Iijima, *Efficient induction of hepatocyte spheroids in a suspension culture using a water-soluble synthetic polymer as an artificial matrix*. *J Biochem (Tokyo)*, 1998. **123**(6): p. 1017-23.
84. Gerlach, J.C., J. Encke, O. Hole, C. Muller, J.M. Courtney, and P. Neuhaus, *Hepatocyte culture between three dimensionally arranged biomatrix-coated independent artificial capillary systems and sinusoidal endothelial cell co-culture compartments*. *Int J Artif Organs*, 1994. **17**(5): p. 301-6.

85. Vidal-Vanaclocha, F., *Role of Sinusoidal Endothelium in the Pathogenesis of Liver Disease*, in *Functional Heterogeneity of Liver Tissue*, F. Vidal-Vanaclocha, Editor. 1997, R. G. Landes Company: Austin, Texas.
86. Powers, M.J., K. Domansky, M.R. Kaazempur-Mofrad, A. Kalezi, A. Capitano, A. Upadhyaya, P. Kurzawski, K.E. Wack, D.B. Stolz, R. Kamm, and L.G. Griffith, *A microfabricated array bioreactor for perfused 3D liver culture*. *Biotechnol Bioeng*, 2002. **78**(3): p. 257-69.
87. Powers, M.J., D.M. Janigian, K.E. Wack, C.S. Baker, and L.G. Griffith, *Functional behavior of primary rat liver cells in a 3D perfused microarray bioreactor*. *Biotechnology and Bioengineering*, 2001. **in press**.
88. Domansky, K., A. Sivaraman, and L.G. Griffith, *Micromachined Bioreactor For In Vitro Cell Self-assembly And 3D Tissue Formation*, in *Lab-on-a-chips for Cellomics: Micro and Nanotechnologies for Life Science*, H. Andersson and A. Van Den Berg, Editors. 2004, Kluwer Academic Publishers: Dordrecht, The Netherlands. p. 319-346.
89. Papadaki, M. and S.G. Eskin, *Effects of fluid shear stress on gene regulation of vascular cells*. *Biotechnol Prog*, 1997. **13**(3): p. 209-21.
90. Fisher, A.B., S. Chien, A.I. Barakat, and R.M. Nerem, *Endothelial cellular response to altered shear stress*. *Am J Physiol Lung Cell Mol Physiol*, 2001. **281**(3): p. L529-33.
91. Davies, P.F., *Flow-mediated endothelial mechanotransduction*. *Physiol Rev*, 1995. **75**(3): p. 519-60.
92. Kan, P., H. Miyoshi, K. Yanagi, and N. Ohshima, *Effects of shear stress on metabolic function of the co-culture system of hepatocyte/nonparenchymal cells for a bioartificial liver*. *Asaio J*, 1998. **44**(5): p. M441-4.
93. Powers, M.J., K. Domensky, A. Upadhyaya, M.R. Kaazempur-Mofrad, P. Kurzawski, K.E. Wack, D.B. Stolz, R. Kamm, and L.G. Griffith, *A microfabricated array bioreactor for perfused 3D liver culture*. *Biotechnology and Bioengineering*, 2001. **in press**.
94. Boardman, K.C. and M.A. Swartz, *Interstitial flow as a guide for lymphangiogenesis*. *Circ Res*, 2003. **92**(7): p. 801-8.
95. Helm, C.E., M.E. Fleury, A.H. Zisch, F. Boschetti, and M.A. Swartz, *Synergy between 3D flow and VEGF directs capillary morphogenesis in vitro: Experiments and theoretical mechanisms*. *Proceedings of the National Academy of Sciences*, 2005. **In press**.
96. Michalopoulos, G.K. and M. DeFrances, *Liver regeneration*. *Adv Biochem Eng Biotechnol*, 2005. **93**: p. 101-34.

97. Michalopoulos, G.K. and M.C. DeFrances, *Liver regeneration*. Science, 1997. **276**(5309): p. 60-6.
98. Kim, T.H., W.M. Mars, D.B. Stolz, B.E. Petersen, and G.K. Michalopoulos, *Extracellular matrix remodeling at the early stages of liver regeneration in the rat*. Hepatology, 1997. **26**(4): p. 896-904.
99. Fausto, N., A.D. Laird, and E.M. Webber, *Liver regeneration. 2. Role of growth factors and cytokines in hepatic regeneration*. Faseb J, 1995. **9**(15): p. 1527-36.
100. Taub, R., *Liver regeneration: from myth to mechanism*. Nat Rev Mol Cell Biol, 2004. **5**(10): p. 836-47.
101. So, P.T., C.Y. Dong, B.R. Masters, and K.M. Berland, *Two-photon excitation fluorescence microscopy*. Annu Rev Biomed Eng, 2000. **2**: p. 399-429.
102. Denk, W., J.H. Strickler, and W.W. Webb, *Two-photon laser scanning fluorescence microscopy*. Science, 1990. **248**(4951): p. 73-6.
103. Harlow, E. and D. Lane, *Using antibodies: a laboratory manual*. 1999, Cold Spring Harbor, N.Y.: Cold Spring Harbor Laboratory Press. xiv, 495 p.
104. Powers, M.J. and L.G. Griffith, *Adhesion-guided in vitro morphogenesis in pure and mixed cell cultures*. Microsc Res Tech, 1998. **43**(5): p. 379-84.
105. Smedsrod, B. and H. Pertoft, *Preparation of pure hepatocytes and reticuloendothelial cells in high yield from a single rat liver by means of Percoll centrifugation and selective adherence*. J Leukoc Biol, 1985. **38**(2): p. 213-30.
106. Schreiber, B.M., *Use of Gene Expression to Characterize Heterogeneous Liver Cell Populations*, in *Biological Engineering*. 2004, Massachusetts Institute of Technology: Cambridge, MA. p. p.120.
107. Voyta, J.C., D.P. Via, C.E. Butterfield, and B.R. Zetter, *Identification and isolation of endothelial cells based on their increased uptake of acetylated-low density lipoprotein*. J Cell Biol, 1984. **99**(6): p. 2034-40.
108. Powers, M.J., D.M. Janigian, K.E. Wack, C.S. Baker, D. Beer Stolz, and L.G. Griffith, *Functional behavior of primary rat liver cells in a three-dimensional perfused microarray bioreactor*. Tissue Eng, 2002. **8**(3): p. 499-513.
109. Enis, D.R., B.R. Shepherd, Y. Wang, A. Qasim, C.M. Shanahan, P.L. Weissberg, M. Kashgarian, J.S. Pober, and J.S. Schechner, *Induction, differentiation, and remodeling of blood vessels after transplantation of Bcl-2-transduced endothelial cells*. Proc Natl Acad Sci U S A, 2005. **102**(2): p. 425-30.

110. Koike, N., D. Fukumura, O. Gralla, P. Au, J.S. Schechner, and R.K. Jain, *Tissue engineering: creation of long-lasting blood vessels*. Nature, 2004. **428**(6979): p. 138-9.
111. Stroh, M., J.P. Zimmer, D.G. Duda, T.S. Levchenko, K.S. Cohen, E.B. Brown, D.T. Scadden, V.P. Torchilin, M.G. Bawendi, D. Fukumura, and R.K. Jain, *Quantum dots spectrally distinguish multiple species within the tumor milieu in vivo*. Nat Med, 2005. **11**(6): p. 678-82.
112. de Haas, R.R., R.P. van Gijlswijk, E.B. van der Tol, J. Veuskens, H.E. van Gijssel, R.B. Tijdens, J. Bonnet, N.P. Verwoerd, and H.J. Tanke, *Phosphorescent platinum/palladium coproporphyrins for time-resolved luminescence microscopy*. J Histochem Cytochem, 1999. **47**(2): p. 183-96.
113. Hohne-Zell, B., A. Galler, W. Schepp, M. Gratzl, and C. Prinz, *Functional importance of synaptobrevin and SNAP-25 during exocytosis of histamine by rat gastric enterochromaffin-like cells*. Endocrinology, 1997. **138**(12): p. 5518-26.
114. Curry, F.E., V.H. Huxley, and R.H. Adamson, *Permeability of single capillaries to intermediate-sized colored solutes*. Am J Physiol, 1983. **245**(3): p. H495-505.
115. Lightman, S.L., L.E. Caspers-Velu, S. Hirose, R.B. Nussenblatt, and A.G. Palestine, *Angiography with fluorescein-labeled dextrans in a primate model of uveitis*. Arch Ophthalmol, 1987. **105**(6): p. 844-8.
116. Rabkin, M.D., M.B. Bellhorn, and R.W. Bellhorn, *Selected molecular weight dextrans for in vivo permeability studies of rat retinal vascular disease*. Exp Eye Res, 1977. **24**(6): p. 607-12.
117. Hakamata, Y., K. Tahara, H. Uchida, Y. Sakuma, M. Nakamura, A. Kume, T. Murakami, M. Takahashi, R. Takahashi, M. Hirabayashi, M. Ueda, I. Miyoshi, N. Kasai, and E. Kobayashi, *Green fluorescent protein-transgenic rat: a tool for organ transplantation research*. Biochem Biophys Res Commun, 2001. **286**(4): p. 779-85.
118. Yuasa, C., Y. Tomita, M. Shono, K. Ishimura, and A. Ichihara, *Importance of cell aggregation for expression of liver functions and regeneration demonstrated with primary cultured hepatocytes*. J Cell Physiol, 1993. **156**(3): p. 522-30.
119. Tong, J.Z., O. Bernard, and F. Alvarez, *Long-term culture of rat liver cell spheroids in hormonally defined media*. Exp Cell Res, 1990. **189**(1): p. 87-92.
120. Landry, J., D. Bernier, C. Ouellet, R. Goyette, and N. Marceau, *Spheroidal aggregate culture of rat liver cells: histotypic reorganization, biomatrix deposition, and maintenance of functional activities*. J Cell Biol, 1985. **101**(3): p. 914-23.

121. Koide, N., K. Sakaguchi, Y. Koide, K. Asano, M. Kawaguchi, H. Matsushima, T. Takenami, T. Shinji, M. Mori, and T. Tsuji, *Formation of multicellular spheroids composed of adult rat hepatocytes in dishes with positively charged surfaces and under other nonadherent environments*. *Exp Cell Res*, 1990. **186**(2): p. 227-35.
122. Malik, R., C. Selden, and H. Hodgson, *The role of non-parenchymal cells in liver growth*. *Semin Cell Dev Biol*, 2002. **13**(6): p. 425-31.
123. Maher, J.J., D.M. Bissell, S.L. Friedman, and F.J. Roll, *Collagen measured in primary cultures of normal rat hepatocytes derives from lipocytes within the monolayer*. *J Clin Invest*, 1988. **82**(2): p. 450-9.
124. Zeilinger, K., G. Holland, I.M. Sauer, E. Efimova, D. Kardassis, N. Obermayer, M. Liu, P. Neuhaus, and J.C. Gerlach, *Time course of primary liver cell reorganization in three-dimensional high-density bioreactors for extracorporeal liver support: an immunohistochemical and ultrastructural study*. *Tissue Eng*, 2004. **10**(7-8): p. 1113-24.
125. Block, G.D., J. Locker, W.C. Bowen, B.E. Petersen, S. Katyal, S.C. Strom, T. Riley, T.A. Howard, and G.K. Michalopoulos, *Population expansion, clonal growth, and specific differentiation patterns in primary cultures of hepatocytes induced by HGF/SF, EGF and TGF alpha in a chemically defined (HGM) medium*. *J Cell Biol*, 1996. **132**(6): p. 1133-49.
126. Braet, F., R. De Zanger, T. Sasaoki, M. Baekeland, P. Janssens, B. Smedsrod, and E. Wisse, *Assessment of a method of isolation, purification, and cultivation of rat liver sinusoidal endothelial cells*. *Lab Invest*, 1994. **70**(6): p. 944-52.
127. Ito, T., A. Suzuki, E. Imai, M. Okabe, and M. Hori, *Bone marrow is a reservoir of repopulating mesangial cells during glomerular remodeling*. *J Am Soc Nephrol*, 2001. **12**(12): p. 2625-35.
128. Iwatani, H., T. Ito, E. Imai, Y. Matsuzaki, A. Suzuki, M. Yamato, M. Okabe, and M. Hori, *Hematopoietic and nonhematopoietic potentials of Hoechst(low)/side population cells isolated from adult rat kidney*. *Kidney Int*, 2004. **65**(5): p. 1604-14.
129. Malick, L.E. and R.B. Wilson, *Modified thiocarbonylhydrazide procedure for scanning electron microscopy: routine use for normal, pathological, or experimental tissues*. *Stain Technol*, 1975. **50**(4): p. 265-9.
130. Braet, F., R. De Zanger, and E. Wisse, *Drying cells for SEM, AFM and TEM by hexamethyldisilazane: a study on hepatic endothelial cells*. *J Microsc*, 1997. **186 (Pt 1)**: p. 84-7.
131. Cukierman, E., R. Pankov, D.R. Stevens, and K.M. Yamada, *Taking cell-matrix adhesions to the third dimension*. *Science*, 2001. **294**(5547): p. 1708-12.

132. Harada, K., T. Mitaka, S. Miyamoto, S. Sugimoto, S. Ikeda, H. Takeda, Y. Mochizuki, and K. Hirata, *Rapid formation of hepatic organoid in collagen sponge by rat small hepatocytes and hepatic nonparenchymal cells*. J Hepatol, 2003. **39**(5): p. 716-23.
133. Shakado, S., S. Sakisaka, K. Noguchi, M. Yoshitake, M. Harada, Y. Mimura, M. Sata, and K. Tanikawa, *Effects of extracellular matrices on tube formation of cultured rat hepatic sinusoidal endothelial cells*. Hepatology, 1995. **22**(3): p. 969-73.
134. Endo, D., K. Kogure, Y. Hasegawa, M. Maku-uchi, and I. Kojima, *Activin A augments vascular endothelial growth factor activity in promoting branching tubulogenesis in hepatic sinusoidal endothelial cells*. J Hepatol, 2004. **40**(3): p. 399-404.
135. Donovan, D., N.J. Brown, E.T. Bishop, and C.E. Lewis, *Comparison of three in vitro human 'angiogenesis' assays with capillaries formed in vivo*. Angiogenesis, 2001. **4**(2): p. 113-21.
136. Villaschi, S. and R.F. Nicosia, *Paracrine interactions between fibroblasts and endothelial cells in a serum-free coculture model. Modulation of angiogenesis and collagen gel contraction*. Lab Invest, 1994. **71**(2): p. 291-9.
137. Ueda, A., M. Koga, M. Ikeda, S. Kudo, and K. Tanishita, *Effect of shear stress on microvessel network formation of endothelial cells with in vitro three-dimensional model*. Am J Physiol Heart Circ Physiol, 2004. **287**(3): p. H994-1002.
138. Martinez-Hernandez, A. and P.S. Amenta, *The extracellular matrix in hepatic regeneration*. Faseb J, 1995. **9**(14): p. 1401-10.
139. Korff, T. and H.G. Augustin, *Tensional forces in fibrillar extracellular matrices control directional capillary sprouting*. J Cell Sci, 1999. **112** (Pt 19): p. 3249-58.
140. Wartenberg, M., F. Donmez, F.C. Ling, H. Acker, J. Hescheler, and H. Sauer, *Tumor-induced angiogenesis studied in confrontation cultures of multicellular tumor spheroids and embryoid bodies grown from pluripotent embryonic stem cells*. Faseb J, 2001. **15**(6): p. 995-1005.
141. Cross, M.J., J. Dixelius, T. Matsumoto, and L. Claesson-Welsh, *VEGF-receptor signal transduction*. Trends Biochem Sci, 2003. **28**(9): p. 488-94.
142. Yancopoulos, G.D., S. Davis, N.W. Gale, J.S. Rudge, S.J. Wiegand, and J. Holash, *Vascular-specific growth factors and blood vessel formation*. Nature, 2000. **407**(6801): p. 242-8.
143. Domansky, K., W. Inman, S. J., and L.G. Griffith, *3D Perfused Liver Microreactor Array in the Multiwell Cell Culture Plate Format*. Proceedings of the Ninth International Conference on Miniaturized Systems for Chemistry and Life Sciences (μ TAS), 2005. **Submitted**.

144. Akrawi, M., V. Rogiers, Y. Vandenberghe, C.N. Palmer, A. Vercruysse, E.A. Shephard, and I.R. Phillips, *Maintenance and induction in co-cultured rat hepatocytes of components of the cytochrome P450-mediated mono-oxygenase*. *Biochem Pharmacol*, 1993. **45**(8): p. 1583-91.
145. Clement, B., C. Guguen-Guillouzo, J.P. Campion, D. Glaise, M. Bourel, and A. Guillouzo, *Long-term co-cultures of adult human hepatocytes with rat liver epithelial cells: modulation of albumin secretion and accumulation of extracellular material*. *Hepatology*, 1984. **4**(3): p. 373-80.
146. Morin, O. and C. Normand, *Long-term maintenance of hepatocyte functional activity in co-culture: requirements for sinusoidal endothelial cells and dexamethasone*. *J Cell Physiol*, 1986. **129**(1): p. 103-10.
147. Donato, M.T., M.J. Gomez-Lechon, and J.V. Castell, *Drug metabolizing enzymes in rat hepatocytes co-cultured with cell lines*. *In Vitro Cell Dev Biol*, 1990. **26**(11): p. 1057-62.
148. Goulet, F., C. Normand, and O. Morin, *Cellular interactions promote tissue-specific function, biomatrix deposition and junctional communication of primary cultured hepatocytes*. *Hepatology*, 1988. **8**(5): p. 1010-8.
149. Jurima-Romet, M., W.L. Casley, J.M. Neu, and H.S. Huang, *Induction of CYP3A and associated terfenadine N-dealkylation in rat hepatocytes cocultured with 3T3 cells*. *Cell Biol Toxicol*, 1995. **11**(6): p. 313-27.
150. Wu, F.J., M.V. Peshwa, F.B. Cerra, and W. Hu, *Entrapment of Hepatocyte Spheroids in a Hollow fiber Bioreactor as a Potential Bioartificial Liver*. *Tissue Eng*, 1995. **1**(1): p. 29-40.
151. Gomez-Lechon, M.J., R. Jover, T. Donato, X. Ponsoda, C. Rodriguez, K.G. Stenzel, R. Klocke, D. Paul, I. Guillen, R. Bort, and J.V. Castell, *Long-term expression of differentiated functions in hepatocytes cultured in three-dimensional collagen matrix*. *J Cell Physiol*, 1998. **177**(4): p. 553-62.
152. Eschbach, E., S.S. Chatterjee, M. Noldner, E. Gottwald, H. Dertinger, K.F. Weibezahn, and G. Knedlitschek, *Microstructured scaffolds for liver tissue cultures of high cell density: morphological and biochemical characterization of tissue aggregates*. *J Cell Biochem*, 2005. **95**(2): p. 243-55.
153. Matsumoto, K., H. Yoshitomi, J. Rossant, and K.S. Zaret, *Liver organogenesis promoted by endothelial cells prior to vascular function*. *Science*, 2001. **294**(5542): p. 559-63.
154. Lacorre, D.A., E.S. Baekkevold, I. Garrido, P. Brandtzaeg, G. Haraldsen, F. Amalric, and J.P. Girard, *Plasticity of endothelial cells: rapid dedifferentiation of freshly isolated high endothelial venule endothelial cells outside the lymphoid tissue microenvironment*. *Blood*, 2004. **103**(11): p. 4164-72.

155. Gerritsen, M.E., R. Soriano, S. Yang, C. Zlot, G. Ingle, K. Toy, and P.M. Williams, *Branching out: a molecular fingerprint of endothelial differentiation into tube-like structures generated by Affymetrix oligonucleotide arrays*. *Microcirculation*, 2003. **10**(1): p. 63-81.
156. Oh, H., H. Takagi, A. Otani, S. Koyama, S. Kemmochi, A. Uemura, and Y. Honda, *Selective induction of neuropilin-1 by vascular endothelial growth factor (VEGF): a mechanism contributing to VEGF-induced angiogenesis*. *Proc Natl Acad Sci U S A*, 2002. **99**(1): p. 383-8.
157. Liu, W., A.A. Parikh, O. Stoeltzing, F. Fan, M.F. McCarty, J. Wey, D.J. Hicklin, and L.M. Ellis, *Upregulation of neuropilin-1 by basic fibroblast growth factor enhances vascular smooth muscle cell migration in response to VEGF*. *Cytokine*, 2005.
158. Braet, F., M. Shleper, M. Paizi, S. Brodsky, N. Kopeiko, N. Resnick, and G. Spira, *Liver sinusoidal endothelial cell modulation upon resection and shear stress in vitro*. *Comp Hepatol*, 2004. **3**(1): p. 7.
159. Asahina, K., H. Sato, C. Yamasaki, M. Kataoka, M. Shiokawa, S. Katayama, C. Tateno, and K. Yoshizato, *Pleiotrophin/heparin-binding growth-associated molecule as a mitogen of rat hepatocytes and its role in regeneration and development of liver*. *Am J Pathol*, 2002. **160**(6): p. 2191-205.
160. Sudo, R., T. Mitaka, M. Ikeda, and K. Tanishita, *Reconstruction of 3D stacked-up structures by rat small hepatocytes on microporous membranes*. *Faseb J*, 2005. **19**(12): p. 1695-7.
161. Arai, M., O. Yokosuka, T. Chiba, F. Imazeki, M. Kato, J. Hashida, Y. Ueda, S. Sugano, K. Hashimoto, H. Saisho, M. Takiguchi, and N. Seki, *Gene expression profiling reveals the mechanism and pathophysiology of mouse liver regeneration*. *J Biol Chem*, 2003. **278**(32): p. 29813-8.
162. Su, A.I., L.G. Guidotti, J.P. Pezacki, F.V. Chisari, and P.G. Schultz, *Gene expression during the priming phase of liver regeneration after partial hepatectomy in mice*. *Proc Natl Acad Sci U S A*, 2002. **99**(17): p. 11181-6.
163. Mars, W.M., M.L. Liu, R.P. Kitson, R.H. Goldfarb, M.K. Gabauer, and G.K. Michalopoulos, *Immediate early detection of urokinase receptor after partial hepatectomy and its implications for initiation of liver regeneration*. *Hepatology*, 1995. **21**(6): p. 1695-701.
164. Fukuhara, Y., A. Hirasawa, X.K. Li, M. Kawasaki, M. Fujino, N. Funeshima, S. Katsuma, S. Shiojima, M. Yamada, T. Okuyama, S. Suzuki, and G. Tsujimoto, *Gene expression profile in the regenerating rat liver after partial hepatectomy*. *J Hepatol*, 2003. **38**(6): p. 784-92.
165. Lai, H.S., Y. Chen, W.H. Lin, C.N. Chen, H.C. Wu, C.J. Chang, P.H. Lee, K.J. Chang, and W.J. Chen, *Quantitative gene expression analysis by cDNA microarray during liver regeneration after partial hepatectomy in rats*. *Surg Today*, 2005. **35**(5): p. 396-403.

166. White, P., J.E. Brestelli, K.H. Kaestner, and L.E. Greenbaum, *Identification of transcriptional networks during liver regeneration*. J Biol Chem, 2005. **280**(5): p. 3715-22.
167. Xu, C., C. Chang, J. Yuan, H. Han, K. Yang, L. Zhao, W. Li, Y. Li, H. Zhang, S. Rahman, and J. Zhang, *Identification and characterization of 177 unreported genes associated with liver regeneration*. Genomics Proteomics Bioinformatics, 2004. **2**(2): p. 109-18.
168. Xu, C.S., C.F. Chang, J.Y. Yuan, W.Q. Li, H.P. Han, K.J. Yang, L.F. Zhao, Y.C. Li, H.Y. Zhang, S. Rahman, and J.B. Zhang, *Expressed genes in regenerating rat liver after partial hepatectomy*. World J Gastroenterol, 2005. **11**(19): p. 2932-40.
169. Xu, C.S., J.Y. Yuan, W.Q. Li, H.P. Han, K.J. Yang, C.F. Chang, L.F. Zhao, Y.C. Li, H.Y. Zhang, S. Rahman, and J.B. Zhang, *Identification of expressed genes in regenerating rat liver in 0-4-8-12 h short interval successive partial hepatectomy*. World J Gastroenterol, 2005. **11**(15): p. 2296-305.
170. Kinnecom, K. and J.S. Pachter, *Selective capture of endothelial and perivascular cells from brain microvessels using laser capture microdissection*. Brain Res Brain Res Protoc, 2005.
171. de Bruin, E.C., S. van de Pas, E.H. Lips, R. van Eijk, M.M. van der Zee, M. Lombaerts, T. van Wezel, C.A. Marijnen, J.H. van Krieken, J.P. Medema, C.J. van de Velde, P.H. Eilers, and L.T. Peltenburg, *Macrodissection versus microdissection of rectal carcinoma: minor influence of stroma cells to tumor cell gene expression profiles*. BMC Genomics, 2005. **6**: p. 142.

Appendix 1 - Isolation and Viability Test of Primary Liver Endothelial Cells

Materials:

PBS (Gibco 10010-031); Percoll (Sigma-Aldrich P-4937); EGM-2 (Cambrex CC-3162); Hoechst (Molecular Probes H-3570); Sytox Orange (Molecular Probes S11368)

Procedure:

1. Perform perfusion as usual except the flow rate should be changed to 15mL/min.
2. After perfusion is done, perform isolation as usual. Reserve the supernatant from the first two 50g spins. Save the hepatocyte pellets if desired.
3. During the waiting time of all these spin cycles, start preparing the percoll layer. In a 50mL conical tube, mix 15mL Percoll and 15mL PBS – 50% Percoll. In another tube, mix 22.5mL PBS and 7.5mL Percoll – 25% Percoll. Divide 25% percoll evenly into two conical tubes. Use a 10mL pipette, draw up about 14.5mL 50% Percoll. Place the pipette tip at the bottom of the 25% Percoll and then raise it a bit so that the pipette tip is not blocked. Very slowly load the 50% Percoll underneath the 25% Percoll. Take care not to generate bubbles at the end of loading so the layer separation is undisturbed. When taking out the pipette, pull it up against the tube wall. If the separation layer is not visible, start over. (This step should be done during waiting time. Do not let cells wait for you.)
4. From this point on, the procedure should be carried out at room temperature. Set the centrifuge to 24°C. Spin the supernatant at 100g for 5min. Reserve the supernatant and discard the pellets.
5. Spin the supernatant at 350g for 7 min. Discard the supernatant. Break up the pellets before re-suspending them in a total of 20mL of PBS.
6. Carefully load 10mL of cell suspension onto the top of 25% Percoll. First wet the wall a little, then slowly move the pipette around the wall to release the liquid so that it slowly trickles down the wall from different points.

7. Carefully carry these two tubes to the centrifuge. Set brake setting to 0 and acceleration to 1. (Eppendorf 5804R) Spin at 900g for 20min.
8. Carefully suction off the top two layers until the total liquid measures at 20mL. Collect the cell layer (at about 15mL mark) until about 10mL is left in the tube. You should now have 20mL of cell suspension in PBS/Percoll collected from 2 tubes.
9. Add to this tube equal volume of PBS. Spin at 900g for 10min. Suction off the supernatant, break up the pellet, and re-suspend the pellet in EGM-2.
10. Combine 900 μ l of EGM-2, 2 μ l of Hoechst, 2 μ l of Sytox Orange, and 100 μ l of cell suspension. Count in a Hemocytometer using the DAPI filter. Sytox orange (dead nuclei) show up as bright green, and Hoechst (all live nuclei) show up as blue.
11. The cells are ready to be used.

Appendix 2 - HGM formulation

HGM is made with the base medium DMEM (Gibco 11054-020) with the additives listed below.

For every 500mL bottle of DMEM add the following:

Chemical name	Amount to add	Final concentration	Stock concentration	Order information
L-proline	0.015g	0.03g/L	N/A	Sigma P-4655
L-ornithine	0.05g	0.1g/L	N/A	Sigma O-6503
Niacinamide	0.153g	0.305g/L	N/A	Sigma N-0636
D-(+)-glucose	0.5g	2g/L	N/A	Sigma G-7021
D-(+)-galactose	1g	2g/L	N/A	Sigma G-5388
Bovine serum albumin	1g	2g/L	N/A	Sigma A-9647
Trace metal:				
ZnCl ₂	5µl of stock	0.0544 mg/L	5.44 mg/mL	
ZnSO ₄ ·7H ₂ O	5µl of stock	0.075 mg/L	7.5 mg/mL	
CuSO ₄ ·5H ₂ O	5µl of stock	0.02 mg/L	2 mg/mL	
MnSO ₄	5µl of stock	0.025 mg/L	2.5mg/mL	
Sterile filter the solution and add the following				
Penicillin-Streptomycin ¹	0.5 mL	10 unit/mL 10 µg/mL	10,000 unit/mL 10 mg/mL	Sigma P-0781
L-glutamine ²	2.5 mL	1 mM	200 mM	Gibco 25030-081
Insulin-Transferrin-Sodium Selenite ³	500 µl	5 mg/L 5 mg/L 5 µg/L	5 g/L 5 g/L 5 mg/L	Roche 1074547
Dexamethasone ⁴	400 µl	0.1 µM	0.05 mg/mL	Sigma D-8893
EGF ⁵	200 µl	20 ng/mL	0.050 mg/mL	Collaborative 40001

1. Dispense Pen/Strep stock into aliquots of 5.1 mL and store at -20°C
2. Dispense L-glutamine stock into aliquots of 2.6 mL and store at -20°C
3. Dissolve 50 mg or 250 mg powder in 5 mL or 25 mL sterile milli-Q water using a syringe. Dispense into 520 µl aliquots and store at -20°C
4. Dissolve 1 mg in 1 mL ethanol using a syringe. After powder is dissolved, add 19 mL PBS and mix thoroughly. Dispense into 420 µl aliquots and store at -20°C
5. Dissolve 100 µg powder in 2 mL sterile milli-Q water. Dispense into 220 µl aliquots.

Appendix 3 - Protocol for Assembling Milli-F Reactors

(Adapted from Anand Sivaraman)

Disposable Materials (these should not be re-used):

Normal silastic tubing, ID 0.062" (VWR 508-008); C-Flex tubing; Female luer PP fittings 1/16" ID (Cole-Palmer EW-06359-27); Straight Connectors (Cole-Palmer EW-06365-11); 00105GF 1/16"x1/16" Luer Adaptor (Cole-Parmer); BUNA o-ring 8x1 cross section 1mm², I.D. 8mm, width 1mm, 70 Durometer (McMaster); PP T-CONNECTOR 1/16" ID (Cole-Palmer EW-00105-GF); Male luer lock 1/16" hose barb (Cole-Palmer EW-30504-00); Polypropylene male luer lock plug (Cole-Palmer EW-30504-20)

Parts that should be autoclaved for 45 min of sterilization under the dry cycle:

1. 4 port connectors (beige color)
2. Five screws (4 mm screws), one blue autoclave sheet
3. One 5 µm pore size custom cut durapore filter
4. Two silicon scaffolds
5. One thick gasket
6. One thin gasket
7. One retaining ring with attached o-ring
8. One blocking screw (needed for 1-pump experiment)
9. One polypropylene reservoir
10. Screw driver, hexagonal connector driver, flat steel forceps, plastic forceps
11. Custom cut tubing pieces – as shown below

Tubing Lengths

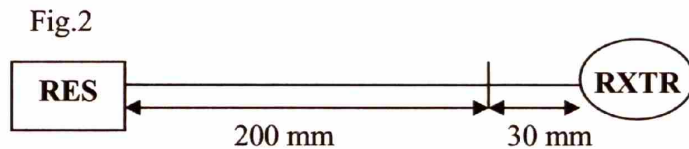
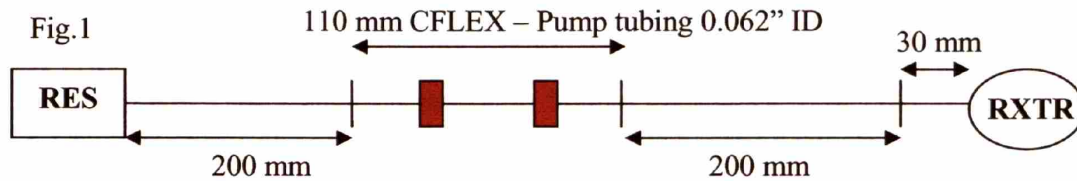
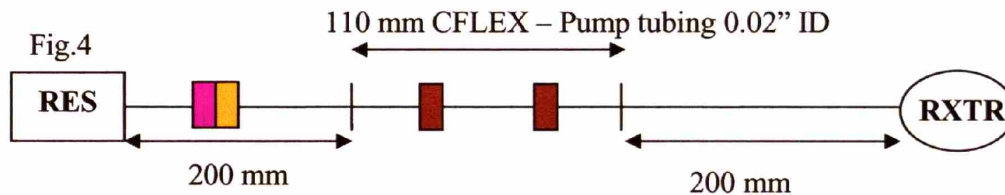
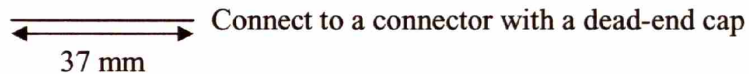


Fig.3



Legend: RES: Reservoir;
RXTR: Reactor; Pink and
orange boxes: luer connectors
for inline filter

Assembly of Milli-F Reactors:

1. Place the Durapore filter in BSA solution in a petri dish (35 mm), one of the silicon scaffolds in collagen solution ($30\mu\text{g}/\text{mL}$), and the polycarbonate reactor body in ethanol solution in a 100 mm petri dish. Remove any bubbles that may be present in the chips placed in collagen solution.
2. The reactor body must be placed completely under 70% ethanol solution for at least 35 minutes.
3. To begin, place the autoclaved blue sheet on the working surface of the hood.
4. Transfer the reactor body parts from the ethanol solution to a 100 mm petri dish with 25 mL PBS solution. Make sure that the reactor parts are completely immersed in PBS. Make sure

that all the ethanol is rinsed out. Since there is a significant surface tension difference between PBS and ethanol, one can see the reactor parts moving around on a film of ethanol in PBS, when initially placed in PBS. However, if the reactor is well rinsed and forcefully immersed into PBS, it will sink to the bottom.

5. Using the autoclaved plastic scalpel, transfer the reactor polycarbonate parts to the blue paper. Using vacuum and a pasteur pipette, remove excess PBS solution on the reactor. Take care not to scratch the reactor, especially the optical window. Hold the pasteur pipette horizontal to the reactor to minimize scratches. Do not remove the PBS completely from the optical window trough. A small amount of PBS will provide the necessary surface tension to hold the gasket in place.
6. Using the plastic forceps place the thin gasket into the trough of the optical window. While the steel scalpel may be used to remove the gasket from the autoclave and placed on the reactor part, the actual placement of the gasket into the trough should only be done with the plastic forceps.
7. Using the steel forceps transfer the silicon chip from collagen solution to the reactor trough. Make sure that you rinse the chip in PBS before transferring the chip to the reactor. This can help remove collagen from the top of the chip.
8. Adjust the chip in the trough using the syringe piston rubber.
9. Using the steel/plastic forceps transfer the filter from BSA solution to the reactor trough. Drop it on top of the silicon scaffold. Again, use the syringe piston rubber to press the filter to the scaffold. Make sure you break (with the syringe piston) and remove all bubbles formed between the filter and the scaffold.
10. Using the scalpel transfer the non-collagen coated silicon scaffold into the trough and place it on top of the filter. Press the scaffold to the filter using the syringe piston.
11. Place the thick gasket on top of the silicon chip.
12. Next place the retaining ring with the o-ring into the trough.
13. Add some PBS solution (1-2 drops using a 1 mL syringe) to the trough, so that the chip sandwich is never kept dry (it's the fluid surface tension that holds the filter to the chip)
14. Place the bottom polycarbonate part on top of the trough, aligning the screw holes with the holes in the top P/C part.

15. Using three of the five 4 mm screws, tighten the bottom part to the top P/C piece. Make sure that you do not tighten any one screw completely at any one time. For even distribution of stress on the o-ring (the main element that provides the seal), tighten the screws evenly.
16. Turn the reactor upside down (so that the optical window now faces you). Using the hexagonal driver, screw the plastic connectors into their respective ports. In case of reactors operating in the 2-pump scheme, use four plastic connectors, else use three. Use a blocking screw in the fourth port (bottom port diagonally opposite to the inlet port).
17. Using the two remaining 4 mm screws, attach the black cover plate to the reactor. This cover plate is needed when the reactor is to be mounted under a microscope.
18. Place 15 mL of medium in the reservoir.
19. Connect the inlet, outlet and cross flow tubing as shown in the figure in the previous page.
20. Use a 0.2 μm Pall filter in the gas exchange tube on top of the reservoir.
21. The reservoir will have a 37 mm inlet short tubing (inside the reservoir) and 2 short (15 mm) tubing for the outlet and cross flow connectors on the lid of the reservoir. In case the reactor is to operate in 2-pump mode, attach a 37mm tubing to the cross flow connector, instead of the 15 mm tubing.
22. Connect the tubing to the reactor and reservoir. Prime the reactor and tubing.

Appendix 4 - Co-culture spheroid formation and bioreactor seeding protocol

Materials:

Autoclaved male luer lock 1/16" hose barb (Cole-Palmer EW-30504-00), 1mL syringes, 100 μ m- and 300 μ m-pore size filter (SEFAR America)

1. The day before perfusion, prepare the spinner flasks by coating its inner walls and paddle attachments with Sigmacote. Let it air dry and rinse with milli-Q water. Autoclave the flask with 100mL of milli-Q water for 45min of sterilization under the wet cycle.
2. On the day of perfusion, seed 60x10⁶ endothelial cells and 20x10⁶ hepatocytes in one spinner flask with 100mL of HEGM. Let it spin at 85rpm in the incubator set at 37°C and 8.5% CO₂.
3. Cut 100 μ m filter into 10cm x 10cm squares and use a rubber band to secure it onto a 100mL glass beaker. Wrap it in foil and then autoclave blue paper. Cut 300 μ m filter into 10cm x 10cm squares and secure a piece onto a plastic funnel with autoclave tape. Wrap it in autoclave blue paper. Autoclave both for at least 45min of sterilization under the dry cycle.
4. On the day of seeding, follow appendix 1 to assemble and prime reactors. In the sterile hood, fill a 100mm Petri dish with 30mL of medium and set it on an ice pack. On the side, prepare another 30mL of medium in a 50mL tube and set it on ice.
5. Retrieve the spinner flask. Remove all spheroids above 300 μ m in diameter by passing all of the solution through the 300 μ m-filter funnel into two new 50mL tubes.
6. Select out all spheroids between 100 μ m and 300 μ m in diameter by pipetting all contents in the 50mL tubes through the 100 μ m-filter beaker.
7. Carefully remove the rubber band and invert and submerge the filter in the Petri dish. Shake it in solution to release all the spheroids. Collect the solution into a 50mL tube.
8. Spin at 40g for 2 minutes at 4°C. Remove supernatant and resuspend cells with the medium set aside earlier. Store it on ice.
9. Reactor fluidics should be primed by now. Fill a 1mL syringe with 0.5mL of medium and attach the connector. Remove bubbles in syringe. Disconnect the reactor outflow line at the connector. Connect the syringe to the outflow line.

10. Remove axial inflow line. Use the syringe to remove bubbles within the flow path. Use a new 1mL syringe and withdraw 1mL of spheroid solution and attach a connector. Remove bubbles and connect to the inflow line.
11. Making sure the cross-flow line is unimpeded, slowly inject spheroid solution into the reactor. Fluid should exit through the cross-flow line, and the outflow syringe should not move. When pressure is felt, stop the injection.
12. Remove the inflow syringe and discard. Remove bubbles in the flow line using the outflow syringe. Re-attach the inflow line to the reactor.
13. Remove the outflow syringe and start the pumps to remove excess spheroids. Re-attach the outflow line.
14. Check under an upright microscope to confirm high seeding density. If desired density is not achieved, repeat step 7-12.
15. Place reactor in the incubator set at 37°C and 8.5% CO₂.

Appendix 5 - Bioreactor cross-flow reversal, medium change protocol

Material: 0.8/0.2 μ m inline filter (Pall PN-4187), 3mL syringe, Autoclaved male luer lock 1/16" hose barb (Cole-Palmer EW-30504-00),

1. Warm up 20mL of culture medium to 37°C.
2. Take out one reactor with batteries attached into the hood. Install the inline double filter.
3. Loosen reservoir lid and stop axial flow. Suction off old medium. Replenish with 20mL of new medium. Tighten the lid. Start up main flow.
4. Carefully detach cross-flow line from reactor body (pull straight out. Any bending might break the connector). Connect a 3mL syringe coupled with an autoclaved connector to the tubing. Pull the tubing out of the pump wheel. While applying suction with syringe, tap on the double filter and tubing to get all bubbles out and make sure line is bubble-free. You may need to raise the height of the syringe to let bubbles float in the right direction. There should be ~0.5-1mL of medium in the syringe at the end.
5. Re-introduce the tubing back into the pump wheel. Detach tubing from syringe. Dispose of syringe along with connector. Increase cross-flow pump rate until a meniscus appear at the end of tubing. Stop the cross-flow pump and re-attach tubing to reactor.
6. Remove the screw-cap on the dead end tubing. Stop the axial flow pump. Clamp the outflow line. Start the cross-flow pump at a high rate. Make sure the back chamber of reactor is starting to fill up and rid of bubbles. Tap the reactor if some bubbles are resisting the flow. Keep pumping until the dead-end line is full and liquid has reached the connector. Return the pump rate to normal operation and stop the pump.
7. Unclamp the out flow line. Screw back on the dead-end line's cap. Restart both pumps.
8. Return reactor to incubator.

Appendix 6 - Sample Preparation for Scanning Electron Microscopy

Materials:

10% Glutaraldehyde (EMS Sciences); PBS (Gibco); 4% Osmium Tetroxide solution (EMS); Thiocarbohydrazide (Sigma-Aldrich); Hexamethyldisilazane (Sigma-Aldrich)

Procedure:

1. Fix sample with 2.5% Glutaraldehyde in PBS for 1 hour
2. Wash with PBS three times, 15 minutes each.
3. Incubate with 1% Osmium Tetroxide in PBS for 1 hour
4. Wash with PBS three times (see step 5), 15 minutes each
5. During the first wash, make up the 1% Thiocarbohydrazide (TCH) solution with Milli-Q water. Warm the water to 55°C on a heat block to help solublize TCH. **Do not heat dry TCH solids directly as it may explode.** Mix it with water before heating.
6. Incubate with 1% Thiocarbohydrazide for 30 minutes.
7. Wash with PBS three times, 15 minutes each.
8. Incubate with 1% Osmium Tetroxide for 1 hour.
9. Wash with PBS three times, 15 minutes each.
10. Incubate with 1% TCH for 30 minutes.
11. Wash with PBS three times, 15 minutes each.
12. Incubate with 1% Osmium Tetroxide for 1 hour.
13. Wash with PBS three times, 15 minutes each.
14. Serial ethanol dehydration with 30%, 50%, 70%, 95% Ethanol for 15 minutes each.
15. Dehydrate with 100% Ethanol three times for 15 minutes each
16. Switch solution to Hexamethyldisilazane (HMDS) by incubating sample in 1:3, 1:1, and 3:1 v/v ratio of HMDS:ethanol for 15 minutes each
17. Incubate sample in 100% HMDS three times, 15 minutes each.
18. Take out most of HMDS in the dish, leave a thin layer of liquid just barely covering sample. Let HMDS evaporate by itself.

19. Store sample in a desiccator when it is completely dry from HMDS. It is now ready for SEM observation. (No Au-Pd coating is necessary)

Appendix 7 - Protocol for RNA isolation from samples in Trizol

(Adapted from the Trizol and RNeasy Kit user manuals)

Materials:

Trizol (Invitrogen), chloroform (Sigma-Aldrich), ethanol, RNeasy Kit (Qiagen), RNase-free water

1. For reactor samples, drop each scaffold into a 2mL eppendorf tube with 700mL trizol. For collagen gel sandwiches in 6-well plates, fill each well with 1mL of Trizol. For tissue samples, cut tissue into chunks as small as possible and drop into 10mL of Trizol in a 50mL tube. Freeze all samples immediately in the -80°C freezer.
2. Thaw samples on ice. For reactor and collagen gel sandwich samples, homogenize the tissue with a 3mL syringe connected with 20-gauge needle for at least 5-10 cycles of pumping in and out. Repeat this step with a 25-gauge needle. For tissue samples, use a tissue homogenizer to break up the tissue. Start from a low setting and work all the way up to the maximum setting.
3. Transfer trizol solution to an eppendorf tube. Each tube should contain 1mL or less of Trizol solution. For every mL of Trizol, add 250µl of chloroform. Vortex on the highest setting and let settle for 2 minutes at room temperature.
4. Spin at 12,000 rpm for 15 minutes in the cold room.
5. Fill an eppendorf tube with RNase-free water and warm it to 55°C.
6. Remove the aqueous phase on top and place into a new eppendorf tube. Add equal volume of ice-cold 70% ethanol. Pipette up and down to mix. If the total volume at this point is more than 650µL, repeat step 6-7 until all solution has been passed through the column. Return the rest of the Trizol sample to -80°C freezer for further DNA or protein isolation.
7. Load the mixture onto an RNeasy column with maximum volume of 650µl. Spin for 15 sec. at 10,000 rpm at room temperature.
8. Collect the flow-through and run it through the column again using step 6. Discard the flow-through.
9. Add 700µl RW1 to the column. Spin for 15 sec. at 10,000 rpm. Discard the flow through and replace the collection tube with a new one.

10. Add 500 μ l RPE buffer (make sure ethanol has been added) and spin for 15 sec. at 10,000 rpm. Discard the flow-through.
11. Repeat the last step.
12. Spin the column again to collect any excess liquid. Discard the collection tube and the flow-through. Place the column into a 1.5mL collection tube with a closeable top.
13. Load 30-50 μ l of 55°C RNAse-free water into the column. Spin for 1 min at 10,000 rpm to elute the RNA.
14. If more than 30 μ g of RNA is expected, repeat the last step with the same tube.
15. Store in the -80°C freezer.

Appendix 8 - Protocol for DNA Isolation from Samples in Trizol

Materials:

Glycogen (Sigma-Aldrich); sodium citrate (Sigma-Aldrich); Hepes (Sigma-Aldrich)

Procedure:

1. Following RNA extraction, spin at 12000g at 4°C for 15 minutes.
2. Carefully remove as much liquid phase as possible without touching the white interface
3. Add 0.3mL 100% Ethanol/1mL Trizol used to the organic phase. Add 5ul of 20mg/mL glycogen to the mixture. Mix by inverting several times.
4. Let the samples sit at room temperature for 3 minutes.
5. Spin at highest speed at 4°C for 10 minutes
6. Remove supernatant into another tube (for further protein purification if desired)
7. Wash pellet with 1mL 0.1M sodium citrate in 10% Ethanol. Leave at room temp for 30 minutes. Mix every now and then by inverting several times.
8. Spin at full speed at 4°C for 10minutes.
9. Repeat steps 6-8.
10. Remove supernatant. Wash with 1.5mL 70% Ethanol per mL of trizol used. Leave for 20 minutes at room temp. Mix by inverting every now and then.
11. Spin at full speed at 4°C for 10 minutes
12. Carefully pipette out the supernatant without disturbing the pellet.
13. Leave the caps open and place the tubes in a 65°C heating block to dry the liquid. Check frequently to promptly remove the tubes when the pellet is almost completely dry.
14. Resuspend in 30ul of 8mM NaOH in Milli-Q water. Use pipette tip to pipette the liquid up and down while also stirring and jabbing the pellet.
15. Place all tubes back at 65°C heating block for 30 minutes to allow more DNA to dissolve.
16. Spin at full speed for 10 minutes at 4°C.
17. Remove supernatant to a clean tube. Add to it 4.8ul of 0.1M Hepes to adjust pH.
18. Store at -20°C.

Appendix 9 - Protocol for Tissue Cryosectioning and Immunostaining

1. For large pieces of fresh tissue (such as liver), immediately place them in liquid nitrogen after excision. After 2 minutes remove tissue from liquid nitrogen and store at -80°C until ready for cryosectioning.
2. For spheroids, fix them with 2% paraformaldehyde (EMS) in PBS for 30 minutes at room temperature. Wash several times with PBS and store in fresh PBS at 4°C until ready to embed in agarose gel.
3. Warm up agarose solution (1% w/v in milli-Q water) to solublize solids and let cool to 37°C . Use 200 mL to resuspend the spheroid pellet and let it solidify in an eppendorf tube.
4. Shake out the gel and place it on a small piece of 42 filter paper (Whatman).
5. In an ice bucket filled with liquid nitrogen equipped with a secondary metal container, pour into the center container 2-methylbutane (Fluka) and wait for it to come to solid-liquid equilibrium. Use a pair of plastic tweezers to hold and submerge the filter paper and the gel into the 2-methylbutane at melting temperature for 30 seconds, and place them in liquid nitrogen for 10 seconds. Store the frozen sample at -80°C until ready for cryosectioning.
6. Cut tissue into 5-10 μm sections on a cryostat and put onto gel-coated slides. Circle the section with PAP-pen (EMS).
7. Keep slides at -20°C until ready for immunostaining.
8. During the procedures below, do not let slides dry up. Keep sections in liquid until the end.
9. Fix in 2% paraformaldehyde for 20 minutes
10. Rehydrate with 5 washes of PBS
11. 5 washes of PBG (1xPBS with 0.15% Glycine, 0.5% BSA).
12. Incubate for 45 minutes in normal goat serum (Sigma-Aldrich), 1:20 dilution
13. 5 washes of PBG
14. Incubate primary antibody for 60 minutes at room temperature or overnight at 4°C .
15. 5 washes of PBG
16. Incubate secondary antibody for 60 minutes
17. 5 washes of PBG
18. 5 washes of PBS

19. Hoechst stain for 1 minute
20. 2 washes of PBS
21. Cover with coverslip and Fluoromount (EMS). Fix coverslips with nail polish and refrigerate overnight before observation.
22. Store at 4°C in the dark.

Appendix 10 - Embedding tissue samples in Technovit8100 and immunohistochemistry

Materials:

16% Paraformaldehyde (EMS Sciences); PBS (Gibco); Sucrose (Sigma-Aldrich); Technovit8100 (EMS Sciences); gelatin capsules (EMS Sciences); Antibodies; bovine serum albumin (Sigma-Aldrich); Trypsin-EDTA solution (Gibco); CaCl₂ (Sigma-Aldrich); Normal goat serum (Sigma-Aldrich)

Procedure:

1. Fix tissue with 2% paraformaldehyde on a nutator at 4°C for 3-4 hours. Tissue size should not exceed 1mm in thickness. If sample is reactor, flow 2% paraformaldehyde for 1 hour at room temp.
2. Wash overnight in PBS containing 6.8% sucrose at 4°C on a nutator.
3. Dehydrate with 100% ethanol at 4°C for 1 hour on a nutator. Exchange ethanol a few times in the first 5 minutes until it runs clear.
4. If sample is in polycarbonate scaffold, cut away edges where there are no channels. Cut the rest into 4-6 parts. Make sure tissue never dries out during cutting. Re-submerge into 100% ethanol if necessary.
5. Dip the sample in a separate tube of infiltrating solution (Technovit 8100 base liquid + Hardener I) to get rid of most of the clinging ethanol. Then place the sample in a fresh eppendorf tube of infiltrating liquid. Put on nutator for 8 hours at 4°C.
6. Prepare embedding solution (15mL of infiltration solution + 0.5mL Hardener II). Print out labels if desired. Put sample in a tube of embedding solution on nutator for 5 minutes. Fill a gelatin capsule with fresh embedding solution. Place sample in it and replace cap. Try to minimize air bubble size. Leave at 4°C overnight.
7. Place into final embedding gelatin capsule. Embed at 4°C overnight
8. Cut away unpolymerized part on top and store sample in a glass vial at -20°C for years, or at 4°C for a month. The cuts can be stored for one week in the fridge.

9. Normal tissue samples are ready to be sectioned now. For reactor samples, bring the block to a microtome. Carefully cut away embedding material until you expose the surface of the scaffold. Use a fresh razor, cut the grids of plastic while leaving the tissue. Use a small needle (>25gauge) to tease away the plastic scaffold parts.
10. Once all plastic parts are removed, re-embed the exposed tissue blocks. No infiltration is needed. Just embed directly in the embedding solution overnight at 4°C.
11. Now the block is ready to be sectioned. Section the samples at thickness 3-5µm on a dry glass knife. Make circles on glass slides with PAP pen and fill circles with milli-Q water filtered through a syringe 0.2µm filter. Float the sections on water on glass slides. Dry the slides on a slide warmer or heat block set at 37°C.
12. As soon as the slides are dry, they can be taken off the warmer and stored at 4°C. It best to use the sections for immunostaining as soon as possible.
13. On the day of staining, dry the slides for 2 full hours on a slide warmer or heat block at 37°C. Make 2%BSA/PBS solution.
14. Incubate the sections in 0.1% trypsin for 30 minutes in an incubator. Our incubators are set at 37°C and 8.5% CO₂. (see below for trypsin recipe) Wash well with 2%BSA/PBS
15. Incubate with normal goat serum (1:20 in 2%BSA/PBS) for 45 minutes in an incubator. Wash well.
16. Incubate primary antibody in 2% BSA/PBS in an incubator for 2 full hours. Every 30 minutes add 10 µl of milli-Q water to each circle.
17. Wash with 2%BSA/PBS at room temp.
18. Incubate with secondary antibody for 1 hour at room temp. (if using the biotin-Strepavidin system, do the biotin for 1 hour, and strepavidin for 30 minutes. Wash very well between each steps)
19. Wash well with 2%BSA/PBS. Then wash well with PBS.
20. Stain with Hoechst stain/PBS (1:1000) for 1 minute.
21. Wash well with PBS. Then leave PBS on for 5 minutes. Wash again. Repeat once.
22. Cover with coverslips and Fluoromount (EMS#17984-25).

Trypsin solution:

According to the book Harlow et al. [103], the recipe goes as follows:

20mM Tris pH 7.8

0.1% Calcium Chloride

0.1% Trypsin

Aliquot and store at -20°C.

Consistent good results were obtained by just mixing the usual trypsin-EDTA solution with 1.67g/L CaCl₂. (See below) EDTA might help on top of the trypsin since it is used in the pressure cooker and microwave methods of antigen retrieval.

Combine and warm up to 37°C before use:

1 mL 0.25% Trypsin and EDTA solution (Gibco 25200-056)

1.5 mL 1.67g/L CaCl₂ in milli-Q water

References

1. Harlow, E. and D. Lane, Using antibodies: a laboratory manual. 1999, Cold Spring Harbor, N.Y.: Cold Spring Harbor Laboratory Press. xiv, 495 p.

Appendix 11 - Notes on maintaining EGFP rat colonies

1. Place one male and one female in the same cage for up to 20 days. Typically mating occurs immediately. The gestation period is 21 days. Females are ready for pregnancy again immediately after giving birth. To avoid exhaustion and to protect newly born pups, females should not be pregnant following birth. This can be achieved by removing the male from the cage.
2. If the mating couple is fighting for an extended period of time, change the mating pairs. But once a successful mating occurs with healthy pups, keep track of the parents and always pair them with each other.
3. Four weeks following birth, the pups can be weaned from the mother. Identify genotype and sex during weaning. Keep males and females separate. Sacrifice whatever is not needed, such as all WT pups.
4. There are four guinea pig cages that are significantly larger than rat cages. These are used as pregnancy/nursing cages. When females are pregnant, they should be placed in nursing cages. Each cage should have only one female. To make things easier, if possible, mating should take place in the nursing cage, and then the male can be removed.
5. Females are more territorial than males. Always try to place a female into a male-occupied cage to avoid fighting.
6. Do not mate rats that are related. Always order a new WT female to mate with an EGFP male if you want to start a new breeding pair.
7. Rats older than 1-year old do not breed regularly. Discard if rats are too old.
8. It is difficult to tell a rat's gender when it is too young. Also disturbing the pups while they are still being nursed could trigger unwanted behaviors from the mother. Hence it is best to check their sex during weaning. The male rats should show their testis when they are left alone and walking around the cage. The genotype can be identified by shining a UV lamp in their eyes in a dark room. EGFP-positive rats have green fluorescent eyes. In fact, even without UV light, the EGFP-positive rats' eyes have a yellow hue under direct sunlight.
9. Homozygous EGFP-positive rats do not live well. All EGFP-positive rats we have are heterozygous. Use EGFP-positive males to mate with WT females. All positive offspring will be heterozygous.

Appendix 12 – Collagen Gel Sandwich Preparation

Materials: 10x PBS (Roche), collagen solution (~3 mg/mL, Cohesion), 1M HCl, glucose (Sigma), sodium bicarbonate

1. Make glucose-enriched PBS by adding glucose and sodium bicarbonate to 10x PBS so that the final concentrations are: 20g/L glucose, 37g/L sodium bicarbonate. Sterile filter this solution and store at 4°C.
2. Sterile filter 1M HCl and store at 4°C
3. Sterile filter milli-Q water and store at 4°C.
4. Under sterile conditions, combine 3.4 mL of collagen solution, 2.4 mL of sterile water, and 650 μ L of glucose-enriched PBS. Add an additional 18 μ L of 1M HCl solution. Mix well and test the pH by pipetting 10 μ L of the solution onto a piece of pH paper. Continue to titrate with HCl until pH reaches 7.4. This titration only needs to be performed the first time the gel is made. Note the total amount of HCl added for future uses.
5. Pipet 600 μ L of the gel solution into each well of a 6-well plate. Avoid any bubbles. Tilt the plate so that all surfaces are covered.
6. Place the plate in the incubator at 37°C and 8.5% CO₂ for at least 1 hour for solution to solidify into a gel.
7. Cells can now be seeded onto the gel. Allow ~2-4 hours for cells to attach, depending on the cell type.
8. Repeat step 4 but half the volume of all components.
9. Aspirate medium and wash once with 37°C PBS. Pipette 300 μ L of mixed solution into each well. Tilt plate to distribute solution.
10. Return plate to the incubator for an hour.
11. Fresh medium can now be added to each well. Medium should be changed every 2 days.



Room 14-0551
77 Massachusetts Avenue
Cambridge, MA 02139
Ph: 617.253.5668 Fax: 617.253.1690
Email: docs@mit.edu
<http://libraries.mit.edu/docs>

DISCLAIMER OF QUALITY

Due to the condition of the original material, there are unavoidable flaws in this reproduction. We have made every effort possible to provide you with the best copy available. If you are dissatisfied with this product and find it unusable, please contact Document Services as soon as possible.

Thank you.

Some pages in the original document contain color pictures or graphics that will not scan or reproduce well.